Removal of thorium and zirconium from aqueous streams by biosorption

A thesis submitted in fulfillment of the requirements for the degree of Doctor of Philosophy

Sayanasri Varala

B.Tech

M.Tech

Chemical and Environmental Engineering, School of Engineering

College of Science, Engineering and Health

RMIT University

August 2017

Declaration

I certify that except where due acknowledgement has been made, the work is that of the author alone; the work has not been submitted previously, in whole or in part, to qualify for any other academic award; the content of the thesis is the result of work which has been carried out since the official commencement date of the approved research program; any editorial work, paid or unpaid, carried out by a third party is acknowledged; and, ethics procedures and guidelines have been followed.

Sayanasri Varala

Acknowledgements

This thesis would never have happened without the help, suggestion, encouragement, evaluation, and support of many great people. It is a pleasure to thank those who made this thesis possible and I express my heartfelt appreciation, especially to the following entities.

I owe my deepest gratitude to my supervisor at RMIT University, ***Dr Rajarathinam Parthasarathy, Associate Professor*** for his detailed and constructive comments, and invariable aid throughout the thesis work. His valuable advice, logical thinking, friendly help and extensive discussions have been of very significant for this thesis.

I am delighted to express my profound sense of indebtedness to my Supervisor at CSIR-IICT***, Dr B Satyavathi, Principal Scientist*** for her kind support, guidance, unfailing attention and constant encouragement throughout my research work that made this thesis possible. She has provided her support in many ways, and I am appreciative of everything she has done for me. I was able to work under her supervision, and I am obliged for all these years. She has my utmost respect and admiration for introducing to this research topic, which has been very interesting and given me great insight into the future work.

It is an honor to be associated with ***Prof Suresh K Bhargava***, Deputy VC and ***Dr Mark Pownceby***, CSIRO. I have great respect towards Prof Suresh K Bhargava for leading CSIR-IICT collaboration research program that gave an opportunity to explore multi-continental research scenario. I gratefully acknowledge the revisions and comments specified by Dr. Mark in the thesis draft that enriched the standards of the thesis.I gratefully acknowledge their mentorship during the research work.

My sincere thanks are expressed to ***Dr M Lakshmi Kantam*****,** Ex-Director, CSIR-IICT for providing me with an opportunity to carry out my research work in IICT and providing financial support through the fellowship program.

I wish to extend my obligations to Mr. D Mallikarjun and Mr. N Balaji for rendering their technical assistance during the experimental work in IICT. I appreciate the support and help provided by all technical and administrative staff of IICT and RMIT during the years. I also acknowledge the moral support rendered by IICT and RMIT friends during the course of time.

I heartily bestow all my besties' especially Dr. Sunitha, Rajesh, Saranya, Vidya, Vivek, Sandeepa and Alka for their ample favours and encouragement even during tough times in PhD pursuit. Finally, and most importantly, I am delighted for the unending support of my family for their immense love, patience, and generosity which have been my strength, inspiration and enthusiasm at every front of my life. They raised me to strive to be the best at whatever I do but to be humble, recognizing that anything I accomplished was a gift from God. My academic career would not have come this far without their full love and encouragement at each step of the way.

Once again I thank everyone.

Sayanasri Varala

Publications:

1. **Sayanasree Varala,** Banala Dharanija, B. Satyavathi*, V.V. Basava Rao, R. Parthasarathy. New biosorbent based on deoiled Karanja seed cake in biosorption studies of Zr(IV): Optimisation using Box–Behnken method in response surface methodology with desirability approach. ***Chemical Engineering Journal*** 302 (2016) 786-800. *Citations-13.*
2. **Sayanasree Varala,** Alka Kumari, B. Dharanija , Suresh K Bhargava, R. Parthasarathy, B. Satyavathi*. Removal of thorium (IV) from aqueous solutions by deoiled Karanja seed cake: Optimisation using Taguchi method, equilibrium, kinetic and thermodynamic studies***. Journal of Environmental Chemical Engineering*** 4 (2016) 405–417. *Citations-6.*
3. **Sayanasri Varala,** R. Parthasarathy, Suresh K Bhargava, B. Satyavathi*. Desorption studies for the recovery of radionuclides (Th and Zr) and optimisation using Taguchi mixed design L_{18} ($2^1 3^2$) - A regeneration step for loaded biosorbent, general mathematical model for multistage operation***. Journal of Environmental Chemical Engineering 5 (***2017) 5396-5405.

Conference Presentations:

1. Sayanasri Varala, B. Satya Sirisha, P.V. Aishwarya, R.Parthasarathy, B. Satyavathi*, "Desorption studies for the recovery of thorium from loaded biosorbent (DKSC): Parameter optimisation and equilibrium modelling" at International Conference on Chemical and Biochemical Engineering (ICCBE) held at Pune , India, 2017.

2. Sayanasri Varala, R. Parthasarathy, B. Satyavathi*, "Desorption of zirconium metal ions from loaded biomass and process optimisation" at Student research Symposium on Water: Effective Technologies and Tools Research Centre (WETT), RMIT University, Melbourne, Australia, 2016.

3. Sayanasree Varala, Alka Kumari, B.Dharanija, R.Parthasarathy, B.Satyavathi, "Equilibrium, kinetic and biosorption studies of thorium from aqueous solutions using deoiled Karanja seed cake" held at International Conference on new frontiers in Chemical, Energy and Environmental Engineering (INCEEE), NIT Warangal, India 2015**.**

Table of Contents

CHAPTER- 3

Results & Discussions

List of Figures

List of Tables

Nomenclature

English

C_e	equilibrium metal ion concentration (mg/l)
q_e	amount of metal ions adsorbed for gram of adsorbent at equilibrium(mg/g),
Q_0	maximum monolayer adsorption capacity(mg/g)
K_L	Langmuir isotherm constant (L/mg)
R_L	separation factor or equilibrium parameter
C_0	initial metal ion concentration (mg/L)
Θ	surface coverage
K_f	Freundlich isotherm constant (mg/g)
N	adsorption intensity
A_T	Temkin isotherm equilibrium binding constant (L/g)
R	Universal gas constant (8.314J/mol/k)
T	Absolute temperature (298 K)
B	constant related to heat of sorption
q_s	theoretical isotherm saturation capacity (mg/g),
K_{ad}	D-R isotherm constant (mol^2/kJ^2),
ε	D-R isotherm constant
q_t	amount of metal sorbed at time- t (mg/g)
k_1	first order rate constant
k_2	second order rate constant
h	initial sorption rate
k_i	intra particle diffusion rate constant
C	Intercept
K_d	Distribution coefficient (L/g)
ΔH^0	enthalpy change
ΔS^0	entropy change
ΔG^0	free energy change
k_{1d}	pseudo-first desorption rate constant
k_{2d}	second order desorption rate constant
$q_{t,d}$	solid-phase concentrations of metal desorbed at any time t

$q_{e,d}$	solid-phase concentrations of metal desorbed at equilibrium
w_1	weight of Petri dish
w_2	initial weight of Petri dish with sorbent
w_3	final weight of Petri dish with sorbent

Abbrevations

DKSC	De-oiled karanja seed cake
Th-DKSC	Thorium loaded biomass
Zr-DKSC	Zirconium loaded biomass
Th-DKSC^R	Regenerated thorium loaded biomass
Zr-DKSC^R	Regenerated zirconium loaded biomass
RSM	Response surface methodology
OA	Orthogonal array
AAS	Atomic absorption spectroscopy
NREL-LAP	National Renewable Energy Laboratory – Laboratory Analytical Procedure
FTIR	Fourier Transform Infrared Spectroscopy
SEM	Scanning Electron Microscopy
EDS	Energy diffraction spectroscopy
pzc	Point zero charge
TCD	thermal conductivity detector

ABSTRACT

Thorium and zirconium are the most stable radionuclides used in various nuclear operations, and the separation of these from aqueous industrial streams is essential. The conventional technologies followed for the treatment of high concentrate nuclear discharges containing these radionuclides are the precipitation, electro precipitation, electro coagulation, cementing, membrane separation, solvent extraction, ion-exchange resins, oxidation–reduction, adsorption, reverse osmosis, and evaporative recovery, etc. However, afore mentioned treatment methods have certain disadvantages like the high cost of implementation and operation, especially for the concentrations below 100 ppm. Hence, the necessity to invent new treatment technologies with acceptable costs is compulsory for the treatment of low concentrate radioactive wastes. One of the promising alternatives is the application of biosorption process that utilizes biomass or bio-based materials as sorbents in the waste water treatment as a pollution control process for most of the industrial discharge. The advantages of biosorption over the conventional methods are low operating cost, selectivity for specific metal, short operational time and no chemical sludge. Biosorption entails the use of living or dead biomass and their derivatives with the involvement of either ligands or functional groups (situated on the outer surface of the biomass) in the mechanism of sorption. This treatment method is based on utilizing the ability of biological materials to accumulate metal ions from liquid wastes either by metabolically mediated or physicochemical pathways.

In the present research, an attempt has been made to explore the potentiality regarding adsorption characteristics of a new agro-industrial by-product namely, de-oiled Karanja seed cake for the removal and recovery of radionuclide metal ions (Th and Zr) from

aqueous solutions via biosorption method. The relevant process conditions for the sorption of these metal ions (pH, sorbent mass, ionic concentration, and temperature) were studied. Furthermore, adsorption isotherm and kinetic sorption modeling, thermodynamics were investigated to determine the probable physical characteristics of the biosorption process. Also, the bound metal ions (Th and Zr) were isolated from the loaded biomass adapting desorption technique using elution agents since biosorption will be more attractive if loaded biomass can be regenerated for reuse in multiple sorption cycles. The biosorption and desorption studies were carried out in batch mode, and the process variables were optimized for the maximum biosorption/desorption efficiency through DOE concepts like Taguchi OA and RSM. The property of new biomass was investigated using characterization techniques like SEM, FTIR, EDX, pH_{pzc} and physicochemical properties.

Deoiled Karanja seed cake has shown good potentiality regarding biosorption capacity in the removal of thorium and zirconium from aqueous streams, and obtained high K_d values when compared to commercially available adsorbents, implying an important feature of DKSC to treat large volumes of low concentration metal wastes. The thorium equilibrium biosorption data fitted very well to the Langmuir isotherm model, whereas the zirconium biosorption data fitted the best with Freundlich model representing the mono-layer sorption and complex heterogeneity of the biomass respectively at optimum conditions. The sorption kinetic data followed pseudo-second order model conveying the chemisorption mechanism by the probable involvement of hydroxyl, carboxyl, amine, and nitro molecular groups. The desorption results revealed that Th ions could be eluted using 0.1M HCl and 0.1M $NaHCO_3$ can be used for eluting Zr ions from the loaded biomass respectively. It was also proved that desorption kinetics follows pseudo-second order model for both thorium and zirconium at optimal

conditions. Also, the regenerated DKSC was found to possess similar properties as of native DKSC. Hence, the research work conveys that proposed biosorption/desorption method using DKSC (new low-cost bi-sorbent) is most cost-effective and efficient treatment method that is suitable for the effluent treatment of nuclear and hydrometallurgical industries. Thus, DKSC could be effectively used as a natural and economic biosorbent for the separation of Th and Zr ions from contaminated sites.

Chapter 1

Introduction

1.1. Research rationale

Henri Becquerel was the first to find about radioactive elements in the 19th century. Ever since more elements have been investigated for their radioactivity and nuclear applications. Among them, thorium and zirconium are important radionuclides with various nuclear applications. The sources, industrial significance, and risks associated with these elements during their processing are discussed in this chapter. The present research is focused on determining the most efficient and economical treatment method that can be used for the isolation of thorium and zirconium from industrial wastewater streams.

1.1.1. Source of Th and Zr, their applications, and risks in their processing

Thorium is a naturally occurring actinide element with nuclear significance. It is the 41st abundant metal disseminated over the earth's crust at an average of 6ppm. It is represented by the symbol Th and its atomic number is 90. Table 1.1 shows a list of the major thorium containing ores. Among them, monazite is the one with significant commercial value. Thorium is mainly refined from monazite-containing heavy mineral sands and also recovered as a by-product in the extraction of other rare-earth containing minerals. According to United States Geological Survey (USGS), United States, Australia, and India have huge reserves of thorium which amount for approximately 25% of the world thorium reserves.

Thirty radioisotopes of thorium ranging from 209 to 238 in mass numbers have been characterised to date. Among them, ^{232}Th and ^{230}Th are the most stable isotopes with half-life periods of 14,100 million years and 75,380 years, respectively. ^{232}Th is the parent primordial radionuclide containing 142 neutrons that accounts for nearly all natural thorium(Boveiri Monji et al., 2014). It is estimated that thorium is more

abundant (about 3 to 5 times) than uranium (Congcong et al., 2014).It is predicted that thorium will be able to replace uranium in the near future as nuclear fuel in nuclear reactors.

Table 1.1: Major sources of thorium.

Ore	Chemical formula	Thwt% (approx. values)
Thorite	$ThSiO_4$	71.59
Thorianite	ThO_2	87.88
Allanite	$Ca(REE,Ca)Al_2(Fe^{2+}, Fe^{3+})(SiO_4)(Si_2O_7)O(OH)$	0.1-2
Monazite	$(Ce, La, Nd, Th)PO_4$	4.83
Zircon	$ZrSiO_4$	≤0.4

In thermal breeder reactors, the fertile isotope ^{232}Th is bombarded by slow neutrons, which leads to neutron capture and the formation of ^{233}Th, which further encounters two consecutive beta decays to become first ^{233}Pa and then the fissile ^{233}U as shown in equation 1.1.

$$^{232}_{90}Th + n \rightarrow {}^{233}_{90}Th + \gamma \xrightarrow[21.8\ min]{\beta^-} {}^{233}_{91}Pa \xrightarrow[27\ days]{\beta^-} {}^{233}_{92}U \xrightarrow[1.5\ X\ 10^5 years]{\alpha} \quad (1.1)$$

^{233}U is fissile and hence can be used as nuclear fuel (as ^{235}U or ^{239}Pu), which can go through nuclear fission. The neutrons emitted from the fission can strike ^{232}Th nuclei, restarting the cycle.

Thorium and its compounds and alloys find widespread use in various applications. It is a main model element for tetravalent actinides (like Np(IV), U(IV), and Pu(IV)) in natural waters and is useful as a tracer when studying environmentally important processes (Yusan et al., 2012, Anirudhan et al., 2010).Thorium oxide finds application as a catalyst, high-temperature ceramic and in high-quality lenses. Thorium is a gamma-emitting by-product of nuclear reactor operations. It is also a toxic element that is widely found in various industrial effluents. Some human activities such as the exploitation of ores associated with thorium, lignite burning in power stations and use

of fertilizers can also concentrate thorium in the environment, especially surface waters (Yusan, 2012, Kuber C. Bhainsa, 2009). The effluents containing Th(IV) are known to cause acute toxicological effects and harmful diseases to humans by localising in the liver, spleen, and marrow, precipitating as hydroxides and resulting in lung, pancreatic and liver cancers(Yang et al., 2015, Bhalara et al., 2014)

Zirconium is a solid transition metal with symbol Zr and atomic number 40. It is a shiny, grayish white material with high metal conductivity, resembling hafnium mostly and titanium to a lesser extent. The most important sources of zirconium are tabulated in Table 1.2., among which zircon ($ZrSiO_4$, a silicate material) is the principal commercial source of zirconium, which is found primarily in Australia, Brazil, India, Russia, South Africa and the United States, as well as in smaller deposits around the world. Besides zircon, baddeleyite and kosnarite are also commercially valuable ores.

Table 1.2: Major sources of zirconium.

Ore	Chemical Formula	Zr wt% (approx. values)
Zircon	ZrSiO4	43.14
Baddeleyite	ZrO_2	72.03
Zirconia	ZrO_2	----

Zirconium is mainly used as a refractory and opacifier and is used in small amounts as an alloying agent for its strong corrosion resistive traits in aggressive environments.It is a major engineering material to carry out certain industrial processes and is mainly used in the manufacturing of photoflash bulbs, moulds for molten metal's, surgical appliances, light filaments, watch cases and tanning of leather(Akhtar et al., 2008). Zirconium-based compounds also have several industrial applications. For instance, zirconium-based carbides and nitrides are refractory solids;

especially carbide is used to make drilling tools and cutting edges. Zirconium dioxide (ZrO_2) is used in laboratory crucibles and metallurgical furnaces. It is also used as a refractory material in space vehicle parts due to its heat resistance and is sintered into a ceramic knife. Zircon ($ZrSiO_4$) is a major value added mineral obtained during the processing of titanium minerals like ilmenite and rutile and is used as gemstones in jewelry. It is also used as a component in some abrasives like grinding wheels and sandpaper. The most extensive utilisation of zirconium is in water-cooled nuclear reactors either in fuel containers or nuclear products to trap fission fragments and neutrons, thus enhancing the efficiency of the nuclear reactor. ^{90}Zr, ^{91}Zr, ^{92}Zr, ^{93}Zr, ^{94}Zr, ^{95}Zr and ^{96}Zr are the naturally occurring isotopes of zirconium, among which ^{90}Zr is the most common making up to 51.45% of all zirconium, and ^{96}Zr is the least common making up only 2.80%.Zr^{93} and Zr^{95} are the main untreated wastes of nuclear discharge released during fission and activation reactions in nuclear reactors and dissolution of "Zircaloy" fuel cladding. These isotopes (Zr^{93} and Zr^{95}) have significant value in nuclear fuel cycle due to their long half-life (1.5×10^6 years). Zirconium has a complex chemistry forming $[Zr_4\ (OH)_8(H_20)_{16})]^{8+}$species in the acidic environment, as in waste streams from nuclear installations, leading to a particulate complex formation above pH 6.0 (Garnham et al., 1993, Akhtar et al., 2008). Due to the large usage of zirconium for its unique physical and chemical properties in various industries, heavy releases of zirconium into the surface water occur from several anthropogenic sources including nuclear power production, ceramic dust, heavy mineral mining, improper waste dumping, accidentalrelease,e.g., leakage, corrosion and from atmospheric fallout.

1.1.2. Purpose of this research

Several industrial activities dealing with thorium and zirconium produce low, intermediate and high-level radioactive wastes that require advanced treatment;

otherwise, the discharges may potentially pollute the surface water. The exact treatment and processing of the industrial streams containing these radioactive nuclides are of a large environmental concerndue to their toxicity and persistence, which pose severe adverse effects on human and ecological health. Even at trace levels, these materials have been a public health problem for many years.They can enter the food chain via bioaccumulation process and disturb the normal functioning of the ecosystem. Also, the segregation of these radionuclides from aqueous media is an important subject of hazardous and nuclear waste management due to their toxicity. The recovery of these ions, therefore, has economic, technical, and commercial importance owing to their nuclear applications. Strict environmental protection legislation and public environmental concerns lead to the search for novel techniques for the recovery of radionuclides from industrial waste water.

Chemical/electro-precipitation, electro floatation, electro deposition, evaporation, ion exchange, reverse osmosis, solvent extraction, membrane separation, and adsorption are some of the conventionally followed separation techniques for the removal and retrieval of radioactive ions (Akkaya et al., 2013, Kütahyalı et al., 2010). Nevertheless, most of these methods are only suitable for large scale treatments and incur a high cost when practiced. Also, they have serious drawbacks such as poor efficiency when they are present at low concentrations (<100 mg/L) necessitating the use of expensive chemicals and accompanying disposal problems. Treatment of dilute wastes (<100 mg/L) is necessary since concentrations at this level are potentially toxic and hazardous to human beings (Ioanna et al., 2013). New technologies with acceptable costs are required for the reduction of these low concentration radioactive ions in industrial effluents.

Compared with conventional methods, biosorption has several advantages and is considered to be quite attractive based on its efficiency. It is one of the easiest, safest and most cost-effective methods because it involves simple operation and easy handling (Siti et al., 2013). The first major challenge for the biosorption operation is to select the most promising biomass type from an extremely large pool of readily available and inexpensive biomaterials. The published works on testing and evaluating the performance of biosorbents in pollution remediation offered a good basis in the search for new and potentially feasible metal biosorbents. Another challenge is that the application of biosorption is facing great difficulties for many reasons like lack of knowledge on the biomass characteristics as sorbent, parameters influencing the biosorption process and sorbent regeneration and reuse. Great efforts have to be made to improve biosorption processes, including immobilisation of biomaterials, improvement of regeneration and re-use, optimissation of biosorption process,etc.

1.1.3. Research Innovation in this work

(a) Application of deoiled Karanja biomass as sorbent

A notable and growing trend is to evaluate the feasibility and suitability of natural, viable, renewable and low-cost materials, which can be used as sorbents to combat the menace of metal pollution. Researchers have examined various biomasses for their potential to be used as sorbents in the removal of metals/organics and classified them into the following categories: bacteria, fungi, yeast, algae, industrial wastes, agricultural wastes and other polysaccharide materials. Much literature has been generated in recent years for the removal of metals from industrial wastewaters using biosorption (Carolin et al., 2017).Recently, agroindustrial wastes have received significant attention due to their abundance in nature, biodegradability, eco-friendly and low cost and they can be used as important sorbents in the removal of metal ions. The annual harvest and processing of

various crops in India yield considerable quantities of agricultural by-products. There is no consistent statistical information about the crops and the associated by-products generated by these plants in India. Some of the agroindustrial wastes include peat, wood, pine bark, banana pith, soya bean, cottonseed hulls, peanut shells, rice husk, sawdust, wool, orange peel, and compost and leaves.

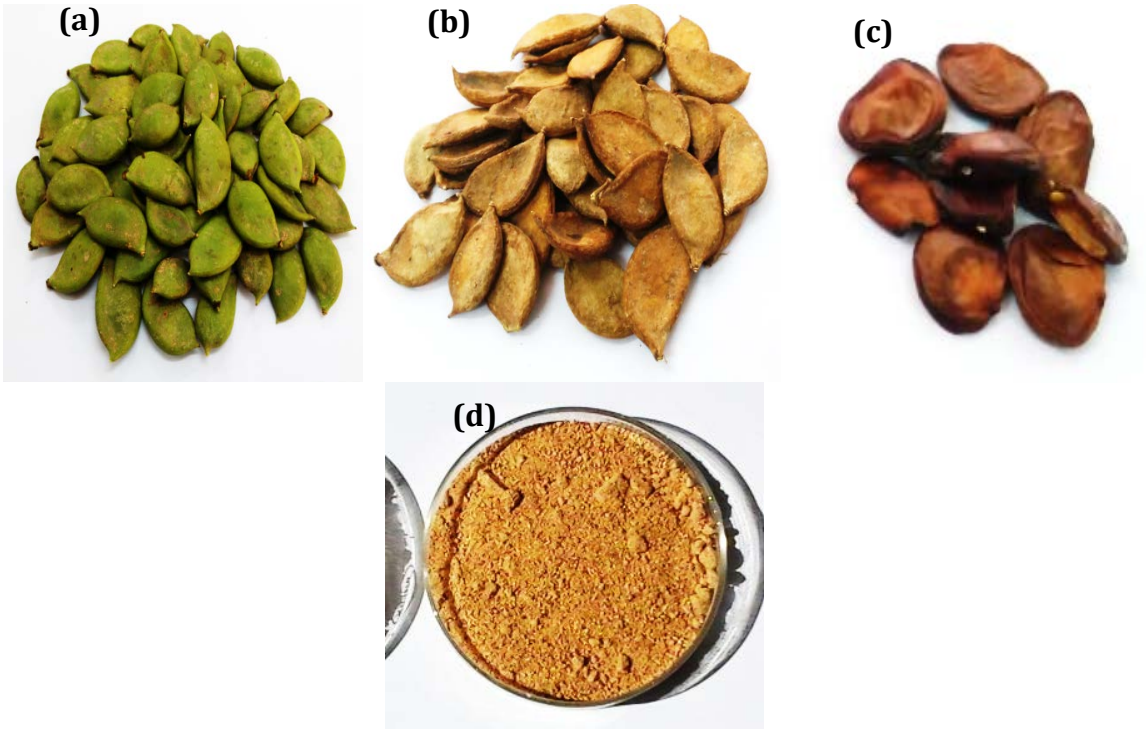

Figure 1.1: (a) Karanja fruits (raw) (b) Dried Karanja seeds (c) Dried Karanja nuts and (d) De-oiled Karanja seed cake

Deoiled Karanja seed cake is one such biomass with little or no economic value that is produced as a residue after extracting oil from Karanja seeds. The bio-oil produced from Karanja is a superior substitute feed for biodiesel production in developing countries such as India. Karanja seeds (Fig. 1.1) are acquired from the Karanja tree, which is known as *Milletiapinnata*, It belongs to the *leguminaceae* species pea family, fabaceae and is a resident of tropical and temperate Asia, Australia, and some Pacific islands. It is regularly known by the synonym *Pongamiapinnata* and commonly called *Karanja* in

India. It is one of the few nitrogen fixing trees and produces bean-like brownish-red seeds (when dried)about 1.5–2.5 centimeters long. The seeds are brittle and contain28-34% of oil with a high percentage of polyunsaturated fatty acids (Muktham, 2016).

The Karanja tree and its seeds, the bio-oil produced from Karanja and the de-oiled Karanja seed cake all have multiple benefits. The plant has been historically used as a medicinal plant in Ayurveda and Siddha systems of Indian medicine. The Karanja tree is famous for its shade, ornamental value, seed oil, and plant fodder. It is a part of social forestry in India. Most parts of the Karanja plant such as the leaves, roots, and flowers, due to their medicinal properties, are used as a crude drug for the treatment of tumors, piles, skin diseases, itches, abscess, painful rheumatic joints, wounds, ulcers, diarrhea, etc. In India, the oil has many applications such as a herbal medicine for the treatment of human and animal skin diseases, in soap making, in tanning industries and mainly as a substitute feed for biodiesel. The Karanja seed cake, due to its ample protein and nitrogen contents and insecticidal and nematicidal activities, finds application as green manure in agriculture and environmental management (Dwivedi et al., 2014).

In the present research, deoiled Karanja biomass has been used as the sorbent for the separation of radionuclides namely, thorium and zirconium from aqueous solutions via biosorption and desorption methods.

(b) Optimisation of process variables using DOE technique

The use of an abundant agro-industrial waste based sorbent for the removal of metals cannot ensure an efficient process. There is a need to optimise and organise process variables to obtain the desired and effective outputs. In developing a process, it is important to understand the influence of process parameters and their interactions on

process performance to determine an optimum set of parameters that will lead to the desired outputs. The classical style of trial and error (change one factor at a time) approach to determine the optimum set of process parameters has many drawbacks. It is time-consuming. There will be a lack of information in this method about the interactions among the variables especially when the number of possible process parameters is high.

On the other hand, Design of Experiments (DOE) technique can help to determine the minimum number of experiments consisting of a possible parameter combination and suggest parameter domains where the process offers the most benefit. DOE is a series of runs/tests that involve purposeful changes to input variables and aids in observing the change in responses at the same time. The main criteria that need to be considered while picking an appropriate DOE that produces the best response include: (i) identifying the number of control factors with their respective levels, (ii) determining the least possible number of runs that can be performed, and, (iii) verifying the impact of cost, time, and availability of chemicals (Douglas 5th edition).

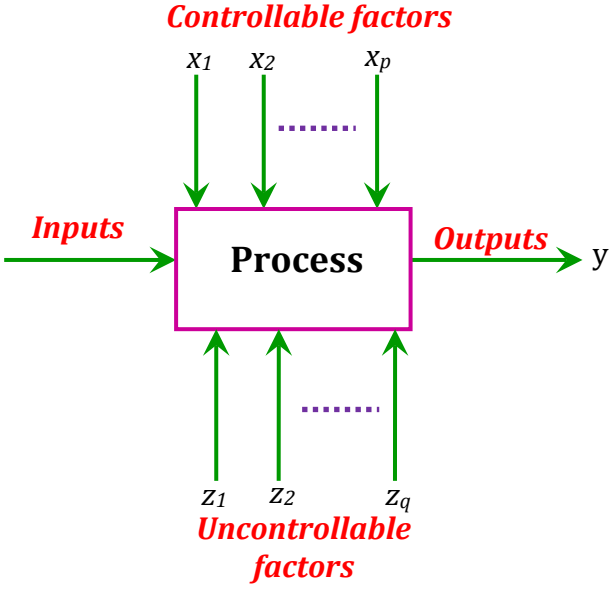

Figure 1.2: General model of a process.

A designed experiment is a series of runs/tests in which the experimenter purposefully makes changes to input variables and observes the responses. In general, experiments are used to study the performance of a process that can be represented by a model as shown in Figure 1.2.

The process consists of desired serial procedures that are required to transform an input into an output that has one or more observable responses. Some of the process variables $x_1, x_2 \ldots x_p$ are controllable, whereas others ($z_1, z_2 \ldots z_q$) are uncontrollable. The general objectives of the experiment include: 1) determining the most influential variables on the response y, 2) determining where to set the influential x's so that y is almost always near the desired nominal value and the variability of y is small, and 3) minimizing the effects of uncontrollable variables $z_1, z_2, \ldots, z_q$. Hence, the experimenter's objective is to plan, conduct and determine the influence of the above factors on the output response of the system. DOE offers the following experimental designs: factorial design, response surface design (RSM), mixture design and Taguchi design.

1.2. Research objectives and questions

The objectives of the present study are

- To examine the potential for using deoiled Karanja biomass as a sorbent for the removal of radionuclides from aqueous solutions
- To obtain equilibrium, kinetic and thermodynamic data to understand the biosorptivebehaviour of Karanja biomass
- To optimise the biosorption process using the principles of design of experiments (DOE)

By conducting this research, the following research questions can be answered:

- What is the efficiency of deoiled Karanja biomass as sorbent in the removal of thorium and zirconium from aqueous solutions?
- What quantity of biomass is required for the treatment of aqueous streams containing radionuclides?
- Is desorption with acidic solutions are proficient for the isolation of thorium from loaded biomass?
- Which eluting agent is the best for the recovery of zirconium by desorption?
- Which of the Taguchi and RSM design approaches gave best the results in process optimisation?

1.3. Structure of the thesis

Chapter 2: Literature review

This section summarises the biosorption method and the theories involved in the concept. Also, it describes the ability of various biomasses in the removal of thorium and zirconium from aqueous and industrial streams. The application of DOE concept in the optimisation of biosorption process is also discussed.

Chapter 3: Materials and methodology

This chapter summarises the experimental procedures followed in the pre-treatment of biomass, biosorption and desorption studies. The techniques adapted for the characterisation of deoiled Karanja biomass and the principles of Taguchi and RSM in DOE are discussed.

Chapter 4: Thorium biosorption and optimisation studies using Taguchi and desirability approach

This chapter discusses the adsorption characteristics of deoiled Karanja biomass which has been employed as a sorbent in the biosorption studies for the removal of thorium metal ions from aqueous solutions. It discusses the effects of process variables and explains the optimisation of parameters used to achieve the maximum biosorption capacity and bio-efficiency using Taguchi robust design, L_{16} (4^3) orthogonal array and desirability approach in multi-variate optimisation for the simultaneous maximisation of responses.

Chapter 5: Zirconium biosorption and optimisation studies using Box-Behnken method in RSM and desirability approach

The chapter discusses the separation of zirconium from aqueous solutions using deoiled Karanja biomass as sorbent. It also discusses the effects of process variables. It explains the optimisation of parameters for achieving the maximum biosorption capacity and bio-efficiency using the Box-Behnken method with 3^3design in response surface methodology (RSM). It discusses how the same responses are maximised employing a desirability approach in multivariate optimisation.

Chapter 6: Desorption and optimisation studies for the recovery of radionuclides (Th and Zr) from loaded-sorbent using Taguchi mixed level design

This section describes the mechanism underlying the desorption of Th and Zr from loaded biomass. It discusses the influence of the process parameters in achieving the maximum desorption. It also presents the Taguchi mixed level design L_{18} ($2^1 3^2$)that was used in the optimisation of the process variables for maximum recovery efficiency.

Chapter 7: Characterisation of deoiled Karanja biomass, a novel sorbent for radionuclides

The chapter describes the characterisation of Karanja biomass which was employed in the current research as biosorbent. It discusses the results of characterisation techniques such as SEM, FTIR and standard NREL methods which help to investigate the possible mechanisms of the biosorption and desorption of Th(IV) and Zr(IV).

Chapter 8: Conclusions and recommendations

This chapter summarises the major findings of the present research and recommends possible future studies in this area.

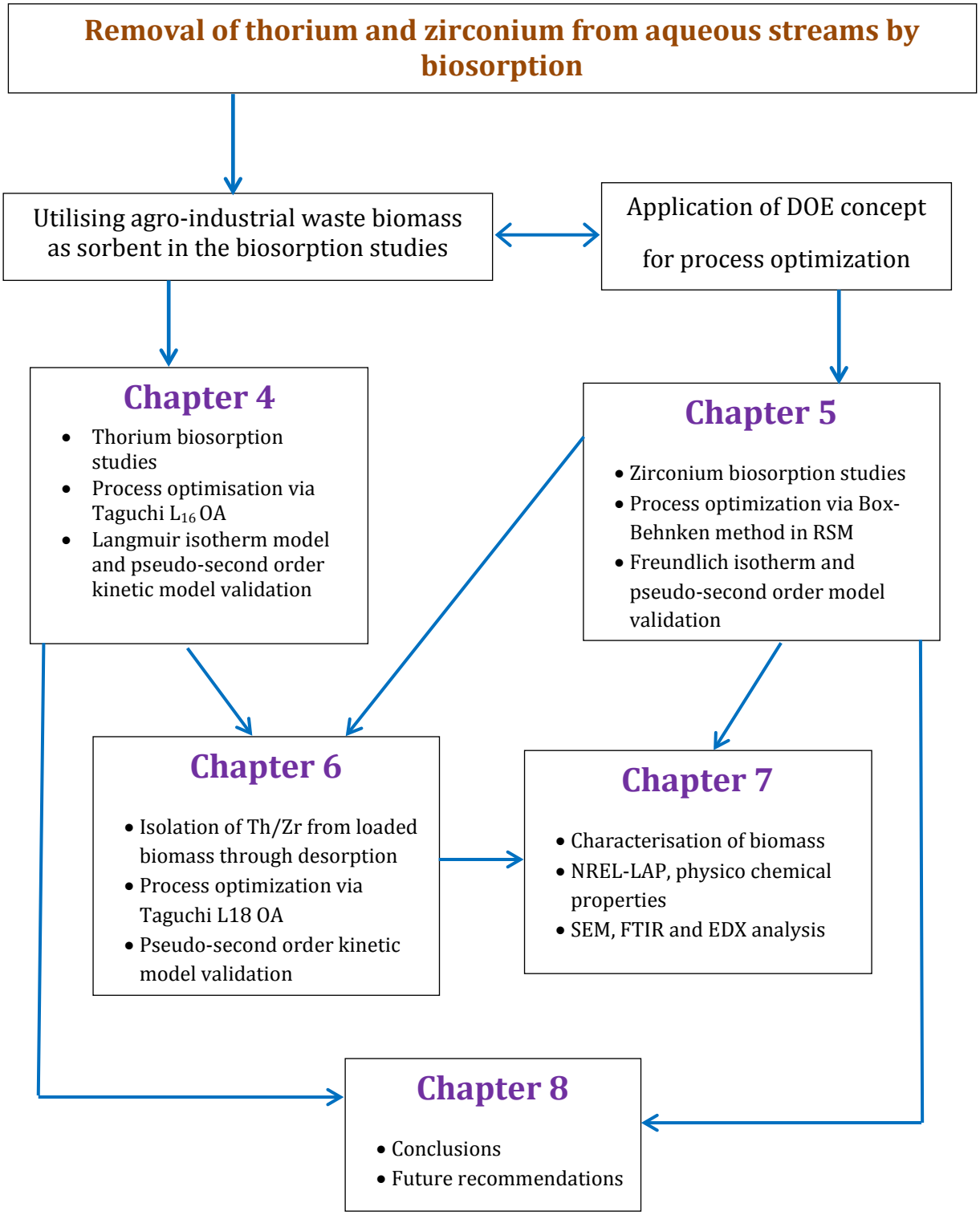
Removal of thorium and zirconium from aqueous streams by biosorption
Utilising agro-industrial waste biomass as sorbent in the biosorption studies
Application of DOE concept for process optimization
Chapter 4
Thorium biosorption studies
Process optimisation via Taguchi L_{16} OA
Langmuir isotherm model and pseudo-second order kinetic model validation
Chapter 5
Zirconium biosorption studies
Process optimization via Box-Behnken method in RSM
Freundlich isotherm and pseudo-second order model validation
Chapter 6
Isolation of Th/Zr from loaded biomass through desorption
Process optimization via Taguchi L18 OA
Pseudo-second order kinetic model validation
Chapter 7
Characterisation of biomass
NREL-LAP, physico chemical properties
SEM, FTIR and EDX analysis
Chapter 8
Conclusions
Future recommendations

Chapter 2
Literature Review

Thorium and zirconium are toxic and shows adverse effects. Thus, industries that use these materials are advised to treat their radioactive wastes systematically so that the extent of active sites can be minimised. Treatment methods for the removal of most radioactive wastes include physical, chemical and biological technologies. A summary of conventional methods that are used in the treatment of industrial streams containing radioactive wastes is given in Table 2.1 with their merits and demerits.

2.1. Biosorption and desorption techniques

Biosorption has been universally accepted as one of the most efficient pollutant removal processes with several advantages especially for industrial discharges with low pollutant concentration (Table 2.1). Biosorption is based on utilising the ability of biological materials including microorganisms (living or dead organisms), agricultural and vegetable wastes as sorbents to remove the metal ions/ pollutants from liquid wastes. It is the adsorption characteristics of biomasses that enable the binding and concentrating of the metal ions from dilute aqueous solutions (Gok and Aytas, 2013).

A general mechanism involved in the removal of pollutants in a typical biosorption method is shown in Figure 1.1. The biosorption process includes a solid phase (sorbent or biosorbent; biological material) and a liquid phase (solvent, generally water) containing the dissolved species to be sorbed (sorbate, metal ions). The solid-liquid mixture is agitated at controlled conditions until equilibrium is established between the solid-bound sorbate species and its portion remaining in the solution.

Table 2.1: Merits and demerits of treatment methods employed for treating radioactive wastes (Wang et al., 2009).

Technology	Merits	Demerits
Ion exchange	• Commercially available • Effective on co-occurring contaminants • Well-understood, well-accepted by metal industry	• Resin regeneration and replacement is costly • Not efficient on all metals • Produces metal-laden waste brine • Overall, high initial, capital, and operational/maintenance costs • Cannot be used for large scale • Ineffective for low concentrated wastes
Reverse osmosis	• Effective removal method • Accepted benchmark technology	• Capital intensive • Low throughput • Produces metal-laden waste • Membranes are expensive • Quickly foul up • Elevated pressure • Sensitivity to suspended solids and organics
Chemical Precipitation	• Effective • Low capital cost • Simple operation • Non-metal selective	• Inadequate • Requires tight operational controls • Post-treatment needs are required • Secondary sludge generation • Ineffective for 1-100 mg/L
Biosorption	• Inexpensive • Metal selectivity • Smooth operation • High efficiency • High versatility • Tolerance to contaminants • results in small volumes of high-concentration wash solutions suitable for subsequent metal recovery • Free of secondary pollution	• Not very well understood • Difficulty in developing generic technologies
Membrane filtration	• Less production of solid waste • Low chemical consumption	• High initial capital and maintenance costs • Low flow rates • Cannot be used for large scale • Ineffective for low concentrated wastes
Electrochemical treatment	• Metal selective • Potential treat effluent > 2000 mg/L	• High initial capital cost, • Ineffective for 1-100 mg/L

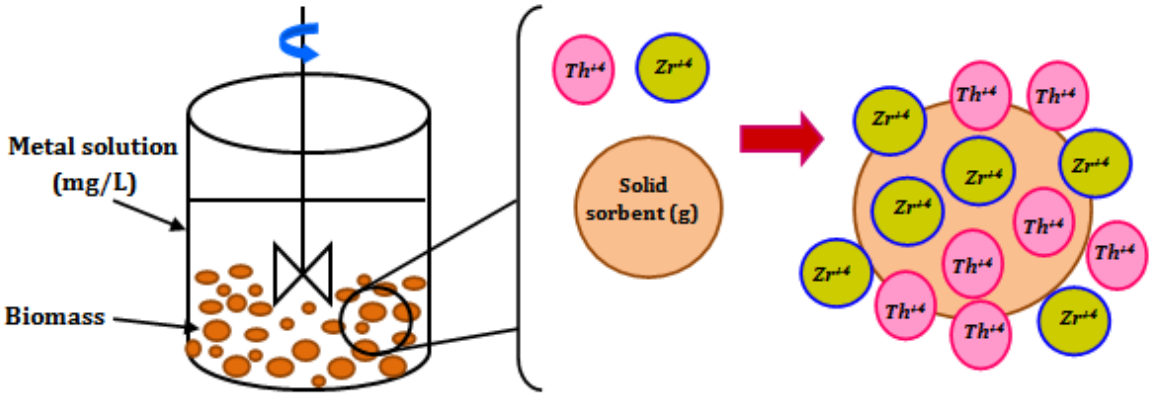

Figure 2.1: General mechanism of biosorption process

Due to higher affinity between the sorbent and sorbate species, the latter is attracted and bound to the sorbent surface by one or more possible combinations of mechanisms such as ion exchange, complexation, coordination, adsorption, electrostatic interaction, chelation and micro precipitation either by physical bonding via London-Vander Waals forces or electrostatic attraction, or by chemical bonding such as ionic or covalent bonding.The underlying mechanism in biosorption is yet to be understood especially if the biomass is a derived material. The degree of sorbent affinity towards the sorbate determines its distribution between the solid and liquid phases. Studies have shown that the biosorption mechanisms depend on the type of functional groups on the surface of the biomass, the nature of the metal, and the characteristics of the matrix around the sorbent species (Boveiri Monji et al., 2008).

Biosorption has gained most recognition for sequestration of radionuclide metal ions (Th and Zr) from aqueous effluent streams due to its excellent separation characteristics. Till date, numerous authors have investigated the ability of various kinds of biomass in the separation of thorium and zirconium from aqueous streams (Table 2.2). Most of the research used synthetic thorium and zirconium metal ions in aqueous media (prepared from their respective nitrate/chloride salts) as feed to

determine the metal uptake capacity of various biosorbents. Only a few have used real waste samples such as sea water containing 100 mg/L of Th in 1L of sea water (Anirudhan et al., 2010) and a Th-rich monazite mineral (river sand type) (Boveiri Monji et al., 2014). Their findings have demonstrated that biosorbents are not effective in the removal process probably due to the interference from other cations, for the sorption sites on biosorbents. The results of thorium biosorption studies showed that the process is mainly influenced by the initial pH of the feed solution and the biosorption efficiency is the highest in the pH range of 4 to 6 (Sayanasree et al., 2016). Zolfonoun et al. (2010) demonstrated the adsorptive characteristics of rice bran for the removal of zirconium ions from leach liquor containing zircon concentrate. They reported that the efficiencies of adsorption of other allied metal ions such as Ti (IV), La (III), Ce (III), Al (III) and Fe (III) were considerably lower than that of Zr (IV) adsorption. They therefore concluded that rice bran is an excellent sorbent for the selective uptake of zirconium from acidic aqueous solutions.

The method of using biosorption from aqueous effluent streams can be applied to a low-cost water pollution control process for the efficient recovery of bound metal ions from industrial discharge and the subsequent regeneration of biosorbent(Kuyucak and Volesky, 1989, ALDOR et al., 1995). Desorption of the metal ions from the loaded biosorbent is accomplished using an elution process that involves the use of an appropriate eluting/desorbing medium to elute metals from the loaded biosorbent. This results in a small, concentrated volume of metal in the eluting solution after the desorption (Njikam and Schiewer, 2012, Vı´tor J.P. Vilar, 2007). Desorption process is metal-selective, economically viable, and ensures the recovery of bulk metals which can be reused in process applications. It also simplifies the disposal and discarding

problems due to the effective reuse of biomass in multiple cycles (Diniz and Volesky, 2006).

Table 2.2: Literature on sorption of Th and Zr using biomass as sorbent.

Radionuclide	Type of sorbent		q_e	R%	Reference
Th(IV)	Microporous Composite P(HEMA-EP)		0.44	--	(Akkaya and Akkaya, 2013)
	Poly(methacrylic acid)-grafted chitosan/bentonite composite matrix		110.5	--	(Akkaya and Akkaya, 2013, Anirudhan et al., 2010)
	S. Sporoverrucosus. Dwc-3		--	>90%	(Ding et al., 2014)
	Fusarium sp. #ZZF51 (living biomass)		--	79.5%	(Yang et al., 2015)
	Rhizopusarrhizus		180	--	MariosTsezos and BohumilVolesky, 1981
	Alginate biopolymers		--	94%	(Gok and Aytas, 2013)
	Rice bran	49.3	>90		(Boveiri Monji et al., 2014)
	Wheat bran	39.7	>70		
	Activated carbon (olive stones)		87	--	(Kütahyalı and Eral, 2010)
	Aspergillusfumigatus		71.94	--	Kuber C. Bhainsa et al., 2009
	Bacillus sp. Dwc-2		10.75	--	Lan etal., 2015
	Bone Meal – 15435		11.5	--	Eduardo et al., 2015
	Actinomycetes		--	--	Akira et al., 2002
	Hyacinth roots		--	--	Ashraf Aly, 2014
Zr(IV)	Microalgae		---	---	(Garnham et al., 1993)
	Cyanobacteria		--	--	
	Candida tropicals		179	--	(Akhtar et al., 2008)
	Aspergillusniger (living)		78.8	--	Kalantari et al.,2014
	Aspergillusniger (dried)		142	--	
	Coriolus versicolor		24.35	--	(Bhatti and Amin, 2013)
	Rice bran		50	--	(Zolfonoun et al., 2010)
	Rice Bran		48.30	99.3	(Boveiri Monji et al., 2008)
	Wheat Bran		34.72	98.5	
	*Platanus orientalis*tree leaves		29.49	92	
	Sugar cane bagasse		107	--	Abida Kausar et al., 2016
			111	--	
			71.5	--	

The mechanisms of desorption and biosorption are similar with both involving ion exchange, i.e., a substitution reaction between anions and cations over the active sorption sites. If the sorption comprises physical bonding, the loosely bound sorbate can

easily be desorbed using distilled water. However, if chemical bonding is present in the sorption mechanism, then the sorbed metal ions can be recovered using proton exchangers or chelating agents. This is especially the case when diverse functional groups such as hydroxyl, carbonyl, carboxyl, amine, amide, and phosphonate groups participate in the adsorption process. The adsorption mechanism with these groups is not restricted to physical bonding (Jnr, 2006).

Although the biomass can be reused after desorption, proper care needs to be taken as the biomass may deteriorate when it is exposed to strong reagents during the recovery process. Hence, the nature and strength of the desorbing medium need to be considered to ensure the reusability of the biomass and minimization of any physico chemical damage. The research related to isolation of radionuclides (Th and Zr) from loaded biomass is scarce. Very few researchers have studied the desorption process using various eluting agents (Bhalara et al., 2014, Gok and Aytas, 2013, Garnham et al., 1993, Akhtar et al., 2008, Kuber C. Bhainsa, 2009). The above studies on desorption have reported that HNO_3, HCl, $NaHCO_3$, and NaCl solutions exhibit high desorption efficiency in the elution process for the recovery of Th and Zr from loaded biomass.

2.2 Theories involved

2.2.1 Adsorption Isotherm Models: Adsorption equilibria are the most desired evidence for proper design and analysis of adsorption data, and they can be achieved through adsorption isotherms. During biosorption, a rapid equilibrium is established between the amount of metal adsorbed on the sorbent (q_e) and the metal remaining in the solution (C_e). There are many theories/models available relating these parameters to illustrate the biosorption phenomena. Among them, the Langmuir, Freundlich, Temkin, and D-R adsorption isotherms are the classical models that are most frequently

used to describe the relationship between equilibrium concentrations. These are provided in Table 2.3 (equations 2.1 to 2.4) and described below:

***(a) Langmuir adsorption isotherm*:** This model describes the coverage of molecules on the outer surface of the sorbent quantitatively. The model is based on three assumptions; adsorption is limited to mono layer coverage, all surface sites are alike and only can accommodate one adsorbed atom, and the ability of a molecule to be adsorbed on a given site is independent of its neighbouring sites. Based upon these assumptions, Langmuir has derived the model (Langmuir, 1918).

(b) Freundlich adsorption isotherm: This model is commonly used to describe the adsorption characteristics of complex surfaces. It assumes the heterogeneous distribution of energetic, active binding sites over the sorbent as well as the interactions between the adsorbed molecules (sorbate) and sorbent (Freundlich, 1906). In the Freundlich model, the smaller the value of $1/n$ (larger value of n), the greater the expected heterogeneity. A $1/n$ value below 1.0 indicates normal adsorption, whereas a value above 1.0 indicates co-operative adsorption. If n lies between 1 and 10, the sorption process is considered favourable.

(c) Temkin isotherm model: This model assumes that the heat of sorption (as a function of temperature) for all molecules within the coverage of the adsorbent surface decreases linearly rather than logarithmically. The adsorption is characterised by a uniform distribution of bonding energies (up to a maximum bonding energy) and is determined by plotting the quantity sorbed, q_e, against $\ln C_e$. The constants are determined from the slope and intercept (Temkin and Pyzhev, 1940).

(d) D-R isotherm model: The D-R isotherm is used to express the adsorption mechanism onto a heterogeneous surface using a Gaussian energy distribution. If the

mean characteristic energy (obtained from the D-R model) falls within the range of 1 to 16kJ/mol, it signifies the involvement of physical electrostatic forces in the sorption process. One of the unique features of the D-R isotherm model is that it is temperature dependent. The approach is usually applied to distinguish the physical and chemical adsorption of metal ions with its mean free energy, E per molecule of adsorbate (for removing a molecule from its location in the sorption space to the infinity) (Dubinin and Radushkevich, 1947).

2.2.2 Kinetic Models: Kinetics plays a significant role in studying the mechanism involved in the biosorption process and is concerned with the rate-limiting steps that include processes such as mass transport and chemical reaction. Various models are available to analyse the kinetics of sorption process. They are: pseudo-first order, pseudo-second order, intra particle diffusion and Elovich models (equations 2.5 to 2.8) Kinetic models are typically used to select the optimum parameter conditions for full-scale batch metal removal processes through their intrinsic phenomenological rate coefficients. Each of the models is discussed below:

(a) Pseudo-first order model: This kinetic model, proposed by Lagergren (Lagergren, 1898), is widely used for relating the sorption of liquid on solid and is based on solid capacity (Azizian, 2004).

(b) Pseudo-second order model: This model is also based on the sorption capacity of the solid phase, and it assumes that the adsorption mechanism is the rate controlling step. The correlation coefficient of the model indicates the level of correlation between the parameters (Plazinski et al., 2013).

Table 2.3: Biosorption and desorption models.

Equation No.			Nonlinear form	Linear form
	Adsorption isotherm models			
2.1.	***Biosorption***	***Langmuir***	$q_e = \frac{Q_0 K_L C_e}{1 + K_L C_e}$	$\frac{1}{q_e} = \frac{1}{Q_0} + \frac{1}{K_L Q_0 C_e}$
2.2.		***Freundlich***	$q_e = K_f C_e^{1/n}$	$\log q_e = logK_f + \frac{1}{n} logC_e$
2.3.		***Temkin***	$q_e = \frac{RT}{b} \ln(A_T C_e)$	$q_e = \frac{RT}{b_T} ln\, A_T + \frac{RT}{b_T} ln\, C_e$
2.4.		***D-R***	$q_e = q_s exp(-K_{ad}\varepsilon^2)$	$\mathrm{Ln}\, q_e = \ln q_s - K_{ad}\varepsilon^2$ Where $\varepsilon = RT \ln\left[1 + \frac{1}{C_e}\right]$
		Kinetic models		
2.5.		***Pseudo-first order***	$q_t = q_e(1 - e^{-k_1 t})$	$\log(q_e - q_t) = log\, q_e - \frac{k_1}{2.303} t$
2.6.		***Pseudo-second order***	$q_t = \frac{k_2 q_e^2}{1 + k_2 q_e t}$	$\frac{t}{q_t} = \frac{1}{k_2 q_e^2} + \frac{1}{q_e} t$
2.7.		***Intraparticle diffusion***	---	$q_e = k_i t^{0.5} + C$
2.8.		***Elovich***	---	$q_t = \frac{ln\alpha A}{\alpha} + \frac{1}{\alpha} \ln t$
2.9.	***Desorption***	***Pseudo-first order***	$\frac{dq_{t,d}}{dt} = -k_{1d}(q_{t,d} - q_{e,d})$	$\log(q_{t,d} - q_{e,d}) = log(q_{0,d} - q_{ed,m}) - k_{1d} t$
2.10.		***Pseudo-second order***	$\frac{dq_{t,d}}{dt} = -k_{2d}(q_{t,d} - q_{e,d})^2$	$\frac{t}{q_{t,d}} = \frac{-1}{k_{2d} q_{ed,m}^2} + \frac{t}{q_{ed,m}}$

(c) Intra-particle diffusion model: This is a complex mathematical relationship proposed by Weber and Morris (Weber and Morris, 1963) as a function of the geometry of the biosorbent particle. If intra particle diffusion is the rate limiting step, the metal uptake varies proportionally with the half power of the time,$t^{0.5}$ rather than$t$. The intercept of the diffusion plot (q_e versus $t^{0.5}$) gives an idea about the thickness of the boundary layer. The larger the value of the intercept, greater the boundary effect. The

diffusion plot shows multi linearity in the biosorption process and contains three stages as given below,

(i) Diffusion of sorbate through the solution to the external surface of the sorbent.

(ii) Gradual sorption and intra particle diffusion which is the rate limiting step.

(iii) Intra particle diffusion slows down due to an extremely low concentration of metal ion left in the solution and a reduction in the number of active interior sites present on the sorbent. This phenomenon eventually leads to the attainment of equilibrium (Ofomaja, 2010).

2.2.3 Thermodynamic Parameters

Biosorption can be considered as a complex and reversible process at equilibrium. With regards to adsorption processes, its thermodynamics represents the final state of a system. The thermodynamic parameters such as Gibbs free energy, enthalpy and entropy play a vital role in designing separators for industrial biosorption processes. These parameters are calculated at different temperatures. The enthalpy change (ΔH^0), entropy change (ΔS^0), and free energy change (ΔG^0) are estimated using the following equations.

$$\ln K_d = \frac{\Delta S^0}{R} - \frac{\Delta H^0}{RT} \qquad (2.11)$$

$$\Delta G^0 = \Delta H^0 - T\Delta S^0 \qquad (2.12)$$

The values of $\Delta H^0$and ΔS^0aredetermined from the slope and intercept respectively, of the plot of $\ln K_d$ vs. $1/T$. Gibbs free energy is then calculated using Eq. (2.12). The calculated values of the thermodynamic parameters ($\Delta G^0, \Delta H^0$and ΔS^0) are examined to verify spontaneity, feasibility and the nature of the process. The nature of

the biosorption process can be specified by the thermodynamic parameters as tabulated in Table 2.4.

Table 2.4: Ranges of thermodynamic parameters and the nature of the biosorption process.

Range	Nature of Process
ΔG^0<0	feasible and spontaneous
ΔG^0>0	not feasible and non-spontaneous
ΔH^0>0	endothermic
ΔH^0>0	exothermic
ΔS^0>0	increase in randomness

2.2.4. Desorption kinetic models: The kinetic equations proposed by Tseng (2009) to describe the desorption mechanism are shown in Table 2.3 (equations 2.9 and 2.10).

2.3. Conclusions:

Although various biomasses have been described in the literature for the separation of radionuclides from aqueous streams via biosorption, studies using agro-industrial waste based biomasses as sorbents are limited. Furthermore, only a few researchers have attempted the isolation of the radionuclides from loaded biomass and also for the optimisation of process variables.

Thus, in the present research work, application of an agro-industrial byproduct as sorbent for the sequestration of radionuclides (Th and Zr) from aqueous solutions via biosorption and desorption studies and simultaneous optimisation of process variables through DOE techniques have been explored.

Chapter 3

Materials and methodology

Summary

This chapter discusses the materials and equipment used in the present research. It also describes the experimental procedures followed for the biosorption and desorption studies. Furthermore, the DOE techniques adapted for the optimisation of process variables are discussed. The equations involved and the results expressed are also discussed in detail.

3.1. Materials, chemicals, and equipment used in the experimental studies

Deoiled Karanja biomass was acquired from Maruti Agro Chem., Hyderabad, India. The following chemicals were purchased from SD Fine-Chem Limited, India; zirconyl chloride octahydrate ($ZrOCl_2.8H_20$, LR Grade), xylenol orange tetra sodium salt dry powder ($C_{31}H_{28}N_2O_{13}SNa_4$), ethanol (99% assay), glacial acetic acid (EP grade), sodium acetate anhydrous extra pure (98% assay), sodium chloride extra pure (99.5% assay), sodium hydroxide pellets purified (97.0% assay), sodium carbonate (93% assay), sodium bicarbonate (96% assay) and Whatman filter paper no. 40 (ashless). Thorium AAS standard (1000 µg/µl in 5% HNO_3) and zirconium AAS standard (1000 µg/µL Zr in HNO_3: HF) were procured from Inorganic Venture, USA and supplied by Crystal Scientific, India. Thorium nitrate pentahydrate ($Th(NO_3)_4.5H_2O$, reagent grade) and nitric acid (69-71% assay) were obtained from Finar chemicals (India) Private Limited. Hydrochloric acid (35-37% assay) and sulphuric acid (98% assay) were supplied by Molychem, India. All chemicals were used in the experiments as received without any modifications.

A Radleys- RR98072 magnetic stirrer was used for washing the Karanja biomass, and a Jeio Tech model OV-12 vacuum oven was used for drying the Karanja biomass in the pre-treatment method. A high precision Citizen balance with an accuracy of ±0.0001g

was used for weighing. A Sartorious PB-11 pH meter was utilized to measure the pH of the samples and a water bath supplied by Sun Labtek Equipment India Pvt Ltd. was used for boiling the samples. The equilibrium studies were carried out using a shaking incubator (Model No.-LSI4018R) provided by Daihan Labtech India Pvt Ltd., capable of maintaining the temperature within $\pm 0.1^0$C. A Lab Companion RW-2025GA refrigerated and heating bath circulator was usedfor maintaining a constant temperature of the experimental apparatus, and a Heidolph (RZR 2021 model) overhead motor and PTFE anchor type impeller (75mm dia) was used for the kinetic and thermodynamic studies. A vacuum pump procured from Heidolph Instruments GmbH & Co., Germany, was used for the vacuum filtration of the loaded biosorbent in the desorption studies.

3.2. Pre-treatment and characterisation of DKSC, a new biosorbent

3.2.1. Physical treatment of Karanja biomass

The purchased biomass was washed with distilled water multiple times at ambient conditions to remove dirt, metallic and soluble impurities. The washed biomass was then sun dried for 2-3 days to remove excess moisture. The sun dried biomass was then grounded using a mortar and pestle and sieved using Taylor series screens. The average size of the sieved particles used in the experiments was <325μm. The sieved biomass was further oven dried at 150°C to remove any residual moisture content and then stored in a sealed polythene bag to prevent moisture absorption from the environment. The resulting biomass, designated as DKSC, was used as the sorbent in all experiments. The steps involved in the pre-treatment of DKSC biomass are shown in Fig. 3.1.

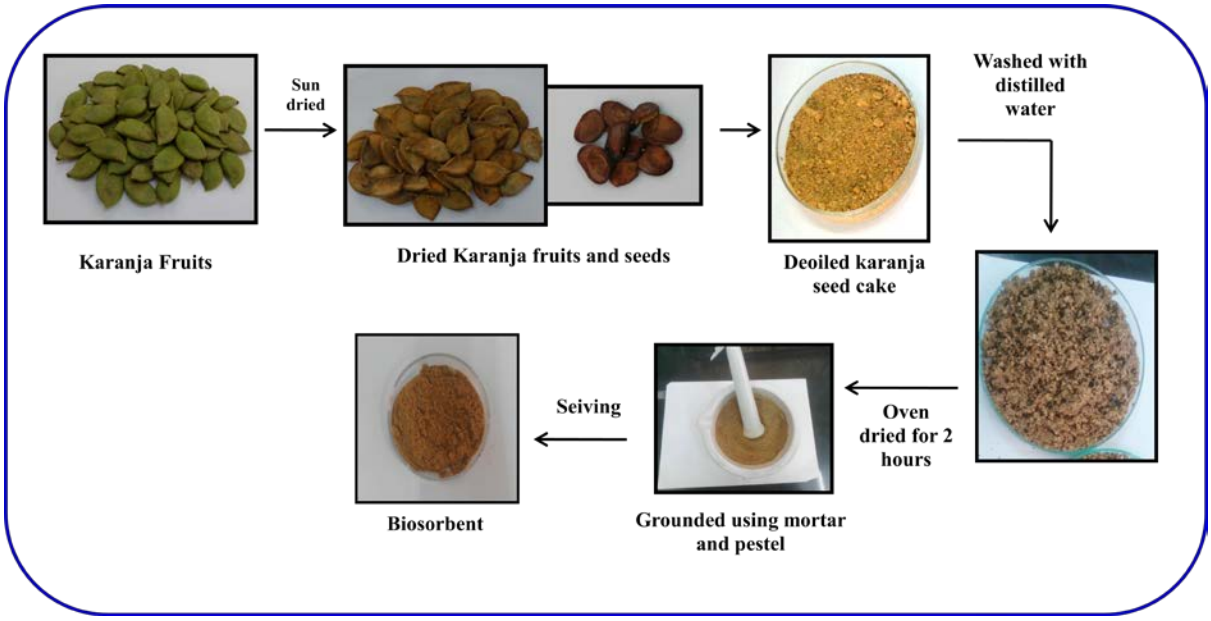

Figure 3.1: Procedure for the preparation of biosorbent.

3.2.2. Characterisation of pre-treated biomass

The DKSC was characterised by standard NREL-LAP (National renewable energy laboratory – laboratory analytical procedure) methods for estimating its physicochemical properties, ultimate analysis (CHNX), Fourier transform infrared spectroscopy (FTIR) for determining its surface functional groups and Scanning Electron Microscopy (SEM) for determining its surface morphology at different stages in the removal and recovery of radionuclides.

(a) Physico-chemical properties: The physicochemical properties of DKSC namely pH, moisture content, bulk density, surface area were determined by adapting NREL standard LAP's for biomass (Radha kumari, 2014) and are discussed below.

- *pH:* To determine the pH of the sorbent, 1g of DKSC was placed into a 250 ml Erlenmeyer flask, and 100 ml of distilled water was added. The mixture was boiled for 5 minutes. The solution was then diluted to 200 ml using distilled water and allowed to

cool to room temperature. The pH of this solution was measured, and the readings were noted.

- *Moisture content:* 5g of DKSC was weighed into a Petri dish and oven dried for 5hours at 105^{o}C. The sample was then removed from the oven and placed in a desiccator immediately to avert any moisture uptake from the atmosphere. This procedure was repeated several times until a constant weight of the sorbent was achieved. The moisture content of the sorbent at each trial was determined using the equation,

$$\%\ Moisture\ content = \frac{w2-w3}{w2-w1}\ X\ 100 \qquad (3.1)$$

where w_1 is the weight of Petri dish, w_2 is the weight of Petri dish plus sorbent before drying, and w_3 is the weight of Petri dish plus sorbent after drying.

- *Bulk Density:* An empty 10 ml measuring cylinder was dried and weighed initially. The measuring cylinder was then filled with DKSC up to the top and weighed again. The difference in the weights of cylinder +DKSC and empty cylinder provided the weight of DKSC. The bulk density of DKSC was determined using the equation

$$\text{Bulk Density} = \frac{w2-w1}{v} \qquad (3.2)$$

where w_1 is the weight of the empty measuring cylinder, $w_2$is the weight of the cylinder plus sorbent and v is the volume of the measuring cylinder.

- *Specific surface area:* Sears' method (Jr, 1956) was used for the determination of the surface area of DKSC. Half a gram of DKSC sample was placed in an Erlenmeyer flask and acidified using 0.1M HCl solution until the pH was 3-3.5. Fifty ml of distilled water and 10g of NaCl were added to the sample. The entire mixture was titrated with

standard 0.1M NaOH solution until pH increased to 4, and then to pH 9.0. The volume of NaOH required to raise the pH from 4.0 to 9.0 was determined as V. The specific surface area (S)was estimated from the equation,

$$S\ (m^2/g) = 32V\text{-}25 \qquad (3.3)$$

- pH_{pzc}*:* The pH_{pzc} of DKSC was evaluated by following the method described by (Zolgharnein et al., 2013). Fifty ml of 0.01M KNO_3 solution was placed in a Erlenmeyerflask, and 0.1g of DKSC was added to it after adjusting the pH of the solution to the desired value in the range of 2-11 using 0.1M HCl/NaOH solution. The mixture was mildly agitated for 48h at the ambient condition to make sure equilibrium was reached. The final pH of the solution was noted as pH_f. The difference (ΔpH) between the initial and final pH values was calculated and plotted against initial pH (pH_i). The x-intercept of the linear curve is designated as point zero charge (pH_{pzc}).

(b) Elemental Analysis (CHNX):

Elemental analysis to determine the mass percentages of carbon, hydrogen, nitrogen, hetero atoms (halogens, X) and oxygen of a sample based on the principle of 'Dumans Method,' which comprises the complete and instantaneous oxidation of the sample by 'flash combustion.' This analysis gives information that helps in determining the structure and purity of unknown /synthesized compounds.

Fig. 3.2 depicts the working principle and the major components of a typical CHNX analyzer that includes units such as a sampler, a combustion/ignition chamber, a packed column, a chromatographic column, and thermal conductivity detector (TCD). The samples were freeze-dried, crushed, weighed and mixed with an oxidiser in a tin capsule and the resulting mixture was combusted in an ignition chamber at 1000˚C. Tin

promotes the violent reaction (flash combustion) in a temporarily enriched oxygen atmosphere. The combustion products were carried by a constant flow of carrier gas and were passed through a glass packed column and then eluted into the chromatographic column. A TCD detector was used to detect and measure the concentrations of combustion product gases NO_2, CO_2, SO_2, and H_2O. The output signals, which are proportional to the concentration of the individual components of the mixture, were recorded. The chromatographic responses were calibrated against pre-analysed standards and the CHNX elemental compositions were reported in weight percentages.

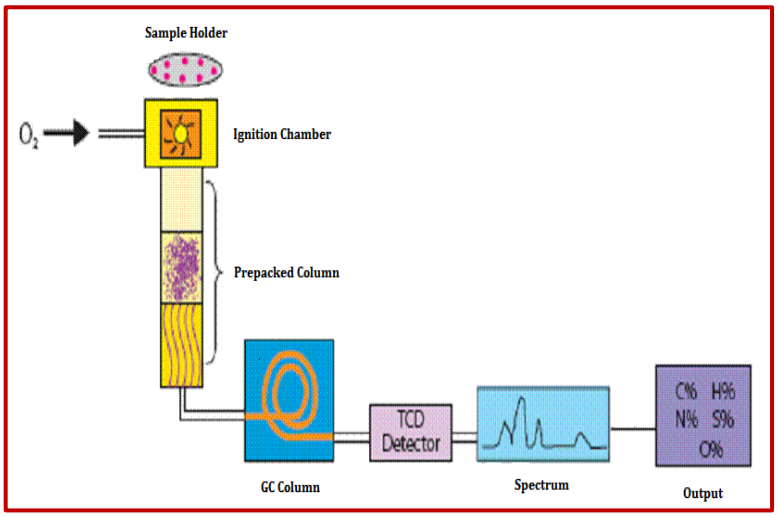

Figure 3.2: Major components of a CHNX analyzer.

An Elementrovario MICRO cube model (made in Germany) CHNX analyser was used for the determination of CHNX compositions in Karanja biomass (deoiled) according to the procedure described above.

(c) FTIR Spectroscopic analysis

FTIR is a quantitative and qualitative analytical technique operating based on the principle that most molecules absorb light in the infrared region of the electromagnetic

spectrum, which can be used to distinguish different organic and inorganic molecules based on their peculiar absorption profile in the fingerprint region. This technique is effective in identifying functional groups, side chains and cross-links involved in different compounds and for characterising covalent bonding information.

The FTIR spectrum of DKSC was obtained following the KBr disk technique. The biomass was ground into a fine powder and mixed with KBr (spectroscopic grade) in the proportion 1 to 2% (w/w). The disk was pressed in a hydraulic press and used in the measurement. The transmittance of the FTIR spectrum was observed over the range 400-4000 cm^{-1} using a Perkin Elmer Spectrum 100 FTIR spectrometer.

(d) SEM analysis:

SEM analysis reveals information about the external morphology (texture), chemical composition (in conjunction with EDS), crystalline structure and orientation of materials making up the sample. The technique is used to produce high-resolution images and show spatial variations in chemical composition.

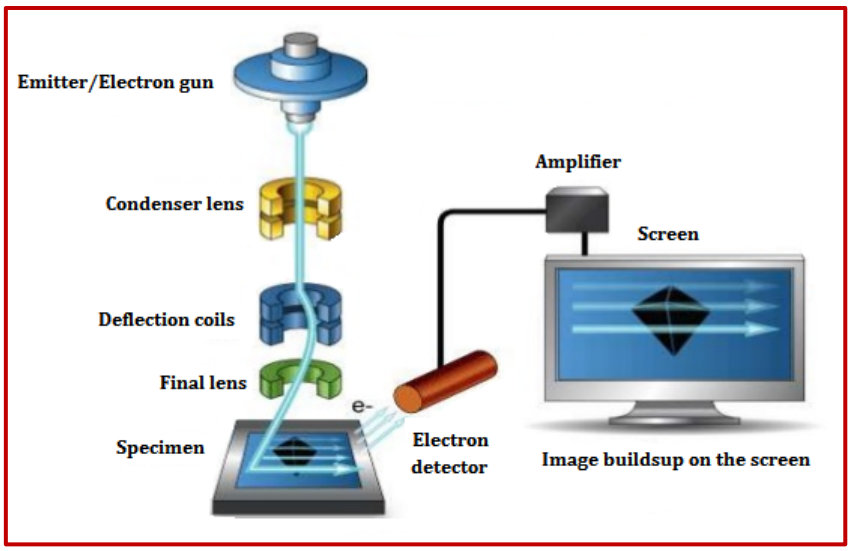

Figure 3.3: Schematic diagram of a typical SEM instrument.

The principle of SEM involves the scanning the surface of the sample using a focused beam of electrons that interact with atoms at various depths within the sample, further generating signals such as secondary and back-scattered electron which convey information about the topography and composition of the sample surface. Fig. 3.3 displays the essential components of SEM including electron source (gun), a condenser lens, deflection coils, final lens aperture and a secondary electron detector. An electron beam emitted from the electron gun is focused by the condenser lens. It passes through a pair of deflector plates in the electron column to the final lens, which deflects the beam. When the electron beam interacts with the sample, the electrons lose energy by repeated random scattering. The absorption of the beam current takes place within the interaction volume of the sample which is detected by specialised detectors (e.g., secondary electron and back-scattered electron detectors plus energy dispersive x-ray detectors to measure composition). An electronic amplifier amplifies the signals generated by the detectors, which are used to create images of the distribution of specimen current. The images are displayed as variations in brightness on a computer monitor or as intensity versus energy spectrum showing characteristic x-rays.

A Hitachi S-3000N scanning electron microscope was employed for characterising the surface morphology of the pre-treated Karanja biomass and metal-loaded biomass. The sample preparation method was as follows. The biomass samples were initially degreased, washed with solvents and dried thoroughly. The powder sample was then compressed into small disks and mounted on carbon tape on a specimen stub. The sample holder was turned upside down before analysis to ensure the removal of loosely bound materials.

3.3. Preparation of thorium and zirconium stock solutions

A thorium stock solution of 1000 mg/L was prepared by dissolving exactly 2.4571 g of $Th(NO_3)_4.5H_2O$in demineralized water and acidified with 1ml of concentrated $HNO_3$to prevent hydrolysis. The stock solution was prepared and stored in an airtight polypropylene container.

A zirconium stock solution of 1000 mg/L was prepared by dissolving exactly 3.53g of $ZrOCl_2.8H_2O$ in 1000ml of 0.1M hydrochloric acid. The stock solution was prepared and stored in an airtight polypropylene container. The glassware used in experiments were immersed in 10% (v/v) HNO_3solution overnight and rinsed several times with demineralised water before used in experiments.

3.4. Quantification of thorium and zirconium by UV/Vis spectrophotometry

3.4.1. Working principle of UV/Vis spectrophotometry

Spectrophotometry is a technique that uses the absorbance of light by a substance at a certain wavelength to determine the analyte concentration. UV/VIS uses light in the ultra violet and visible spectral region. This technique is based on Beer-Lambert law which states that the absorbance of the sample at a given wavelength is proportional to the absorptivity of the substance (constant at each wavelength), the path length (the distance the light travels through the sample) and the concentration of the absorbing substance. It is expressed in the form the following equation:

$$A = a\ X\ b\ X\ c \qquad (3.4)$$

where A is the absorbance of the sample, a is the absorptivity of the substance, b is the path length, and c is the concentration of the substance.

The minimum elements required in a UV/Vis instrument are the following (Fig. 3.4); light source, usually a tungsten lamp for the visible region of the spectrum or a deuterium lamp (D_2) for ultraviolet wavelengths, a monochromator to produce a beam of single radiation selected from a wide range of wavelengths via filters, and cuvettes quartz or silica cells for holding the analyte to be measured and also to introduce the samples into the light path, and detectors.

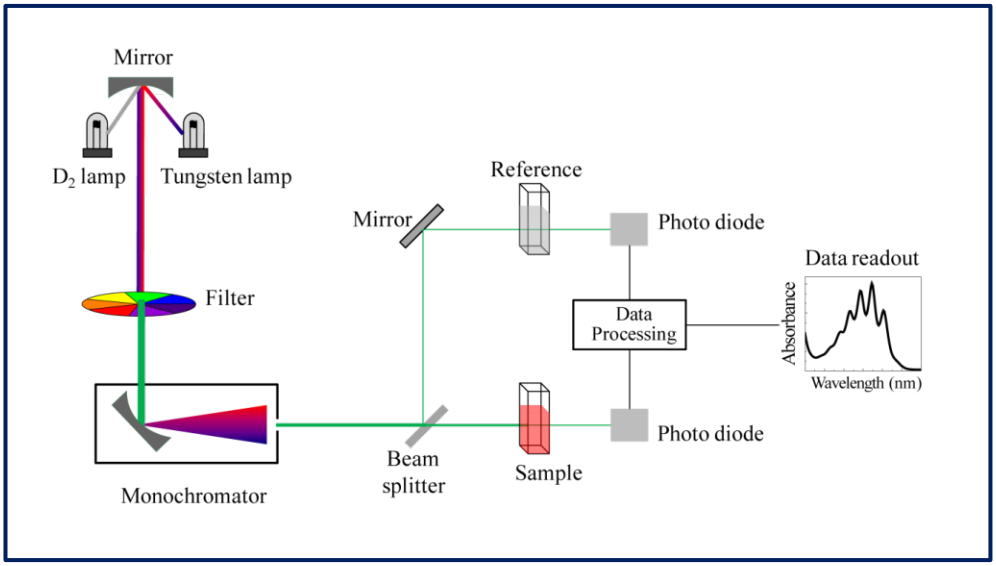

Figure 3.4: Schematic diagram showing the principles of UV-Vis spectrophotometry.

3.4.2. Quantification of Thorium:

A spectrophotometric technique was carried out to estimate the total Th^{+4} metal ion concentration in the sample aliquots. The analytical methodology is based on the complex formation of thorium with xylenol orange developed by Mukherji (1966).

Calibration curve: A standard calibration curve was generated using the Thorium AAS standard, which was diluted with demineralised water to obtain the desired thorium concentrations in the range 2-15mg/L. The standards were then buffered with 10ml of acetate buffer to maintain a constant pH. Five ml of xylenol orange reagent solution was added to the thorium solution and allowed to stabilise for approximately 3 hours. The absorbances of these standards were measured using the UV-Vis spectrophotometer at 575nm using 1cm cell quartz cuvettes calibrated against blank. The calibration plot for thorium is shown in Fig. 3.5 (a). The correlation coefficient obtained for the calibration curve was 0.9989.

The concentrations of thorium present in the samples from the experiments were determined from this standard curve using the absorbance measured using the UV-Vis spectrophotometer.

(a) Xylenol orange solution (10^{-3}M): The reagent solution was prepared by dissolving 0.7606g of xylenol orange tetra sodium salt dry powder in 50% ethanol (v/v). The reagent was always prepared fresh.

(b) Sodium Acetate Buffer Solution: Sodium acetate buffer of pH = 6±0.2 was prepared by mixing an appropriate portion of 0.01M glacial acetic acid with 0.01M sodium acetate solution.

- *0.01M glacial acetic acid:* It was prepared by diluting 0.3mL of glacial acetic acid with 500ml of demineralised water.
- *0.01M sodium acetate:* It was prepared by dissolving 4.1g of sodium acetate anhydrous with 500ml of demineralised water.

3.4.3. Quantification of zirconium:

The concentration of Zr(IV) in the sample aliquots was quantified using a spectrophotometric technique based on the reaction of zirconium with xylenol orange as discussed by (Akkaya and Akkaya, 2013).

Calibration Curve: A standard calibration curve was generated using standard Zr solutions in the concentration range of 0.05-2.5 mg/L. These were prepared by diluting Zirconium AAS standards with demineralised water. The standard sample was mixed with xylenol orange solution reagent in the ratio of 20:2(v/v)and allowed to stand for approximately 30 minutes. Xylenol orange reacts slightly with zirconium to form a complex that has the best absorbance at 535nm (Akthar et al., 2008). Thus, the absorbance was measured at 535nm using 1cm cuvettes calibrated against reagent blank. The calibration curve is shown in Fig. 3.5(b) and the correlation coefficient for the calibration curve was 0.9682. The concentration of Zr(IV) present in the experimental sample was measured using this standard calibration curve. The calibration experiments for Zr were repeated 3 times and the trends in the calibration curves were found to be similar. The percentage variation in the data was found to vary ± 2%.

(a) Xylenol Orange reagent solution (0.05%):The solution was prepared by dissolving the xylenol orange tetra sodium salt dry powder in 0.6N hydrochloric acid. The reagent was always prepared fresh.

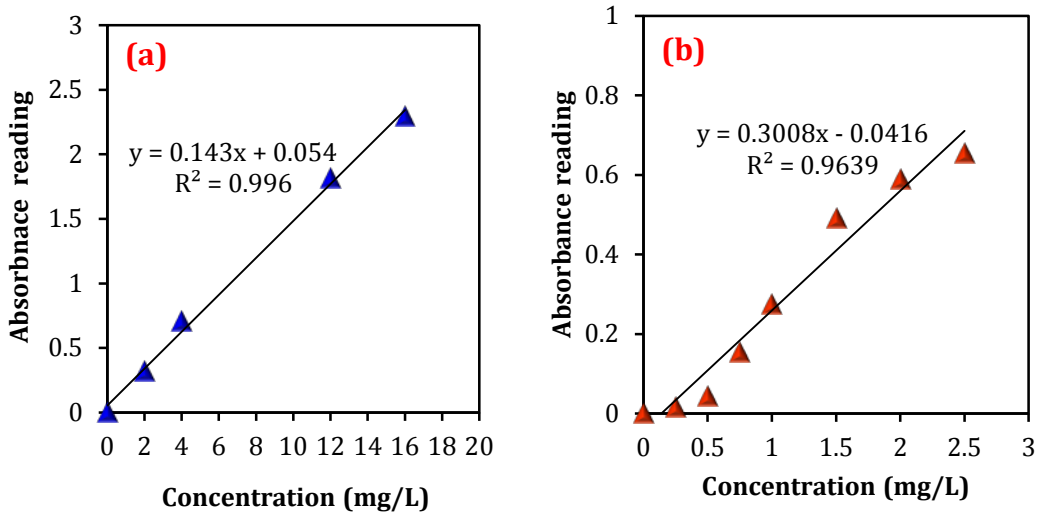

Figure 3.5: Calibration curves for Th(IV) and Zr(IV) quantification using UV-Vis Spectrophotometer; (a) thorium absorbance at 575nm and (b) zirconium absorbance at 535nm.

3.5. Biosorption and desorption experimental procedures

3.5.1. Biosorption experiments for the removal of radionuclides:

All the experiments were conducted in batch mode and the experimental procedures were established from the thorough understanding of the preliminary studies. Equilibrium studies were performed at 25˚C in 250 ml Erlenmeyer flasks using a shaking incubator operating at 200rpm. The predetermined concentrations in metal solutions (mg/L) of required volume were prepared by serial dilution of a metal stock solution with demineralised water. The pH of the metal solutions was achieved by adding the necessary amounts of 0.1M HCl/NaOH solution. The pH of the aqueous solution was measured to ensure a consistent pH value during the entire experimental run. This is because the pH values used in the experiments were chosen according to the experimental design. A known weight of DKSC was added to the metal solution, and the flasks were agitated for a fixed time until equilibrium was attained. The solid-liquid

mixture was separated after equilibrium by filtration using Whatman filter paper. The filtrate was then analysed to determine the metal concentration (Th/Zr) using the spectrophotometric methods discussed above (Section: 3.4).

For all the biosorption experiments, only the initial pH of the metal solution was recorded because there were negligible changes in the pH values of the solution during the experiment as can be seen from the data presented in Fig 3.6.

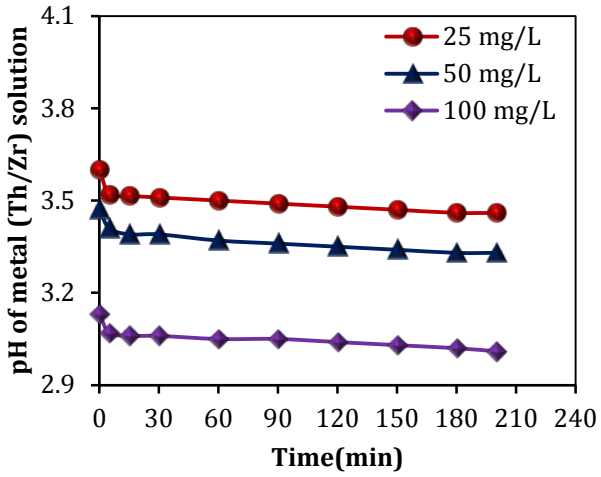

Figure 3.6: Effect of contact time on solution (Th/Zr) pH during biosorption process.

The kinetics and thermodynamic studies were performed in a four-necked 250 ml jacketed reactor equipped with a thermostat for temperature control and overhead motor for stirring. Vigorous stirring was provided to the solid-liquid mixture using a PTFE (ploy tetra flouro ethylene) anchor type impeller to overcome the external mass transfer resistance. The kinetic studies were carried out at 25˚C by varying the initial metal concentration (mg/L) of thorium and zirconium in the feed (working volume 200ml) using a predetermined DKSC loading for 5 hours. Samples were withdrawn from the reactor vessel at regular time intervals and analysed for the metal concentration. The procedure followed for the thermodynamic studies was similar to that used for the kinetic studies except that the temperature was different for thermodynamic studies

(15 to 45˚C). The experimental setup used for the kinetic and thermodynamic studies are shown in Fig. 3.7.

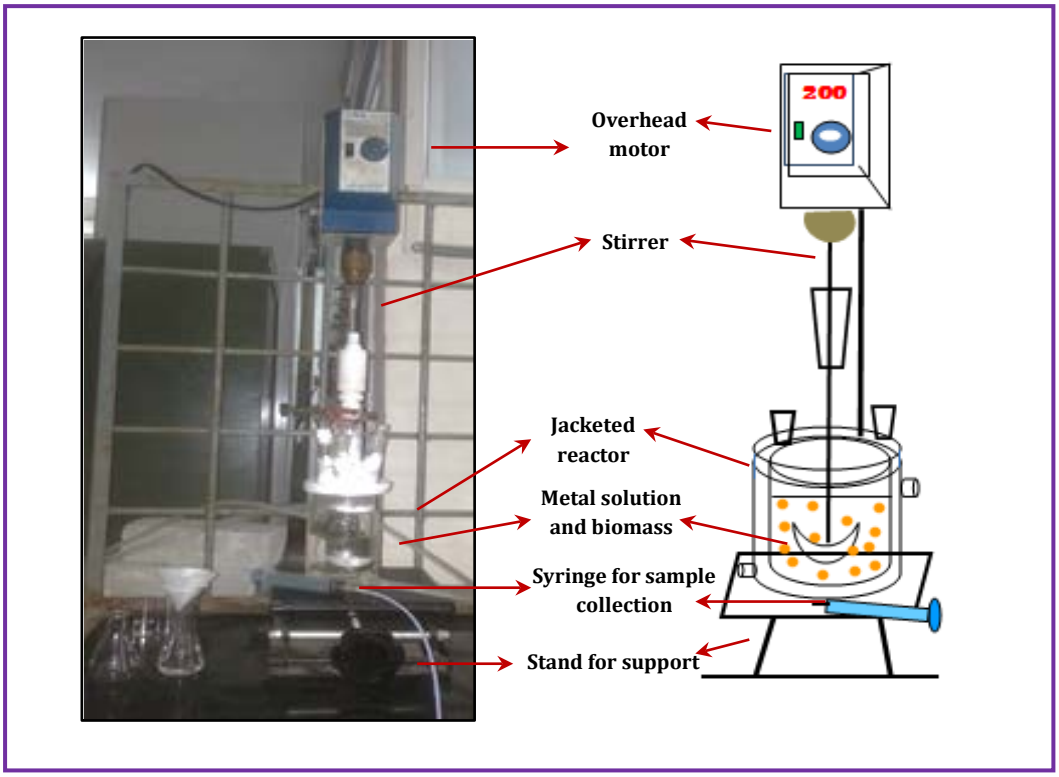

Figure 3.7: Experimental setup used for kinetic and thermodynamic studies in biosorption and desorption studies.

The experimental results were used to determine metal uptake capacity or biosorption capacity (metal ions sorbed per gram of biosorbent) (q_e, mg/g), the bio-removal efficiency ($R, \%$) and the distribution coefficient (K_d, L/g) using the following equations

$$q_e = \frac{(C_i - C_e)V}{m} \qquad (3.5)$$

$$R(\%) = \frac{C_i - C_e}{C_i} \times 100 \qquad (3.6)$$

$$K_d = \frac{C_i - C_e}{C_e} \times \frac{V}{m} \qquad (3.7)$$

where C_i and C_e are the initial and the equilibrium concentrations of the metal solution before and after biosorption in mg/L, V is the working volume of metal solution in L, and m is the mass of DKSC in g.

3.5.2. *Desorption experiments for the recovery of radionuclides from loaded biomass:*

Desorption experiments were performed in batch mode using metal (Th/Zr)-loaded DKSC obtained from the biosorption experiments. The loaded DKSC was vacuum filtered on Whatman filter paper, washed multiples times with distilled water over the filter paper to remove loosely bound metal ions and then air dried overnight and secured in an airtight bag.

The equilibrium studies for desorption was performed in Erlenmeyer flasks. The volumes of eluant and loaded sorbent were chosen to obtain a fixed L/S ratio. The eluant and loaded DKSC mixture was stirred at 25°C in a shaking incubator operating at 200rpm for six hours. The desorbed DKSC was filtered from the eluant using Whatman filter paper, and the eluantwas subjected to spectrophotometric analysis for the quantification of metal ions present in the eluant.

Kinetics and thermodynamic experiments performed for desorption studies were similar to those for biosorption studies. The desorption experimental results were used to determine the desorption capacity, q_{des} (mg/g), and the desorption efficiency, D%, using the following equations:

$$q_{des} = \frac{C_{des}}{m} X\ V \qquad (3.8)$$

$$D\% = \frac{q_{bio} - q_{des}}{q_{bio}} X\ 100 \qquad (3.9)$$

where C_{des} is the concentration of the metal ions in the eluant in mg/L, V is the volume of eluant in L, m is the mass of loaded sorbent in g, and q_{bio} is the biosorption capacity of DKSC in mg/g (obtained from the biosorption studies).

3.6. Design of Experiments (DOE) technique for the process optimisation

In an experimental study involving a number of process parameters, it is important to understand the influence of process parameters and their interaction on process performance to determine an optimum set of parameters that ensure the desired outputs. The classical style of trial and error approach to determine the optimum set of process parameters has drawbacks especially when the number of possible process parameters is high because it fails to elucidate the effects of interaction between the parameters. On the other hand, the design of experiments (DOE) technique helps to determine the minimum number of experiments that consists of a possible parameter combination. DOE also suggests parameter domains where the process offers the most benefit. DOE is a series of runs/tests that involve purposeful changes to input variables and observing the change in responses. The main criteria that need to be considered while picking an appropriate DOE are:(i) it should identify the number of control factors with their respective levels, (ii) it should determine the least possible number of runs that should be performed and (iii) it should minimise the impact of cost, time, and use of chemicals.DOE includes various techniques/methods that can be applied for successful optimisation of the process to attain maximum benefit. They include: (a) Factorial designs, (b) Response Surface designs(c) Mixture designs and (d) Taguchi designs.

In the present research, Taguchi and Response Surface (RSM) designs were adapted to optimise the thorium and zirconium biosorption process parameters.

3.6.1. Taguchi robust design

Dr. Genichi Taguchi, a scientist in Electronic Control Laboratory in Japan, carried out a major research and proposed the theory of robust design in DOE, commonly known as Taguchi method in early 1980's in the USA. The Taguchi approach is a new form of DOE with unique application principles and experimental strategies that can be inexpensive in optimisation. It attempts to improve the performance quality, and it is achieved via reducing variation in a process through the robust design of experiments (Kamaruddin et al., 2010).

Taguchi design contains specially constructed tables called orthogonal arrays (OA), which is a combination of control and noise factors selected by a number of factors (variables) and levels (states). With OA, the design is balanced with all the factors and levels weighing equally. Each factor can be evaluatedindependently, and the effect of one factor does not influence the estimation of another factor. The selection of an appropriate orthogonal array depends on the total degrees of freedom of the parameters involved in the process study (Daneshvar, 2007).

Unlike full factorial combinations, Taguchi tests a certain pair of combinations affecting the process and the levels as the particular parameter space is varied. This allows the collection of the necessary data to determine which factors affect the product quality the most with minimum experimental trials, thus saving time, cost, labour and resources. This method is best suited for an intermediate number of variables (3 to 50), few interactions between variables, and only when a few variables contribute significantly. The experimental data collected is transformed into a signal-to-noise (S/N) ratio which is a measure of response variations and is also a performance parameter to measure the sensitivity of quality characteristic deviating from the

measured values. It is the log transformation of the mean square deviation of the desired response, where the signal (S) is the desirable effect (mean), and the noise (N) is the undesirable effect (signal disturbance). The data from the arrays can be analysed by plotting the data and performing visual analysis, analysis of variance (ANOVA),Fisher's exact test, or Chi-squared test to test significance (Daneshvar et al., 2007). The general steps involved in Taguchi approach are shown in Fig. 3.8.

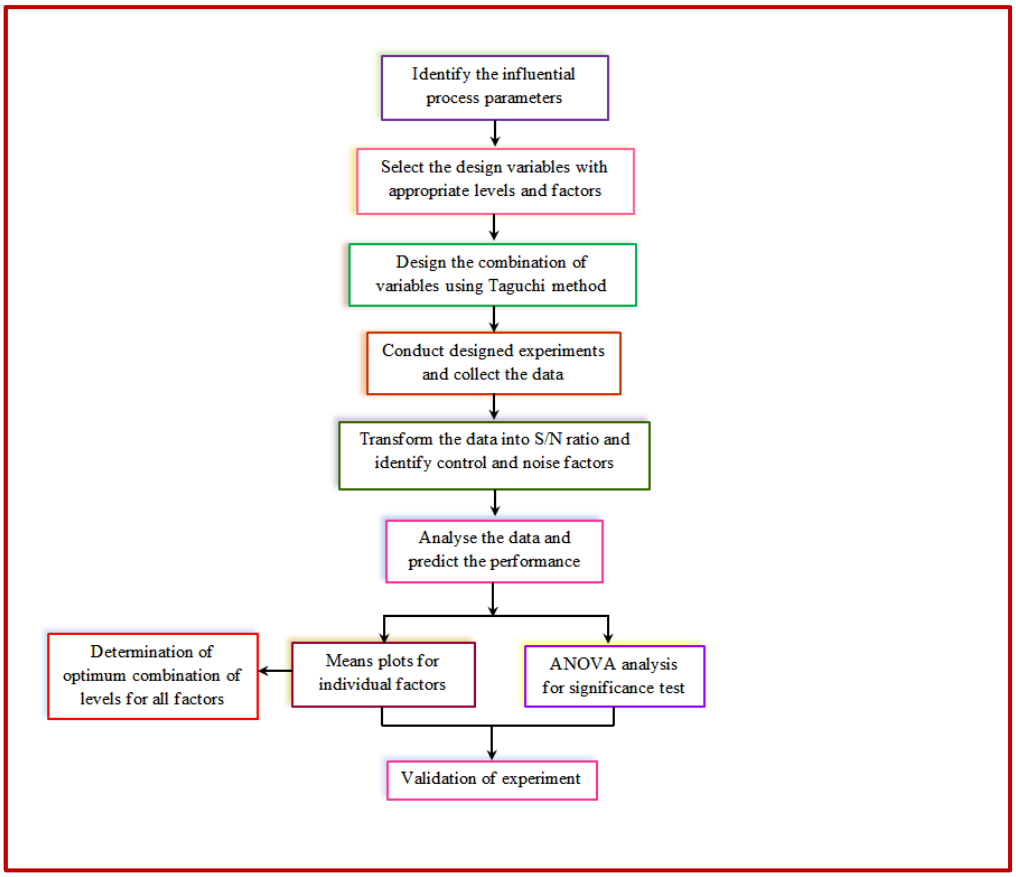

Figure 3.8: Algorithm for Taguchi approach.

Usually, there are three categories of quality characteristic in the analysis of the S/N ratio, i.e lower-the-better, higher-the-better, and nominal-the-better. An appropriate criterion for the S/N ratio must be chosen depending on the goal for the optimisation of the process parameters.

(1) *Lower-is-better*: If the aim is to minimise the performance, the value of the S''/N ratio should be low.

$$\frac{S''}{N_i} = -10\ log_{10}\left[\frac{1}{n_i}\sum_{i=1}^{n} Y_i^2\right] \quad (3.8)$$

(2) *Higher-is-better*: If the goal is to maximise the performance, the value of the S'/N ratio should be high.

$$\frac{S'}{N_i} = -10\ log_{10}\left[\frac{1}{n_i}\sum_{i=1}^{n} \frac{1}{Y_i^2}\right] \quad (3.9)$$

(3) *Nominal-is-better*: If the goal is to achieve a predetermined S/N, then the value of S'''/N need to be a target value.

$$\frac{S'''}{N_i} = -10\ log_{10}\left[\frac{1}{n_i}\sum_{i=1}^{n} \left[\frac{Square\ of\ mean}{variance}\right]_i\right] \quad (3.10)$$

where $Y_i$is the response variable for n observations.

3.6.2. RSM - Box-Bohnken experimental design:

Response Surface Methodology is a proficient statistical tool involving a set of mathematical and a statistical technique used for modeling and analysis of problems and is mainly used by industrial engineers to optimise process parameters as it offers a fewer number of runs at a specific position of design points that can reduce time, cost and resources. It is the most effective and powerful experimental design when considered in comparison to other response surface designs like central composite, Doehlert matrix and 3-level full factorial designs(Sharma et al., 2009, Islam et al., 2009, Douglas and Montgomery)). RSM involves a stepwise procedure for optimising a process via statistical evaluation of the designed experiments, estimation of the coefficients in a mathematical model, and testing the adequacy of the model. The detailed steps involved in this approach are shown in Fig. 3.9.

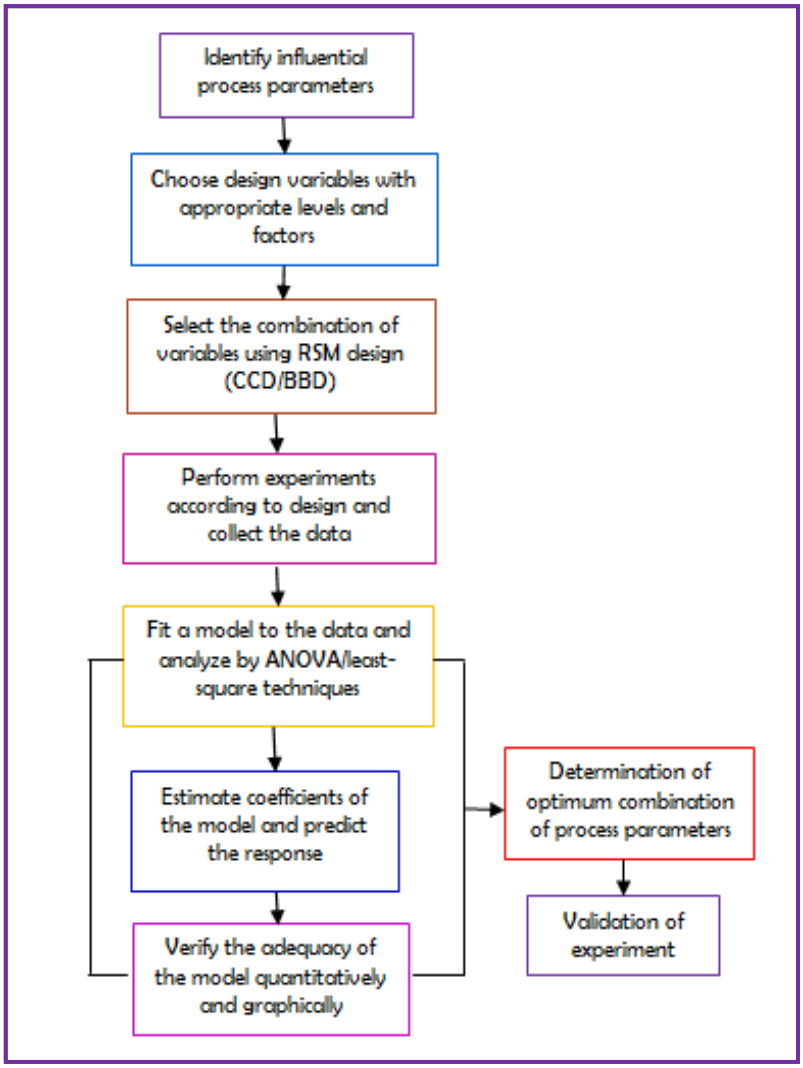

Figure 3.9: Sequential steps required for RSM

The response Y is influenced by many process variables and a relationship between them is established by the RSM technique. Analysis of a response, *Y* which is dependent on process variables X_1, X_2,. ..,X_n, is done using the correlation:

$$Y = f(X_1, X_2, \cdots X_n) \pm \varepsilon \qquad (3.11)$$

where f is the real response function (its format isunknown), and ε is the error which describes the differentiation that can be integrated by the function f.

Box–Behnken is a spherical design consisting of central and middle points at the edges of the cube circumscribed on the sphere. The number of experiments required in this

design can be decided according to equation 3.12 (Mourabet et al., 2012, Aravind Kumar, 2008)).

$$N = 2k(k-1) + c_p \quad (3.12)$$

where k is the independent factor and c_p is the replicate number of the central point. In a process involving three independent variables (X_1, X_2, X_3), the relationship between response (Y) and the variables can be approximated by a quadratic second order polynomial;

$$Y = \beta_0 + \beta_1X_1 + \beta_2X_2 + \beta_3X_3 + \beta_{12}X_1X_2 + \beta_{13}X_1X_3 + \beta_{23}X_2X_3 + \beta_{11}X_{21} + \beta_{22}X_{22} + \beta_{33}X_{23} \quad (3.13)$$

where Y is the predicted response, β_0 is the model coefficient at the centre point, β_1, β_2, β_3 are the linear coefficients, β_{12}, β_{13} and β_{23} are the cross-product coefficients, β_{11}, β_{22} and β_{33} are the quadratic coefficients. Multiple regression analysis can be done to obtain the values of coefficients, and the equation can be used to predict the response. The goodness-of-fit of the quadratic model can be determined by the coefficient of determination (R^2) (Akar et al., 2014, G. Annadurai, 1998).

3.6.3. Percentage contributions :

The total percentage contributions (TPC) for all the possible first-order, interaction and quadratic terms were obtained by the method adopted by Yetilmezsoy (2009) using the following equations.

$$TPC_i = \frac{\sum_{i=1}^{n} SS_i}{\sum_{i=1}^{n}\sum_{j=1}^{n} SS_i + SS_{ii} + SS_{ij}} \times 100 \quad (3.14)$$

$$TPC_{ij} = \frac{\sum_{i=1}^{n}\sum_{j=1}^{n} SS_{ij}}{\sum_{i=1}^{n}\sum_{j=1}^{n} SS_i + SS_{ii} + SS_{ij}} \times 100 \quad (3.15)$$

$$TPC_{ii} = \frac{\sum_{i=1}^{n}\sum_{j=1}^{n} SS_{ii}}{\sum_{i=1}^{n}\sum_{j=1}^{n} SS_i + SS_{ii} + SS_{ij}} \times 100 \quad (3.16)$$

where TPC_i, $TPC_{ij}$and TPC_{ii} are the total percentage contributions of the first-order, interaction and quadratic terms, respectively. Similarly, SS_i, SS_{ij}, SS_{ii} are the computed sum of squares for the first-order, interaction and quadratic terms, respectively.

3.6.4. Desirability approach for multi-variate optimisation :

The desirability method is an established technique for the simultaneous determination of the optimum settings of input variables that can determine the optimum performance levels for one or more responses. Depending on whether a particular response Y_i is to be maximised, minimised or assigned a target value, different desirability functions d_i (Y_i) are used (G. Derringer, 1980).

As an example, let L_i, U_i and T_i be the lower, upper and target values, respectively, that are desired for response Y_i, with $L_i \leq Y_i \leq U_i$. If the response is the "target is the best" kind, then its desirability function is given by equation (3.14),

$$d_i = \left(\frac{Y_i - L_i}{T_i - L_i}\right)^p \quad \text{if } L_i \leq Y_i \leq T_i$$

$$d_i = \left(\frac{Y_i - U_i}{T_i - U_i}\right)^q \quad \text{if } L_i \leq Y_i \leq T_i \qquad (3.17)$$

$d_i = 1$ if $Y_i = T_i$

$d_i = 0$ if $Y_i \leq L_i$ or $Y_i = L_i$

where the exponents p and q determine how important it is to hit the target value.

If a response is to be maximised instead, the individual desirability is defined as shown in equation (3.15),

$d_i = 0$ if $Y_i \leq L_i$

$$d_i = \left(\frac{Y_i - L_i}{T_i - L_i}\right)^p \quad \text{if } L_i \leq Y_i \leq T_i \qquad (3.18)$$

$d_i = 1$ if $Y_i \geq T_i$

Finally, if a response is to be minimised, the individual desirability (d_i) is calculated according to equation (3.19),

$d_i = 1$ if $Y_i \leq T_i$

$$d_i = \left(\frac{Y_i - U_i}{T_i - U_i}\right)^q \quad \text{if} \quad T_i \leq Y_i \leq U_i \tag{3.19}$$

$d_i = 0$ if $Y_i \geq U_i$

In a multi-response circumstance, the ideal case is that the all responses' desirability value is equal to 1 and the whole response's desirability value also equals 1. If any response cannot achieve the requirement, the ideal case of the whole response cannot be achieved and is considered as the unacceptable case. Moreover, if the desirability value of any response equals to 0, the whole response will also be considered to be the unacceptable case. To complete the requirement, the whole response's desirability value can take the geometric average of all responses' desirability value, i.e.

$$D = (d_1 \times d_2 \times d_3 \times \ldots\ldots \times d_n)^{1/n} = \left(\prod_{i=1}^{n} d_i\right)^{1/n} \tag{3.20}$$

where d_i represents the desirability value of the i^{th} response, and n represents the number of responses in the measure, i=1, ... n. In other words, D equals 1 when all responses achieve the target, and the D equals 0 when any one response cannot achieve the requirement.

It can be extended to:

$$D = (d_1^{\alpha 1} \, x \, d_2^{\alpha 2} \, x \ldots\ldots x d_n^{1/n})^{1/n}, \tag{3.21}$$

where $0 \leq \alpha_i \leq 1$, (i = 1,2,3,....n), $\alpha_1 + \alpha_2 + \cdots \ldots . + \alpha_n = 1$

where d_i indicates the desirability of the different responses, Y_i (I = 1,2,3,...n) and α_i represent the importance of responses. So, maximum overall desirability function D depends on the α_i (importance) value.

Chapter 4

Thorium biosorption and optimisation studies via Taguchi and desirability approach

Summary

The research presented in this chapter discusses the sequestration of thorium from aqueous solutions by applying the biosorption method as a separation technique. An agro-industrial waste biomass namely deoiled Karanja biomass was employed as the sorbent in the biosorption studies for the removal of thorium metal ions. The effects of process variables including initial metal concentration, pH of the feed solution and DKSC loading were examined. Design parameters were optimised to obtain the maximum biosorption capacity and bio-removal efficiency using a fractional factorial design of experiments and a desirability approach for multivariate optimisation. A Taguchi robust design, L_{16} (4^3) orthogonal array was used for the optimisation of process parameters. Using the optimum parameter combination obtained from the Taguchi method gave a maximum efficiency of 91.97% at an initial Th concentration of 130 mg/L, pH of 5.0 and a DKSC loading of 0.25 g/L.

4.1. Introduction

Thorium is a naturally existing radioactive nuclide with nuclear significance and is an active gamma emitting by-product of nuclear reactor operations. The speciation of Th from the nuclear discharge is a significant concern in nuclear waste management and also for environmental pollution control. The methods employed in dealing with this radionuclide from aqueous and industrial waste streams using different kinds of biomass were discussed in Chapter 2.

4.2. Experimental Investigations

Materials and experimental methodologies employed to carry out the present work were described in Chapter 3 (Materials and Methodology).

4.2.1. Preliminary studies:

The parameters such as contact time, mixing speed, pH, and DKSC loading were investigated in preliminary studies. Variables were tested in a univariate fashion (i.e., varying one parameter at a time while keeping remaining constant) and all experiments were conducted in batch mode.

4.2.2. Taguchi L_{16} (4^3) OA design:

A Taguchi L_{16} orthogonal array (OA) comprising of three factors (initial Th(IV) concentration, initial pH and DKSC loading) with four levels each (Table 4.1) was employed to study the effect of process variables towards biosorption capacity(q_e) and bio-removal efficiency (R%) in the thorium biosorption studies.MINITAB17 Statistical software (free trial) was utilised for the generation of the experimental design matrix with the selected factors at their respective levels. The L_{16}OA suggested 16 runs were requiredin the experimental design for the selected factors with their corresponding levels as presented in Table 4.2 along with the results obtained.

Table 4.1: Factors and levels considered in the Taguchi robust design.

Factors/Levels	***1***	***2***	***3***	***4***
Initial Th concentration (mg/L)	15	40	85	130
Initial pH	2	3	4	5
DKSC loading (g/L)	0.25	0.50	0.75	1.00

4.3. Results and discussions

4.3.1. Preliminary investigations

The shaking speed and equilibrium time were identified as the principal process variables that were required to be fixed for the biosorption studies. Thus, those variables were investigated in the initial test work. Visual observations led to the

Table 4.2: Taguchi L_{16} OA design results for the biosorption of thorium studies.

Exp.run order	C_i (mg/L)	pH	DKSC loading (g/L)	C_e (mg/L)	q_e (mg/g)	S/Nratio for q_e	R%	S/Nratio for R%	D
1	15	2	0.5	1.19	27.03	28.64	92.07	39.28	0.31
2	15	3	1.0	1.54	13.45	22.57	89.74	39.06	0.21
3	15	4	1.5	0.15	9.89	19.90	99.92	40.00	0.19
4	15	5	2.0	0.35	7.41	17.39	99.93	40.00	0.17
5	40	2	1.0	39.86	0.14	-17.12	00.35	-9.13	0.00
6	40	3	0.5	29.16	21.46	26.63	27.10	28.66	0.15
7	40	4	2.0	0.86	19.98	26.01	99.95	40.00	0.28
8	40	5	1.5	7.34	21.67	26.72	81.64	38.24	0.26
9	85	2	1.5	60.84	16.11	24.14	28.42	29.07	0.13
10	85	3	2.0	35.17	24.86	27.91	58.62	35.36	0.24
11	85	4	0.5	7.48	154.00	43.74	91.20	39.20	0.73
12	85	5	1.0	1.61	78.82	37.93	98.11	39.83	0.54
13	130	2	2.0	5.03	62.48	35.91	96.13	39.66	0.48
14	130	3	1.5	5.24	83.17	38.40	95.97	39.64	0.55
15	130	4	1.0	0.74	130.00	42.28	99.94	40.00	0.71
16	**130**	**5**	**0.5**	**0.24**	**260.00**	**48.30**	**99.97**	**40.00**	**1.00**

C_i– initial Th(IV) concentration, C_e – equilibrium Th(IV) concentration, D-Desirability

conclusion that, at lower mixing speeds, the biosorption capacity of DKSC was at a minimum due to an inefficient dispersion of sorbent particles in the working solution that led to agglomeration of sorbent particles at the bottom of the reactor vessel. It was also found that a mixing speed of 200 rpm was sufficient for the availability of all surface binding sites in the sorption process. The biosorption capacity reached a maximum value at this mixing speed, and therefore the agitation speed was chosen as 200 rpm for all further batch biosorption studies.

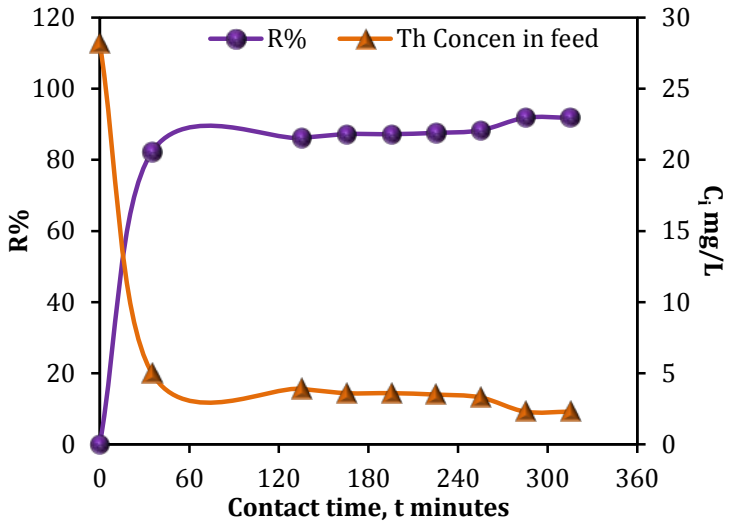

Figure 4.1: Effect of contact time towards bio-removal efficiency (R%) and initial Th concentration in feed (C_i, mg/L).

The effect of shaking time (i.e. contact time) on thorium biosorption onto DKSC was examined up to a maximum of 5 hours using solution with 28 mg/L of initial Th(IV) concentration as the feed with an initial pH of 6 and DKSC loading of 0.1g for 100 ml. The results obtained are displayed in Fig. 4.1. As can be seen in the figure, the initial Th(IV) concentration (C_i mg/L) in the feed decreases with increasing time indicating the biosorptive capability of DKSC in adsorbing thorium ions. Thorium uptake was very rapid in the first 30minutes, and it led to 82% removal efficiency. Equilibrium was attained within 180 minutes. Hence, the equilibrium time was fixed as 180 minutes for all further biosorption experiments. The samples were collected at fixed time intervals, and the time intervals were chosen on the basis of preliminary experiments. The trends in the graphs plotted using the results from the preliminary experiments were similar to those obtained using actual experiments. Thus, more data within the 0-30 minutes were not deemed to be required.

Literature suggested that precipitation of thorium takes place when pH >6 (Sayana et al., 2016). Hence, the pH values were varied from 2 to 6. Precipitation of thorium was also examined in this pH range, and it was found that there was no precipitation up to pH of 6.0. However, thorium was precipitated at higher concentrations when the pH was equal to 6.

4.3.2. Multivariate optimisation of Th(IV) biosorption process using the Taguchi robust design with desirability approach

(a) Statistical analysis of Taguchi L_{16}OA design

The experiments were performed according to the design (Table 4.2) as specified in the section 3.5.1 and the data collected was converted into biosorption capacity (q_e) and bio-removal efficiency (R%) according to equations 3.5 and 3.6, respectively. The results calculated were treated for statistical significance by employing MINITAB17 statistical software (trial version). The q_e and R% values that were calculatedwere transformed into S/N ratios (larger-is-better) according to equation 3.9 and are presented in Table 4.2.

Table 4.3: Response table for signal-to-noise ratios(S/N) - Larger is better.

Levels/Factors	Initial Th(IV) concentration		Initial pH		DKSC loading	
	q_e	$R\%$	q_e	$R\%$	q_e	$R\%$
1	22.13	39.59	17.89	24.72	36.83	36.79
2	15.56	24.44	28.88	35.68	21.42	27.44
3	33.43	35.87	32.98	39.80	27.29	36.74
4	41.22	39.82	32.59	39.52	26.81	38.75
$\Delta_{max-min}$	25.66	15.38	15.09	15.08	15.41	11.31
Rank (q_e)	1		3		2	
Rank ($R\%$)	1		2		3	

$\Delta_{max-min}$:Rangeis the difference between maximum and minimum levels of factors

Response tables for the two responses (q_e and R%) obtained from signal-to-noise ratios (S/N) are shown in Table 4.3. From the observation of the rankings obtained for each variable, it is evident that initial Th(IV)concentration is the most influential variable for the two responses R% and q_e in the biosorption process for thorium, whereas pH and DKSC loading were the least influential factors. The same data has been shown in Fig. 4.2 in terms of percentage contribution from each parameter. Thus, the contribution of initial Th(IV) concentration towards the responses q_e and R% has the greatest effect.

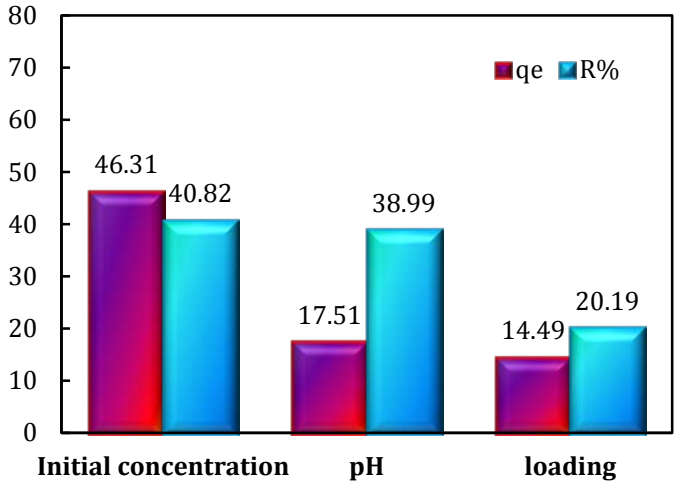

Figure 4.2: Percentage contributions of process variables towards responses $q_e$and R%.

ANOVA (Analysis of variance) was performed for the experimental data to determine the effects of the various factors towards the responses. Results are presented in Table 4.4. An F-test was carried out for experimental results, and the results were compared withcritical values. As is evident from Table 4.4., the initial metal concentration has the largest sum of squares indicating it is the most influential operational parameter. From the calculated F-values, it is clear that no single parameter has a statistical significance at 95% confidence level.

Table 4.4: ANOVA table for q_e and R% in L_{16}OA design.

Factors	SS	DOF	MS	F[a]	F_{cr}[b]	PC
For q_e						
Initial Th concentration	1574	3	524	4.27	9.28	46.31
Initial pH	595	3	198	1.61	4.76	17.51
DKSC loading	492	3	164	1.34	3.86	14.49
Residual	737	6	122	----	----	----
Total	3399	15	----	----	----	----
For R%						
Initial Th concentration	626	3	208	1.68	9.28	40.82
Initial pH	598	3	199	1.61	4.76	38.99
DKSC loading	309	3	103	0.83	3.86	20.19
Residual	743	6	123	----	----	----
Total	2277	15	----	----	----	----

[a]Fischer's ratio; [e]$F_{0.05}(\nu_1, \nu_2)$ where ν_1 is the degree of freedomand $\nu_2 = (a*n - a)$, a is factor number, and n is the number of levels

Fig. 4.3 displays the main effect plots of the S/N ratios for the responses q_e and R% obtained from the Th(IV) biosorption studies. The higher response represents the best level of each variable and can be interpreted as an optimised value for that particular process variable.

- *Effect of Initial Th(IV) concentration*; The initial Th(IV) concentration shows a critical effect towards q_e and R% as it explains the metal uptake mechanism. As perceived from Fig. 4.3.(a) and (b), the biosorption capacity (q_e) and bioremoval efficiency (R%) initially decreased with an increase in Th(IV) concentration from 15 to 40 mg/L and then increased as initial Th(IV) concentration was increased from 40 to 130 mg/L. The decrease in q_e and R% with respect to initial Th(IV) concentration may be due to the formation of a series of polynuclear complexes of thorium such as $Th_2(OH)_2^{6+}$, $Th_6(OH)_{15}^{9+}$ and $Th_2(OH)^{7+}$ with high oxidation numbers along with the anions in the solution. The uptake of these ions onto the sorbent is difficult.

Also, an increase in thorium concentration results in the increasing hydrolyzation among thorium ions which are unable to reach the adsorption sites of the sorbent (Yusan et al., 2012, Gok and Aytas, 2013, M. A. A. Aslani, 2001). The further increase in thorium concentration led to a rising in q_e and R% values since the initial sorbate concentration increases the concentration gradient which in turn increases the main driving force that overcomes all mass transfer resistances between the sorbent-sorbate systems. The parameter q_e increased with respect to the thorium concentration (40 to 130 mg/L) due to the enhancement of electrostatic interactions (relative to covalent interactions) between thorium and DKSC, whereas the R% parameter increased due to the attainment of process equilibrium (Anirudhan et al., 2010, Bhalara et al., 2014, Yusan et al., 2012, Kütahyalı and Eral, 2010)). Hence, qe and R% had higher response values of 260 mg/g and 99.97%, respectively for an initial thorium concentration of 130 mg/L. The values obtained here are the highest compared to those achieved with many other adsorbents reported in the literature (Akkaya et al., 2013, Gok et al., 2013, Gok et al., 2011, Ceren et al.,2010,Innoue et al., 2006). Thus, 130 mg/L can be regarded as an optimum value for initial Th (IV) concentration for the present sorbate-sorbent system.

- *Effect of initial pH;* The pH is one of the important factors that influence the biosorption of radionuclides onto DKSC. It affects the degree of ionisation, surface charge, speciation and precipitation of metal ions. It is well known that surface charge of the sorbent can be modified by changing the pH of the solution, and the chemical species in the solution depends on the pH (Sayana et al., 2016). From Fig. 4.3 (a) and (b), it can be seen that q_e and R% parameters both increased as the pH was increased from 2 to 4 and the maximum biosorption occurred at pH 4 (with nearly 100% of thorium

adsorbed onto DKSC). The increase can be explained based on the state at which the thorium ion exists in aqueous solutions and is dependent on pH.

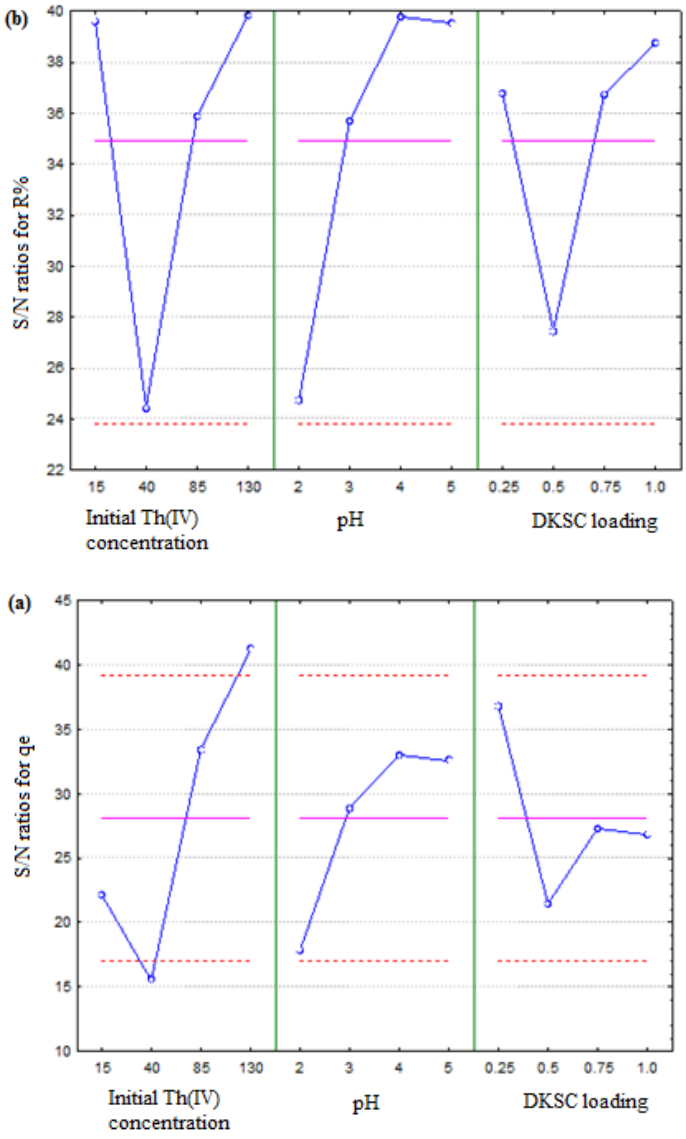

Figure 4.3: Main effects of the major variables (by S/N ratios) on (a) $q_e$and (b) $R\%$.

In acidic solutions, especially when the pH is < 3, thorium is present in +4 oxidation state as highly soluble species (Fig 4.4). Hydroxonium ions (H_3O^+) present in strongly acidic solutions (2<pH<4) may compete with the thorium cations for the sorption sites and hinder the sorption process. When the pH is around 4, 1:1 and 1:2

positively charged thorium acetate complexes $[ThCH_3COO]^{3+}$ and $[Th(CH_3COO)2]^{2+}$ appear as characteristic ions present in the solution (Yusan et al., 2012, Aslani et al., 2001).

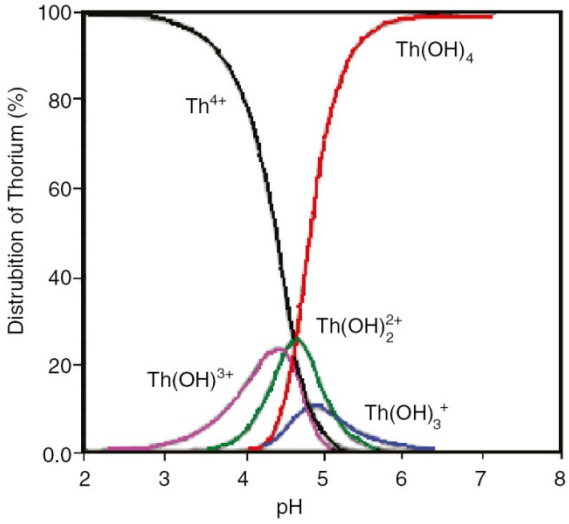

Figure 4.4: Thorium species distribution diagram.

The FTIR results revealed that DKSC contains carboxyl, hydroxyl, amine as major functional groups and the pH_{pzc} of DKSC was determined as 6.2 (Fig. 7.1). The increased biosorption of Th(IV) in the pH range of 4-5 may therefore be caused by the ion-exchange reactions of thorium ions with carboxyl groups due to deprotonation of these functional groups at the surface sites that results in the increase of negative charge. The exchange reactions involved can be shown as follows (Gok and Aytas, 2013, Ding et al., 2014),

$$\text{COOH} + \text{Th}(OH)_3^+ \rightarrow [(COO)Th(OH)_3] + H^+$$

$$n\,COOH + Th(OH)^{3+} \rightarrow [(COO)_nTh(OH)_3]^{(3-n)+} + n\,H^+ \quad \text{(n=1, 2, 3)} \qquad (4.1)$$

$$nCOOH + Th(OH)_2^{2+} \rightarrow [(COO)_nTh(OH)_2]^{(2-n)+} + n\,H^+ \text{ (n=1,2)}$$

- *Effect of DKSC loading;* The DKSC loading determines the sorbate-sorbent equilibrium and also the number of binding sites available for biosorption. Fig. 4.3(b) depicts the plot of DKSC loading against R%, indicating the presence of surplus amounts

of unoccupied sites with the increase in DKSC loading (Anirudhan et al., 2010).The results of the present study are in agreement with those of similar studies reported in the literature (Akkaya and Akkaya, 2013, Yusan et al., 2012).

(b) Multivariate optimisation with desirability approach

The overall desirability values of each response were calculated by considering equation 3.20 (Chapter 3) to verify whether the response is acceptable or not. The independent desirability of each response ($q_e$and R%) was combined to determine the overall desirability and is reported in Table 4.2. It was observed that the combination 212 (Exp. No 5) shows an overall desirability of zero. Thus a S/N ratio cannot be calculated for this case. Therefore, the optimisation of the combination was carried out based on the analysis by means of overall desirability (Nandi et al., 2010). The factors' combination 4-4-1(Exp. No 16) reached an overall desirability value of 1 giving rise to the conclusion that optimum process variables occur at 130 mg/L of initial Th concentration, pH of 5 and a DKSC loading of 0.25 g/L. Thus, the maximum values obtained at the optimum conditions using the desirability approach are 260 mg/g for q_e and 99.97% for R%.

4.3.3. Equilibrium studies and adsorption isotherm modeling

Equilibrium studies were performed to measure the capacity of DKSC in the biosorption of thorium from aqueous streams. The results obtained are presented in Figure 4.4. The results show that q_e increased considerably with Th(IV) equilibrium concentration(C_e) due to the reason that the original Th concentration tends to increase the interactions among DKSC and thorium ions. However, q_e attained almost a constant value with increasing initial concentration due to the saturation of the sorption sites on DKSC (Aly et al., 2013). The distribution coefficient (K_d) is the ratio of the equilibrium

concentration of meal ions in solid to that in the aqueous phase. Fig. 4.5 displays the K_d as a function of C_e for Th(IV) biosorption. High values of K_d is an excellent feature for the sorbent, and the K_d values obtained for DKSC were13.05 L/g for $C_e$of 1.78 mg/L which decreased to 0.2 L/g for $C_e$of 585mg/L using 0.667 g/L of DKSC. A similar trend in K_d was observed as a function of $C_e$by (Akhtar et al., 2008).

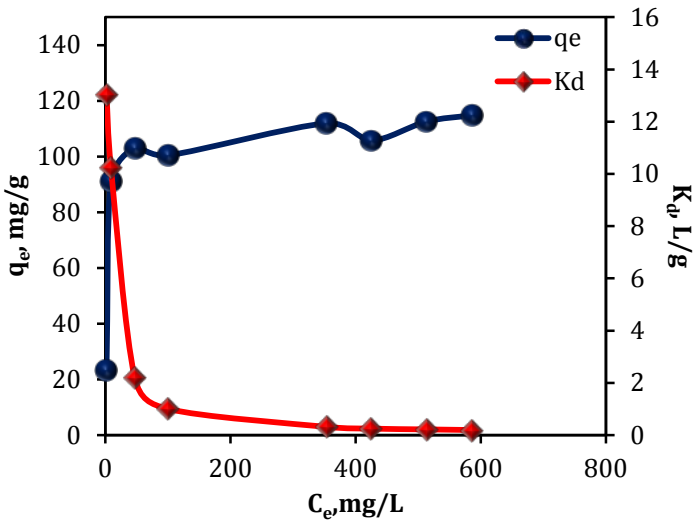

Figure 4.5: q_e and K_d as a function ofC_e.

Also, the equilibrium data were analysed using linear forms of adsorption isotherms namely, Langmuir and Freundlich models (Section 2.2.1, Chapter 2). The graphical representations of the resulting isotherm models are shown in Fig. 4.6. The parameter values were determined using linear regression and are presented in Table 4.5. The high value of 0.98 obtained for the correlation coefficient (R^2) for the Langmuir model suggests that the model fits well with the experimental data indicating monolayer biosorption of thorium ions onto DKSC. The maximum value obtained for Q_0 was 125 mg/g for DKSC. The essential features of Langmuir isotherm model can be elaborated using two dimensionless parameters namely, the separation factor (R_L) and the surface coverage (θ). Fig. 4.6 depicts the plots of R_L and θ against the initial Th

concentration (C_i, mg/L). The results reveal that the R_L values obtained are between 0 and 1 ($0<R_L<1$) suggesting that the biosorption of thorium using the DKSC is favourable. Also, the θ value increased with C_i until the sites on the DKSC were saturated which also indicates sorption with monolayer coverage {Dada et al., 2012, Nagapal et al., 2011, Yuvaraja et al., 2014).

Table 4.5: Parameter values derived from isotherm models.

Langmuir isotherm model		
Q_0	125.00	R^2= 0.98
K_L	0.13	
Freundlich isotherm model		
K_f	1.54	R^2= 0.66
n	4.85	

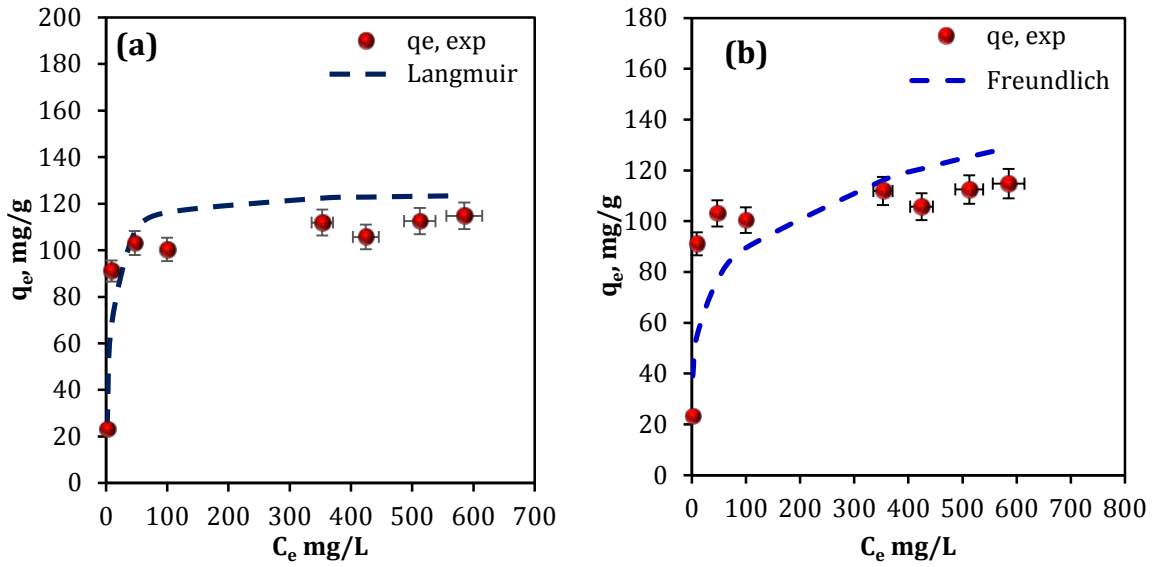

Figure 4.6: Validation of equilibrium data through a comparison of different adsorption isotherm model, (a) Langmuir model and (b) Freundlich model. Error bars are for ±5 % variation.

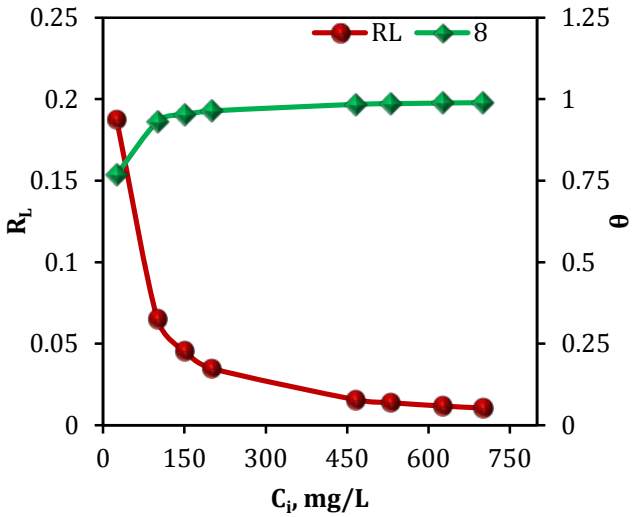

Figure 4.7: Separation factor **(**R_L) and surface coverage (θ) as function of C_i.

4.3.4. Kinetic studies of diffusion and mass transfer modeling

The kinetic studies were carried out using initial Th(IV) concentrations of 25, 50 and 100 mg/L for 3 hours at 25^0C in a working volume of 0.2 L to determine the mechanism of biosorption process. The kinetic data obtained were modeled using the linear forms of the pseudo-first-order, pseudo-second-order, and intraparticle diffusion models (Section 2.2.2, Chapter 2). The performance of each of the models and the model parameters used are presented in Table 4.6.

High correlation coefficient values (R^2 = 0.9999 (25 mg/L), 0.9999 (50 mg/L) and 1.0000 (100 mg/L)) were obtained for the pseudo-second order model for the concentration ranges used indicating that the experimental data fitted well with the model. Further, the close agreement between experimental q_e values and those predicted by the pseudo-second order model suggests that the model was suitable for representing the kinetics of thorium uptake onto DKSC (Fig. 4.8). Also, the results suggest that the overall rate of biosorption may be influenced by chemisorptions which involves ion exchange on the sorption sites (Ahmed et al., 2014, Nagpal et al., 2010).

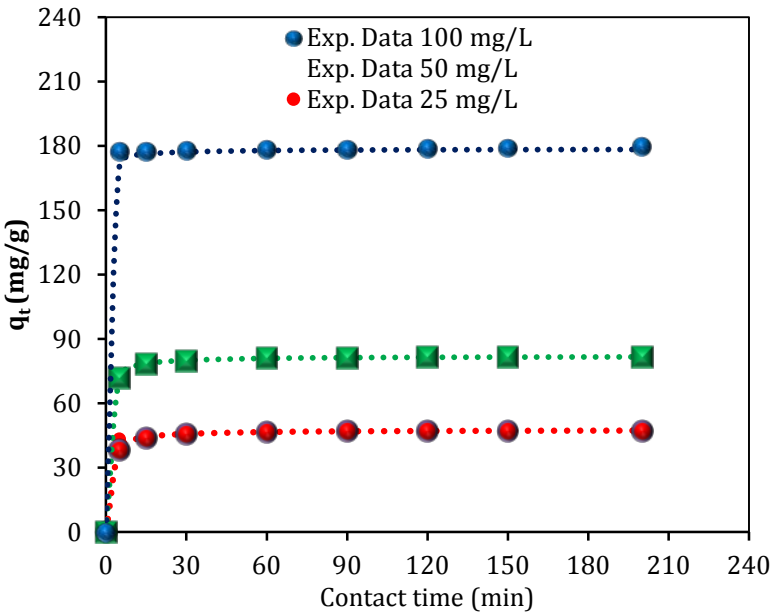

Figure 4.8: Experimental data(●) and Pseudo-second order model (·····).

Table 4.6: Kinetic model parameters for thorium biosorption.

Model parameters	25 mg/L	50 mg/L	100 mg/L
Pseudo-first order			
q_e (exp)	46.67	81.92	179.69
q_e	2.64	2.79	2.77
k_1	0.009	0.012	0.012
R^2	0.78	0.80	0.88
Pseudo-second order			
q_e (exp)	46.67	81.92	179.69
q_e	47.62	81.97	178.57
k_2	0.0172	0.0169	0.0241
H	39.00	113.55	768.48
R^2	0.9997	0.9999	1.0000
Intra-particle diffusion			
k_i	0.219	0.218	0.182
C	43.47	78.76	176.9
R^2	0.82	0.91	0.97

4.3.5. Thermodynamic studies for determining feasibility of the biosorption process

The thermodynamic study (effect of temperature) on biosorption reveals valuable information regarding enthalpy and entropy changes (Azouaou et al., 2010). The biosorption of thorium studies was carried out at different temperatures to determine thermodynamic parameters such as ΔH^0, ΔS^0, and ΔG^0 using distribution coefficients (K_d)(Section 2.2.3, Chapter 2).

The ΔH^0 and ΔS^0 values were determined from the plot of ln K_d vs. 1/T (Fig. 4.9) as 47.04 J/mol (slope) and 184.82 J/mol (intercept) (Table 4.7), respectively. When the ΔH values are <40 J/mol the type of adsorption can be accepted as physical process with weak attraction of forces. Thus, in the present study the ΔH value was obtained as 47.04 J/mol representing the adsorption as chemical process involving chemical reactions. The positive value of enthalpy change suggests that thorium biosorption process is endothermic in nature. The positive value of entropy change designates the increased randomness at the solid-solution interface during the adsorption of thorium onto DKSC, also it favors complexation and stability of the biosorption process.

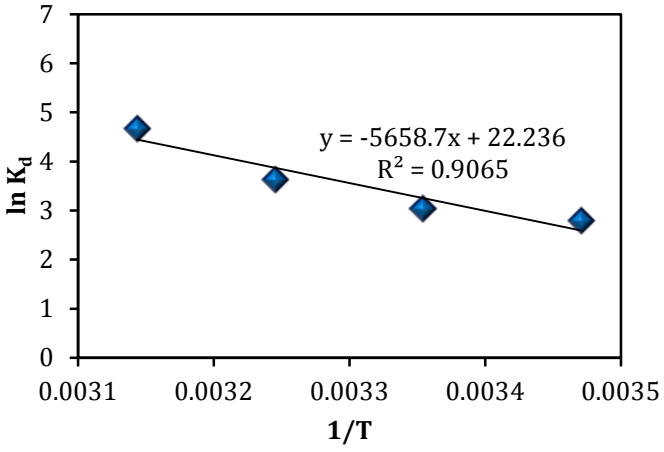

Figure 4.9: Temperature dependence of thorium biosorption process.

The change in Gibbs free energy (ΔG^0) was calculated from equation 2.2 and results are shown in Table 4.7. The ΔG values obtained for the temperatures used in this work are negative confirming the thermodynamic feasibility and reaction spontaneity of the thorium biosorption process with an increase in temperature. Furthermore, the increase in ΔG values with an increase in temperature indicates that thorium biosorption process is favoured at higher temperatures. The increase in adsorption with temperature may be attributed to either increase in the number of active surface sites available for adsorption onto DKSC or the desolvation of the sorbing species. Generally, the absolute magnitude of the change in Gibbs free energy for physisorption is between −20 and 0 kJ/mol, and chemisorption has a range from −80 to −400 kJ/mol. The results found in this study are between −53.21 and −58.75 kJ/mol specifying the sorption to be in between physisorption and chemisorptions, thus interpreting as physical adsorption with an enhancement by chemical effect. Since ΔG values are between 20 and 80 kJ/mol, adsorption type can be explained as chemisorptions with ion exchange reactions. Seemingly the ion-exchange has a range from −20 to −80 kJ/mol, which is consistent with the results found from isotherm and kinetic models.

Table 4.7: ΔG^0 values for thorium biosorption at different temperatures.

ΔH° (J/mol)	**ΔS° (J/mol)**	**ΔG° (kJ/ mol K)**			
		288 K	298 K	308 K	318 K
47.0406	184.8202	-53.2089	-55.0571	-56.9053	-58.7535

4.4. Conclusions

The present work revealed that DKSC was effective in the removal of Th(IV) from aqueous solutions. Its efficiency in removing thorium was examinedin a batch

biosorption experiment. A set of selected process variables were optimised via Taguchi robust design adapting desirability function for multivariate response optimisation. The optimum conditions obtained include the initial Th(IV) concentration at level-4 (130 mg/L), pH at level-4 (5) and DKSC loading at the level-1 (0.25 g/L). These conditions led to a maximum value of 260 mg/g for q_e and 99.97% for R%. The Langmuir isotherm model exhibited a good correlation with the equilibrium data, and a pseudo-second order model fitted well the kinetic data obtained within the concentration range used. The kinetic study suggests that chemisorption occurred during biosorption. The thermodynamic studies revealed that thorium biosorption was a spontaneous process and it was endothermic in nature.

Chapter 5

Zirconium biosorption and optimisation studies via Box–Behnken method in RSM and desirability approach

Summary

The research presented in this chapter discusses the sequestration of zirconium from aqueous solutions using the biosorption method as a separation technique. The biosorptivebehaviour of deoiled Karanja biomass was therefore investigated for the removal of zirconium metal ions. The effects of process variables namely, the initial metal concentration, the pH of the feed solution and the DKSC loading were examined, and the parameters were optimised for the maximum biosorption capacity and bio-efficiency using the Box-Behnken method with 3^3design in response surface methodology (RSM).

5.1. Introduction

Zirconium is a significant engineering material due to its corrosion-resistive traits and has achieved significant implementation in the nuclear industry because of its transparency to neutrons for cladding uranium fuel elements and for trapping fission fragments. The speciation of Zr from nuclear discharge is a chief concern in nuclear waste management and related environmental pollution control. The methods employed for the separation of zirconium from aqueous streams and the use of different kinds of biomasses in the recovery of this metal ion were discussed in Chapter 2 (Literature Review).

5.2. Experimental procedures

Materials and methodologies employed to in this study were described in Chapter 3 (Materials and Methodology).

(a) ***Preliminary studies***

As described in Chapter 4, preliminary investigations used a univariate method to analyse the effect of variables such as contact time, mixing speed, initial pH, and DKSC loading by conducting experiments under batch mode.

(b) ***Box-Behnken design (3^3) in RSM***

A Box-Behnken experimental design containing three factors namely, initial Zr(IV) concentration, initial pH and DKSC loading with three levels (Table 5.1) for each variable was implemented to study the effect of these process variables on q_e and R% in the zirconium biosorption studies. The design matrix was developed using Design Expert software version 9.0 (trial version) that generated 15 experiments including three center points. The details of the experiments are presented in Table 5.2 along with the experimental and predicted responses for bio-removal efficiency (R%).

Table 5.1: Levels of process variables in the Box-Behnken experimental design.

Design Variable	**Coded values**			**Uncoded values**			**∇x_i**
Initial Zr concentration (mg/L)	-1	0	+1	55	65	75	10
Initial pH	-1	0	+1	2	3	4	1
DKSC loading(g/L)	-1	0	+1	3	5	7	2

5.3. Results and discussions

5.3.1. Preliminary studies:

The effect of contact time on the biosorption of zirconium onto DKSC was investigated over a period of 4 hours using 50 mg/L of initial Zr(IV) concentration with an initial pH of 3 and DKSC loading of 0.5 g for 100 ml. The results obtained are shown in Fig. 5.1. They show a reduction in the Zr(IV) concentration (C_i, mg/L) with increasing time

Table 5.2: 3^3 Box-Behnken design matrix for zirconium biosorption studies with experimental and predicted results for R%.

Run order	Coded level of Variables			Actual level of variables			Biosorption capacity, q_e(mg/g)	Bio-removal efficiency (R%)	
	A	*B*	*C*	*A*	*B*	*C*		*Observed response*	*Predicted response*
1	-1	-1	0	55	2	5	8.75	79.53	74.58
2	1	-1	0	75	2	5	9.02	60.13	60.24
3	-1	1	0	55	4	5	10.14	92.22	92.10
4	1	1	0	75	4	5	14.18	94.56	99.50
5	-1	0	-1	55	3	3	16.69	91.05	93.74
6	1	0	-1	75	3	3	23.47	93.87	91.49
7	-1	0	1	55	3	7	7.23	92.07	94.44
8	1	0	1	75	3	7	9.90	92.43	89.74
9	0	-1	-1	65	2	3	8.33	38.43	40.69
10	0	1	-1	65	4	3	17.42	80.41	77.84
11	0	-1	1	65	2	7	4.30	46.34	48.92
12	0	1	1	65	4	7	6.57	70.81	68.56
13	0	0	0	65	3	5	12.18	93.72	93.59
14	0	0	0	65	3	5	12.17	93.63	93.59
15	0	0	0	65	3	5	12.14	93.41	93.59

A-Initial Zr(IV) concentration (mg/L), B- Initial pH of feed, C-DKSC loading

which indicates the capability of DKSC as a sorbent in sequestering zirconium ions from aqueous solutions. The effect of contact time on Zr(IV) metal uptake was investigated using 1.5 g/L DKSC. Zirconium uptake was very rapid in the first 100 minutes leading to nearly 50% of zirconium removal. Equilibrium was attained at 230 minutes. These results indicate that a contact time of approximately 4 hours is suitable for the removal of zirconium from aqueous streams which can be considered very short and economical in commercial prospects for DKSC. Hence, the equilibrium time was fixed as 4 hours in further biosorption

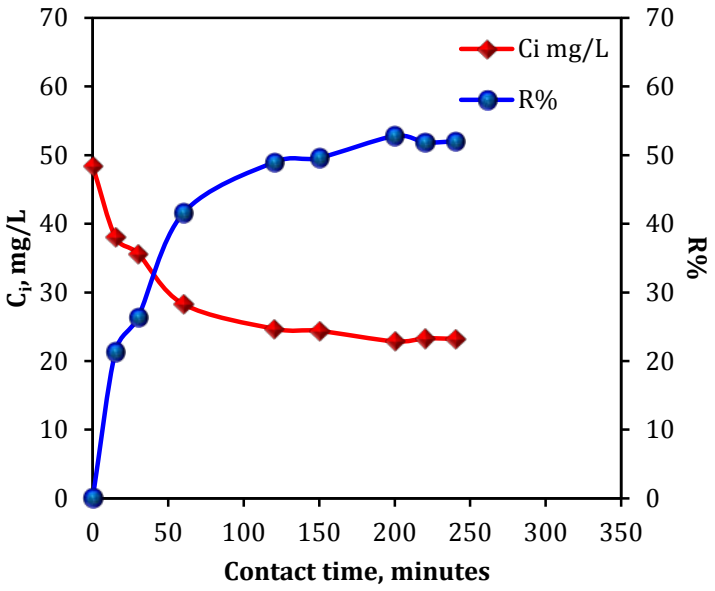

Figure 5.1: Preliminary studies: Effect of contact time on zirconium biosorption onto DKSC.

experiments. The effect of shaker speed in zirconium biosorption was found to have the same effect as discussed in section 4.3.1. The results obtained in the preliminary investigations have led to the idea of fixing levels using the Box-Behnken method for optimisation. The effect of pH on the hydrolysis of zirconium ion concentration in the feed was examined by varying it from 2 to 6. The trials found that the precipitation of zirconium hydroxides in the aqueous solution takes place beyond pH 4 and these precipitates could be observed visually. This may be due to the presence of hydroxide complexes (cationic or anionic) and hydroxide precipitates in the feed solution (Sayana et al., 2016).

Monomeric hydrolysed species such as $MO(OH)^{-1}$, $M(OH)_2^{2-}$, $M(OH)_3^{-}$and polymeric hydrolysed species with general form $[M(OH)_x^{4-x}]_n$were the most soluble zirconium species present in the pH range 2-4. Also, the formation of insoluble colloidal zirconium hydroxides occurs beyond pH 4 as reported in literature(Boveiri Monji et al., 2008). Hence, pH values up to 4 were considered in further studies in this work. The

biosorption capacity was found to be lower for DKSC loading below 3 g whereas it was almost constant for DKSC loading above 7 g. Thus, the levels of DKSC loading for this work were chosen as 3, 5 and 7 g.

5.3.2. Multivariate optimisation of Zr(IV) biosorption process using Box-Behnken method in RSM using desirability approach

(a) Statistical analysis of Box-Behnken (3^3) experimental design

Experiments were conducted according to the design specified in Section 3.5.1 and the data collected were converted into biosorption capacity (q_e) and bio-removal efficiency (R%) according to equations 3.5 and 3.6, respectively. The results calculated were analysedfor statistical significance employing Design Expert software version 9.0 (trial version). The predicted values of response were obtained by full quadratic model fitting using the software mentioned above. An empirical second-order polynomial equation (quadratic model) relationship involving response and variables shown in equation 5.1 can be used to predict the response at given levels for each factor.

$$R\% = 93.59 - 1.74A + 14.20B - 0.26C + 10.69A^2 - 22.67B^2 - 11.92C^2 + 5.43AB - 0.6BC - 4.38BC \quad (5.1)$$

The correlation between the predicted and observed responses is shown in a parity plot (Fig. 5.2). As is evident from the plot, the data points fall very close to the straight line with 45°slopeimplying a good correlation between the observed and predicted responses thereby confirming the quality of the model. The statistical significance and goodness-of-fit of the model were tested using the analysis of variance (ANOVA), and the results are shown in Table 5.3.The values obtained for the coefficient of determination $R^2$and adjusted R^2 are 0.9798 and 0.9435, respectively which are in reasonable agreement with those found from experimental results. The R^2 (coefficient

of determination) value obtained in the present study suggests that 97% of the total variationfor Zr(IV) biosorption can be revealed by the model and only 3% is left to residual variability. The predicted R^2 obtained a value of 0.67 which implies that the present model has a block effect and adequate precision obtained a value of 16.26 (Table 5.3) which can be used to navigate the design space in the present study. The coefficient of variation (CV) for this model is the error expressed as a percentage of the mean. Results obtained in the present study are in agreement with those previously reported (Mourabet et al., 2012).

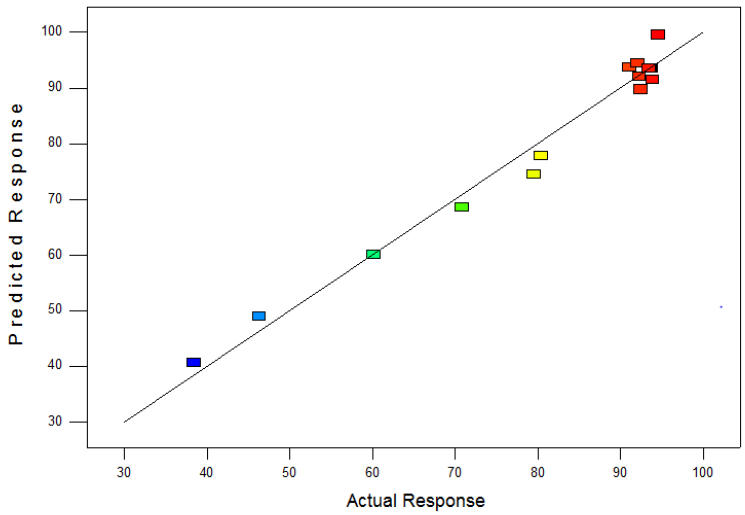

Figure 5.2: Predicted response versus observed response (R%).

According to the results obtained using ANOVA from the quadratic model, the model F-value (26.96), the model constant (β_0), pH (B), and the lack of fit (LOF) and interaction terms ($AB, A^2, B^2,$ andC^2) are statistically significant whereas BC is marginally significant at a 95% probability level (Kousha et al., 2012). The LOF analysis has proven that the quadratic model chosen for the present system is acceptable (Islam et al., 2009). The sum of squares (SS) obtained from ANOVA was used to calculate the

percentage contribution (PC) for each model term as SS strengthens the significance of the corresponding source in the undergoing process (Feza Geyikci et al., 2012).

Table 5.3: ANOVA for response surface quadratic model.

Source	SS	df	Mean Square	*F* Value	p-value Prob> F	Model Coefficient	Coefficient Estimate	SE	PC, %
Model	4761.81	9	529.09	26.96	0.0010 Significant	β_0	93.59	2.56	----
A	24.10	1	24.10	1.23	0.32	β_1	-1.74	1.57	0.51
B	1612.53	1	1612.53	82.17	0.03 Significant	β_2	14.20	1.57	34.48
C	0.56	1	0.56	0.028	0.87	β_3	-0.26	1.57	0.01
AB	118.11	1	118.11	6.02	0.06	β_{12}	5.43	2.21	2.52
AC	1.51	1	1.51	0.077	0.79	β_{13}	-0.61	2.21	0.03
BC	76.63	1	76.63	3.90	0.10	β_{23}	-4.38	2.21	1.64
A^2	421.75	1	421.75	21.49	0.01 Significant	β_{11}	10.69	2.31	9.02
B^2	1897.18	1	1897.18	96.67	0.00	β_{22}	-22.67	2.31	40.56
C^2	524.81	1	524.81	26.74	0.00	β_{33}	-11.92	2.31	11.22
Residual	98.12	5	19.62						
Lack of Fit	98.07	3	32.69	1311.18	0.0008 Significant				
Pure Error	0.050	2	0.025	Adequate Precision=16.261					
Cor Total	4859.93	14	CV=5.48						

R^2=0.9798, Pred.R^2=0.6771, Adj.R^2=0.9435

Percentage contribution of each of the model terms was calculated using equations (3.14) to (3.16) as discussed in section 3.6.3 and is shown schematically in Fig. 5.3. As depicted in the figure, the quadratic terms (A^2, $B^2$and C^2) demonstrated the highest level-of-significance with a total contribution of 61%, followed by the interaction terms (AB, BC and AC) with a total contribution of 35%. First-order terms (A, B and C) showed the lowest level of significance with a total contribution of only 4% representing an insignificant effect in predicting Zr(IV) biosorption efficiency. Among the three factors considered, only the initial pH of feed (B) showed the highest level of

significance with a contribution of 40.56% (quadratic term) and 34.48% (first-order term) followed by DKSC loading with 11.22% (quadratic term) as compared to other components. Similar results were reported by previous authors(Yetilmezsoy et al., 2009, Singh et al., 2010, E. Ozdemir, 2011, Kumar Anupam, 2011).

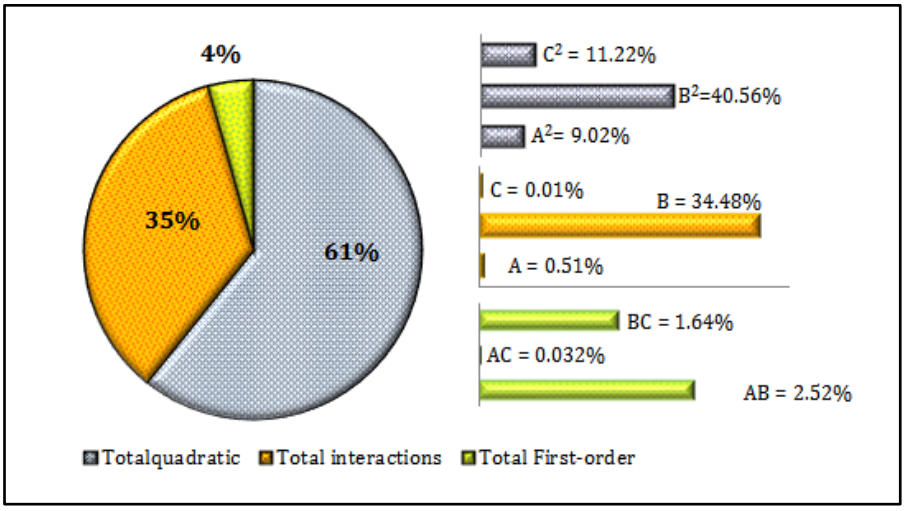

Figure 5.3: Schematic representation of percentage contribution.

- *Interaction effect of process parameters:*

Fig. 5.4 represents the 3D surface plots of the combined effects from the AB, AC and BC parameters for Zr(IV) biosorption using DKSC. The interactions of the parameters AB have a significant positive effect towards the response R% where as AC and BC have an insignificant effect. Fig. 5.4.(a) depicts the interaction of AB (initial Zr concentration-initial pH) with response (R%) and the response plot can be explained as follows. At a constant DKSC loading (5g/L), for an initial Zr concentration (A) at 55 mg/L and at a pH (B) of 2, the R% obtained was 79.52%. The value increased to 94.56% as the pH was increased to 4 with the same initial Zr concentration. In comparison, when the initial Zr concentration was increased to 65mg/L and the pH decreased to 3,

the R% dropped to 93.6%. At an initial Zr concentration of 75 mg/L and a pH of 2, the lowest R% value of 60.13 % was obtained.

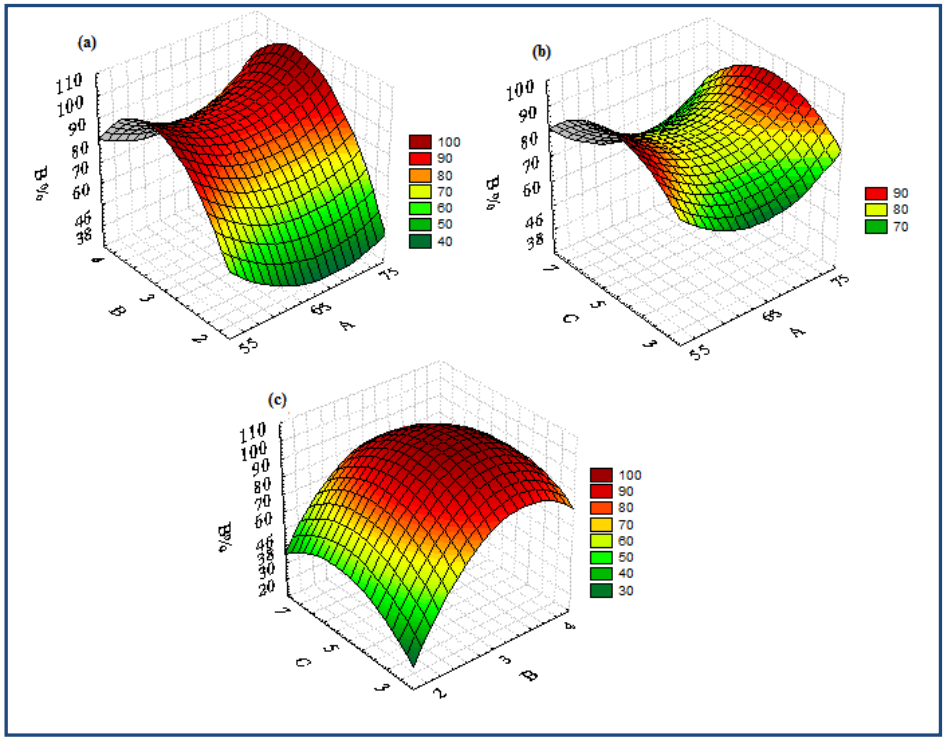

Figure 5.4: 3D response surface plots for (a) *AB*with R%, (b) *AC* with *R*% and (c) *BC* with *R*%.

Similarly, the interaction of *AC* (initial Zr concentration-DKSC loading) with response (R%) is illustrated in Fig. 5.4.(b). For an initial Zr concentration of (*A*) 55 mg/L and DKSC loading (*B*) of 3 g/L, the R% value was 91.05% at a constant pH of 3.An increase in DKSC loading from 3 to 7 g/L with the same initial Zr concentration increased the R% value to 92.07%. A further increase in initial Zr concentration to 65 mg/L at a DKSC loading of 5 g/L led to an increase in R% to 93.58%. At 75 mg/L of initial Zr concentration and with a DKSC loading of 3 g/L, R% attained the highest value of 93.87%. Fig.5.4. (c) represents the interaction of parameters BC (initial pH-DKSC loading) with response (R%). For a constant initial Zr concentration of 65 mg/L at a pH of 2 and a DKSC loading of 3 g/L, R% attained a value of 38.43%. An increase in pH to a value of 3 and a DKSC loading to a value of 5g/L led R% to a maximum value of 93.72%.

From the above observations, it was established that among all the interactions studied (AB, AC and BC), pH and DKSC loading had the most effect on the bio-removal efficiency. It can be inferred that an increase in pH value causes an increase in the R% with a maximum obtained at around a pH of 3-4. The underlying phenomenon can be explained by studying the functional groups involved in the metal binding mechanism. FTIR spectroscopic analysis revealed that methyl, amide, carboxylic and nitro are the potential functional groups that can actively participate in the biosorption of Zr(IV) metal ions onto DKSC depending on the initial pH of the feed solution. At a pH of 3-4, the maximum number of interactions occurs between cations such as Zr^{+4} and the possible functional groups present on DKSC due to electrostatic attraction. At a pH of 2-3, the R% decreases due to the electric repulsion among the Zr^{+4} and molecular groups along the binding sites as H^+ and H_3O^+ions increase (Bhatti and Amin, 2013, P. Senthil Kumar, 2011, H. Kalantari, 2014). The influence of the initial pH towards Zr(IV) biosorption can be explained by considering thepH_{pzc} of the DKSC. At a pH <pH_{pzc}, the surface charge of DKSC is positive leading to the repulsion of Zr(IV) which results in low Zr(IV) sorption onto DKSC and therefore a low R%. While at a pH>pH_{pzc}, the surface charge of DKSCis negative and therefore Zr(IV) gets sorbed onto the DKSC with greater affinity and consequently R% increases. Since the $pH_{pzc}$of DKSC was 6.72, Zr(IV) sorption will be maximised at pH<pH_{pzc}. The highest Zr(IV) biosorption took place in the pH range of 3-4 because at pH >4 zirconium hydroxides are formed and are precipitated in the aqueous solution. An increase in DKSC loading increased the extent of surface area for sorption making more adsorption sites available for exchange; as a result, the activity of functional groups also increased thereby leading to a higher R% (Serencam et al., 2013, Ozdes et al., 2010, Serencam et al., 2014, Reddy et al., 2010).

(b) Multi-response optimisation via a desirability approach

The desirability approach is an established tool for the optimisation of design variables including single and multiple responses. The standard desirability functions are discussed explicitly in section 3.6.4. Design Expert software was used to find the optimum combination of process variables ($A, B\ and\ C$) that maximised the responses (R%and q_e) using the desirability function simultaneously. A maximum level of initial Zr concentration (A), initial pH (B) within range, a minimum level of DKSC loading (C) and a maximum level of responses (R% andq_e) were set for maximum desirability as shown in Table 5.4.

Table 5.4: Optimisation of individual responses (d_i) to obtain overall desirability response (D).

Factor	Goal	Lower limit	Upper limit	Lower weight	Upper weight	Importance
*Initial Zr Concentration (**A**)*	Maximize	55	75	1	1	5
*Initial pH (**B**)*	Within range	2	4	1	1	1
*DKSC loading (**C**)*	Minimize	3	7	1	1	3
R%	Maximize	38.43	93.72	1	1	5
$\boldsymbol{q_e}$*(mg/g)*	Maximize	4.30	23.46	1	1	5

The results show that the initial pH is the major factor that needs to be considered in the biosorption studies of Zr using DKSC, followed by the DKSC loading and the initial Zr concentration. From 16 starting points in the response surface changes, the best local maximum was found to be at an initial Zr concentration (A)of 74.99 mg/L, an initial pH (B) of 3.58, and a DKSC loading (C) of 3.00g/L, which produced a maximum bio-removal efficiency(R%) of 97.80% and biosorption capacity (q_e) of 23.44 mg/g with overall desirability (D) of 0.99 as shown in Fig. 5.5. To validate the optimised parameters,

confirmatory runs were conducted using process parameters. The experimental results obtained were found to be close to optimised values (Table 5.5).

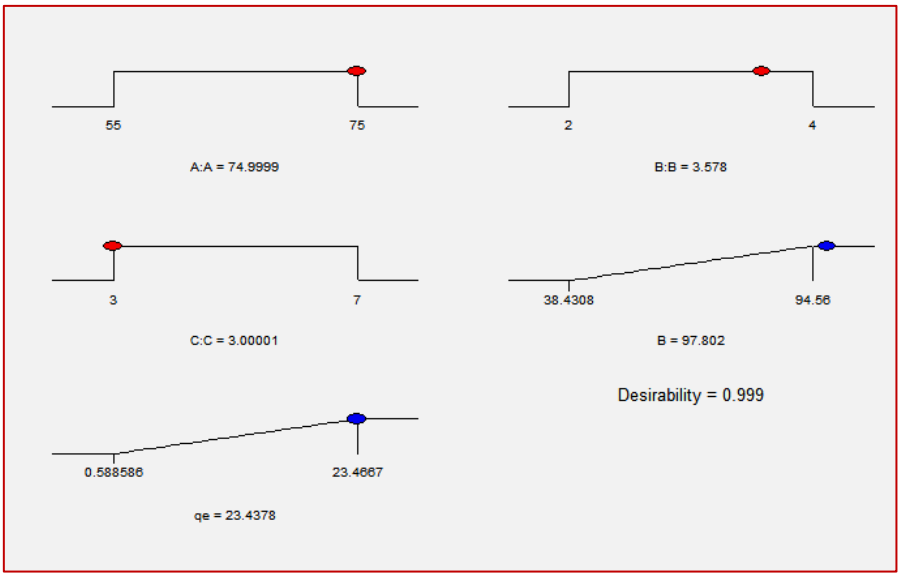

Figure 5.5: Desirability ramp for numerical optimisation of five goals considered

Table 5.5: Optimised and confirmative values of the process parameters for maximum responses ($R\%$ and q_e)

Process parameters	Optimized Values (predicted)	Confirmation Values (experimental)
$\boldsymbol{R}\%$	97.80	95.67
$\boldsymbol{q_e}$, *mg/g*	23.44	22.76
*Initial Zr concentration (**A**), mg/L*	74.99	75
*Initial pH (**B**)*	3.57	3.6
*DKSC loading (**C**), g/L*	3.00	3

5.3.3. Equilibrium studies and adsorption isotherm modeling

Equilibrium studies were carried out using 0.3g of DKSC in 0.1L of working solution. The solutions were mixed at 25^{0}C in a shaker running at 200 rpm for 4 hours. The initial

Zr concentration was varied from 20 to 100mg/L. Fig. 5.6 shows a plot of biosorption capacity (q_e) and distribution capacity (K_d) as a function of equilibrium Zr concentration (C_e). The parameter$q_e$increased considerably with an increase in $C_e$due to the increase in the initial Zr concentration (C_i). As $C_i$increases, the interaction between the sorbate and sorbent also increases (Reddy et al., 2010, Duygu Ozdes et al., 2010, Senthil Kumar et al., 2011). TheK_d value decreased from 2.958 L/g to 1.582 L/g for an increase in C_e ranging from 2 to 16 mg/L at a DKSC loading of 3 g/L. Higher values of K_d were obtained for lower C_e implying an important feature that DKSC has the ability to treat large volumes of low concentration metal wastes. The K_d values achieved in this research were very high when compared to other industrial adsorbents, which have $K_d$values as low as 0.010 L/g (Akhtar et al., 2008).

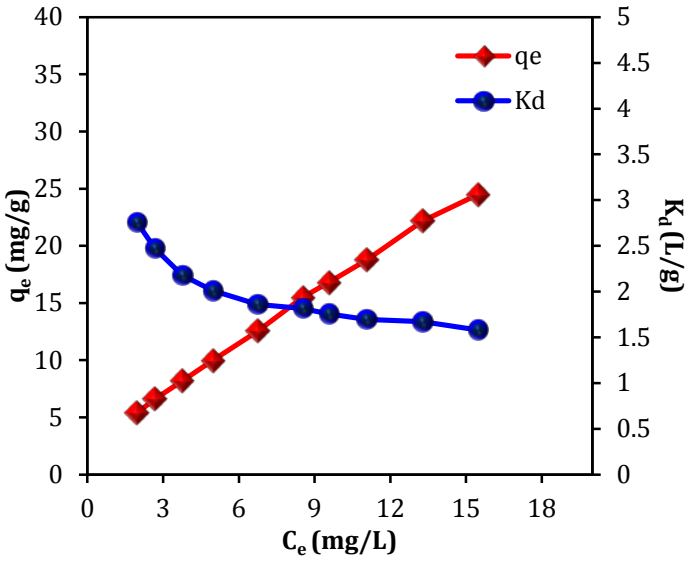

Figure 5.6: q_e and K_d as a function of C_e.

The adsorption isotherms were obtained at a fixed temperature and fixed DKSC loading using isotherm model equations in linearised forms as discussed in Section 2.2.1 (Chapter 2). The graphical representation of model isotherms is shown in Fig. 5.7, and

the calculated model parameters are tabulated in Table 5.6 along with correlation coefficients.

Table 5.6: Isotherm model parameters obtained in the biosorption of Zr(IV) onto DKSC.

Langmuir	**Q_0**	**K_L**	**R^2**	**Freundlich**	**K_{ad}**	**n**	**R^2**
	38.46	0.08	0.98		3.15	1.35	0.99
Temkin	**B**	**A_T**	**R^2**	**D-R**	**q_s**	**K_{ad}**	**R^2**
	0.10	60.81	0.94		17.90	0.14	0.79

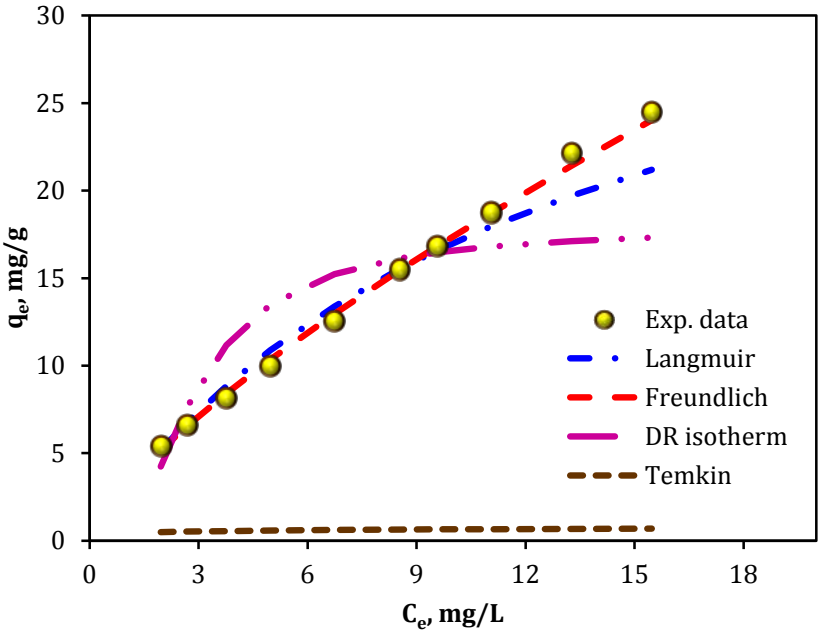

Figure 5.7: Adsorption isotherms at optimised conditions (initial pH: 3.6, DKSC loading: 3 g/L and initial Zr concentration: 18 to 90 mg/L).

High correlation coefficients were obtained for linear plots corresponding to the Freundlich and Langmuir isotherm models indicating that the equilibrium data agreed well with both models thus indicating the heterogeneous multilayer biosorption of Zr(IV) onto DKSC. The parameter values obtained signified a greater extent of biosorption (better K_{ad}) with greater heterogeneity (with $1/n$ = 0.74) and favourable biosorption of Zr(IV) onto DKSC (n=1.35) i.e., indicating the heterogeneous multilayer

adsorption of Zr ions onto DKSC surface (Varala et al., 2016). The $q_{e,model}$ values were estimated from the model equations using regression analysis and are shown in Fig. 5.7 along with experimental data. As can be seen from Fig. 5.7, the Freundlich model fitted the experimental data better compared to other models.

The results suggested that the biosorption of Zr(IV) is proportional to the square of the number of vacant sites on DKSC and the overall rate of biosorption may be affected by chemisorption, i.e., chemical reactions involving an exchange of electrons between DKSC and Zr(IV). Also, the calculated biosorption capacities were comparable to the experimental data within the concentration range used. Most of the previous studies on biosorption reported that the metal biosorption process is a pseudo-second order process and the results of our study confirmed the same (Sharma et al., 2009, Ercan Özdemir, 2011, Ruhan Altun Anayurt, 2009)

5.3.3. Kinetic studies with diffusion and mass transfer modeling

Kinetic studies help to study the effect of contact time and are essential to describe the biosorption rate. The kinetic models assist in determining the rate controlling step for the biosorption process. Kinetic studies in this work were carried out using different initial Zr concentrations of 60 and 80 mg/L in a working volume of 0.2 L using 1.5 g/L DKSC for a constant contact time of 4 hours at 25^0C and using a shaker running at200 rpm.To determine the mechanism of the biosorption process, kinetic models specified in section 2.2.2 (Chapter 2)were applied to the experimental data. The parameters for all kinetic models were calculated from the linear plots and are tabulated in Table 5.7 along with their correlation coefficients. On close examination of correlation coefficients, it can be found that the pseudo-second order model leads to the

best correlation (R^2= 0.99 for 60mg/L and 0.994 for 80 mg/L) for the kinetic data compared to other models.

Table 5.7: Kinetic model parameter values for Zr(IV) sorption onto DKSC.

60 mg/L		*80 mg/L*	*60 mg/L*		*80 mg/L*
Pseudo-first order			***Intraparticle diffusion***		
q_e (exp)	3.04	7.87	q_e (exp)	3.04	7.87
q_e	1.36	4.59	k_i	0.067	0.23
k_1	0.01	0.01	C	1.8	4.19
R^2	0.81	0.88	R^2	0.94	0.81
Pseudo-second order			***Elovich***		
q_e (exp)	3.04	7.87	q_e (exp)	3.04	7.87
q_e	2.89	8.06	A	21.09	5.21
k_2	0.03	0.09	A	3.49	0.90
H	7.77E-4	7.95E-5	B	3.49	0.90
R^2	**0.99**	**0.99**	R^2	0.85	0.89

5.3. Conclusions

The present research focused on the utilisation of an agro-industrial waste biomass namely DKSC as a sorbent for the biosorption of Zr(IV) from aqueous solutions. Multivariate optimisation was carried out for the process variables namely initial Zr concentration, initial pH, and DKSC loading, using Box-Behnken design in RSM along with desirability approach for maximum bio-removal efficiency (R%) and biosorption capacity (q_e).Regression analysis showed that a quadratic model provided the best fit to the experimental data with a coefficient of determination (R^2) value of 0.98 and F-Value of 26.96. The desirability function recorded a maximum R% of 97.8% and a $q_e$of 23.44 mg/g for an initial metal concentration of 74.99 mg/L at a pH of 3.57 and for3.00 g/L of DKSC loading. At a desirability value of 0.99, these conditions were confirmed as the optimised process conditions. The equilibrium data agreed well with the Freundlich

isotherm model and the kinetic data agreed well with a pseudo-second-order equation with a correlation coefficient of 0.99 for the concentration range considered. Data for the distribution coefficient (K_d) obtained in the present study was 2.96 L/g which is much higher than those of other industrial adsorbents.

Chapter 6

Desorption studies for the isolation of radionuclides from loaded biomass

Summary

This chapter focuses on the efficient individual recovery of the radionuclides (Th and Zr) from the loaded DKSC using different eluting media. The desorption step is useful in the isolation of sorbed metal ions as well as in the regeneration of loaded biomass that can be reused in further cycles. The primary factors affecting the desorption were optimised employing the Taguchi L_{18} $(2^1 3^2)$ *mixed level design for the maximum desorption efficiency*$(D\%)$ *and it was found that the eluent concentration was the major factor in desorption. The optimised conditions were found to be as follows: 1M HCl at an L/S ratio of 7 with a recovery of 96%, and 0.1M* $NaHCO_3$ *at an L/S ratio 3 with a recovery of 69% for thorium and zirconium, respectively. It was also proved that the desorption step regenerated the biosorbent which possesses properties similar to that of native DKSC. The desorption kinetics for both thorium and zirconium followed the pseudo-second order rate equation at optimal conditions.*

6.1. Introduction

Desorption of metal ions from loaded biosorbents is accomplished using an elution process that involves the use of an appropriate eluting/desorbing medium (Elwakeel et al., 2014, Elwakeel et al., 2017).The mechanisms of desorption and biosorption are similar with both involving ion exchange. The detailed mechanisms involved in the desorption process were discussed explicitly in Chapter 2(Literature review).

6.2. Experimental investigations

The detailed experimental procedures used for the desorption studies were described in section 3.5.2 (Chapter 3).

(a) Preliminary studies:

Screening experiments were carried out using eight eluents containing competing counter ions (sodium cations), proton exchangers (mineral acids) and complexing agents (chlorine, carbonate and bicarbonate anions). These were used to treat the metal-laden biomass to recover the sorbed metal ions, to determine an effective desorption technique based on the desorption efficiency ($D\%$), and to ascertain the elution potential of each eluent towards the desorption of radionuclides (Th and Zr) from loaded biomass. The L/S ratio and the eluent concentration used in the experiments are shown in Table 6.1.

Table 6.1: Range of parameters considered for the desorption studies

Parameters	Range
Eluent type	HNO_3, HCl, H_2SO_4, NaOH, NaCl, CH_3COONa, Na_2CO_3, $NaHCO_3$
L/S ratio	1
Eluent concentration	0.1M

(b) Taguchi L_{18} ($2^1 3^2$) OA experimental design for metal elution:

A Taguchi orthogonal array L_{18} ($2^1 3^2$) design consisting of 3 factors having mixed levels (one factor at two levels and two factors at three levels) was employed to examine the influence of process variables such as eluent type, eluent concentration, and L/S ratio on the desorption efficiency ($D\%$) for the desorption of thorium and zirconium from loaded biomass. Three typical eluent concentrations of 0.01, 0.1 and 1M were tested along with an L/S ratio in the range 3-10. The factors and their levels were selected based on the preliminary assessment and are shown in Table 6.2. MINITAB17 statistical software (free trial) was used for the generation of the experimental design matrix involving the chosen factors at their respective levels as shown in Table 6.3. $D\%$ was

chosen as the response variable in the present study, and the target was to achieve a higher *D*%; hence, the larger-is-better criterion was selected for the S/N ratio (Equation 3.9).

Table 6.2: Factors and levels considered for the Taguchi mixed design L_{18} ($2^1 3^2$) model.

Factors/Levels		***1***	***2***	***3***	***1***	***2***	***3***
		Thorium desorption			*Zirconium desorption*		
Eluent	*A*	HCl	HNO_3	-	H_2SO_4	$NaHCO_3$	-
L/S ratio	*B*	3	7	10	3	7	10
Eluent Concentration (M)	*C*	0.01	0.1	1	0.01	0.1	1

Table 6.3: Taguchi L_{18} orthogonal array design for the desorption process

Experiment run order	***Eluant***	***L/S ratio***	***Eluant concentration***	***Thorium desorption***		***Zirconium desorption***	
				D%	*S/N ratio*	*D%*	*S/N ratio*
1	1	1	1	7.42	17.41	40.54	32.16
2	1	1	2	42.81	32.63	54.90	34.79
3	1	1	3	92.18	39.29	5.63	15.01
4	1	2	1	24.61	27.82	0.18	14.90
5	1	2	2	82.59	38.34	58.13	35.29
6	1	2	3	96.00	39.64	8.43	18.52
7	1	3	1	17.94	25.08	0.56	5.04
8	1	3	2	14.18	23.03	62.60	35.93
9	1	3	3	66.61	36.47	1.03	0.26
10	2	1	1	13.39	22.53	5.89	15.40
11	2	1	2	69.74	36.87	69.15	36.79
12	2	1	3	90.54	39.14	69.82	36.88
13	2	2	1	28.06	28.97	12.25	21.76
14	2	2	2	63.44	36.05	76.10	37.63
15	2	2	3	83.51	38.43	59.05	35.42
16	2	3	1	1.89	5.53	18.85	25.51
17	2	3	2	56.10	34.98	62.60	35.93
18	2	3	3	73.47	37.32	69.08	36.79

6.3. Results and discussion

6.3.1. Preliminary studies:

The results obtained in the preliminary evaluation are shown on a Pareto chart (Fig. 6.1). As shown in the figure, the results indicated that both HNO_3 and HCl achieved satisfactory values for D% in the metal elution process for thorium. This was due to protonation of carboxyl, carbonyl or hydroxyl groups of the biomass all of which do not attract the positively charged thorium (Th^{+4}) ions.Therefore, the protons replace the bound thorium ions and release the thorium ions into the recovery solution (Wankasi et al., 2005). Similarly, $NaHCO_3$ and HNO_3 led to the highest values of *D*% in the desorption of zirconium.

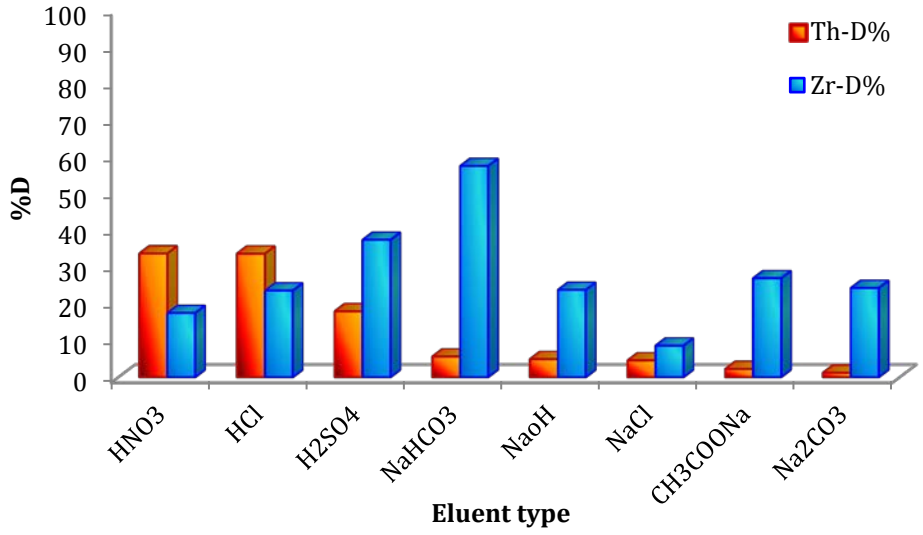

Figure 6.1: Preliminary studies for desorption of thorium (Th-D%) and zirconium (Zr-D%) (0.1M concentration, L/S ratio: 1, 200 rpm and 25°C)

The recovery of Th and Zr in the elution step decreased depending on the recovery media according to the following order;

Thorium desorption : HNO_3 > HCl >H_2SO_4 > $NaHCO_3$ >NaOH>NaCl> CH_3COONa > Na_2CO_3

Zirconium desorption: $NaHCO_3$ > H_2SO_4 > CH_3COONa > Na_2CO_3 >NaOH> HCl > HNO_3 >NaCl.

Based on the results, the eluents HNO_3 and HCl for thorium, and $NaHCO_3$ and HNO_3 for zirconium were chosen for further optimisation studies using the Taguchi design. During desorption experiments, the colour of the biomass was noted to change both in the acidic and basic media in proportion to their strength. Also, the eluate was found to change in colour after desorption as the soluble proteins are eluted from the biomass (ALDOR et al., 1995, Jnr, 2006)).

6.3.2. Statistical significance and optimisation of thorium and zirconium desorption using the Taguchi L_{18} mixed level array design

The experiments were conducted using the Taguchi L_{18} mixed level design matrix (Table 6.3). *D*%was chosen as the response in the optimisation method. The results obtained from the experimental runs were transformed into an S/N ratio (larger-is-better criterion) as the aim was to maximise D%. The Minitab17 statistical software was used for the interpretation of results which are shown in Table 6.3.

(a) Thorium elution from loaded biomass (Th-DKSC)

Response tables for the calculated S/N ratios are shown in Table 6.4. It can be interpreted from the data shown in the table that eluent concentration was the predominant factor that influenced the thorium desorption significantly, followed by L/S ratio and eluent type.

Table 6.4: Response table for S/N ratio (larger-is-better) in the thorium desorption studies

Factors/Levels	Eluent	L/S ratio	Eluant concentration
1	31.08	31.31	21.22
2	31.09	34.87	33.65
3	---	27.07	38.38
Delta	0.01	7.81	17.16
Rank	**3**	**2**	**1**

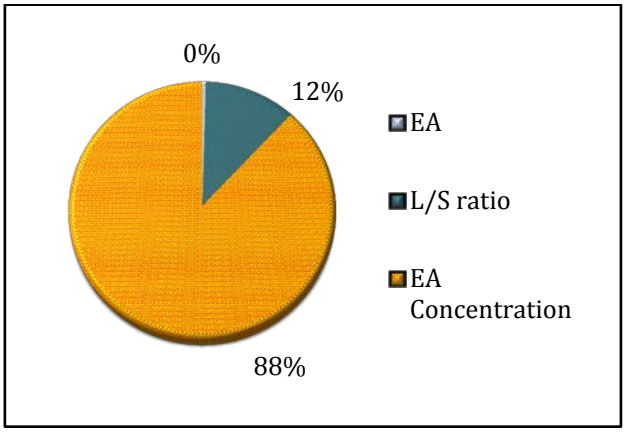

Figure 6.2: Percentage Contribution of factors for thorium desorption

Fig. 6.2 depicts a pie chart showing the percentage contribution (PC) that was calculated using the sum of squares (*SS*)calculated using equations 3.14 to 3.16 (Section 3.6.3). The chart emphasises the significance of the corresponding factor in the process under consideration (Sayanasree et al., 2016). The pie graph further illustrates that the eluent concentration is the leading factor with the highest level-of-significance, contributing 88% for the recovery of thorium. In comparison, the L/S ratio contributed only 12% and eluent type provided the least (nearly 0%) in predicting the desorption efficiency.

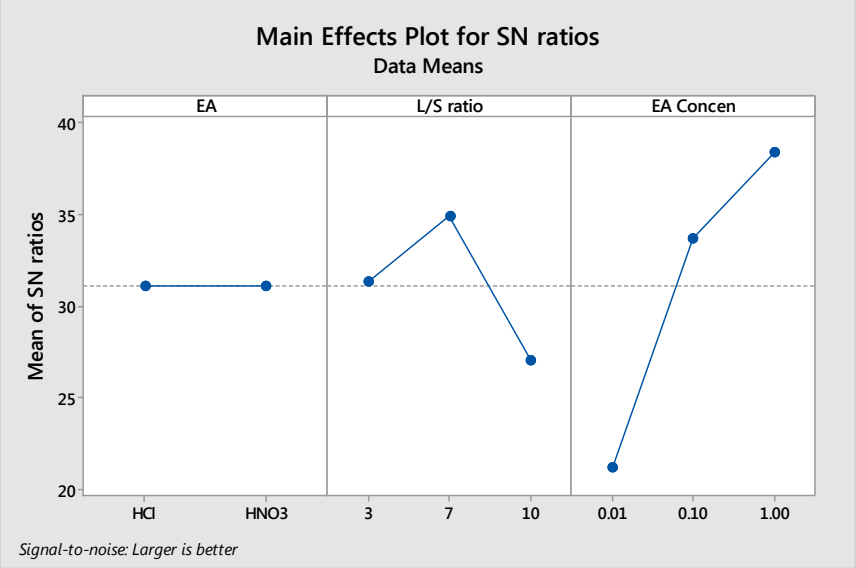

Figure 6.3: Main effect plots of factors by S/N ratios (larger-is-better) for thorium desorption.

Fig. 6.3 shows the main effect plots for three factors (eluent, L/S ratio, and eluent concentration) and S/N ratios (larger-is-better) calculated (obtained from Table 6.3) for thorium in the desorption studies. For the recovery of thorium, both eluents (Eluting agents) HCl and HNO_3 were judged to be suitable due to the fact that thorium metal ions can be desorbed using acidic solutions (Gok and Aytas, 2013, Bhalara et al., 2014, Sayanasree Varala and Satyavathi, 2016, VOLESKY, 1981)Generally, $D\%$ increased with increasing L/S ratio and q_{des}also increased due to the high metal concentrations released into the eluent. A very large increase in L/S ratio results in a decrease in $D\%$ due to an increased accumulation of metal ions over the biomass leading to a new equilibrium. It is preferable to use low L/S ratios because high metal concentration can be achieved using a small volume of eluent (Vı´tor, 2007). An increase in eluent concentration increases $D\%$ due to the accumulation of H^+ ions in the eluant solution that increase the concentration gradient between metal ions and protons and result in an enhancement of the driving force for ion-exchange, thus replacing the metal ions over the biomass surface (Zhang and Wang, 2015, Jnr, 2006). The optimised conditions

can be assessed as $A_1B_2C_3$ and $A_2B_2C_3$i.e., an eluent HCl/HNO_3 of 1M concentration at a L/S ratio of 7 that led to D% values of 96% and 83% (Experiment run order 6 and 15 in Table 6.3) from the Taguchi OA design for thorium. As the $A_1B_2C_3$ combination leads to a maximum D%, these conditions were chosen as the best optimum process parameters for the effective recovery of thorium metal ions from loaded DKSC (Th-DKSC).

(b) Zirconium elution from loaded biomass (Zr-DKSC)

Table 6.4 shows the response tables obtained for the calculated S/N ratios (larger-is-better). It was found that eluent concentration was the major factor that influenced the response most thus ranking first in the zirconium desorption. This was followed by eluent type and L/S ratio of ranks 2 and 3, respectively.

Table 6.5: Response table for S/N ratios (larger-is-better) in the zirconium desorption studies

Factors/Levels	Eluent type	L/S ratio	Eluent concentration
1	16.89	28.51	12.48
2	31.35	22.29	36.06
3	---	21.56	23.81
Delta	14.46	6.94	23.58
Rank	***2***	***3***	***1***

The pie graph (Fig. 6.4) illustrates that eluent concentration is the main factor with the highest level-of-significance contributing 75% for the recovery of zirconium from the loaded biomass. The L/S ratio and eluent type are the second and third major factors contributing 24% and 1% towards predicting the desorption efficiency of zirconium.

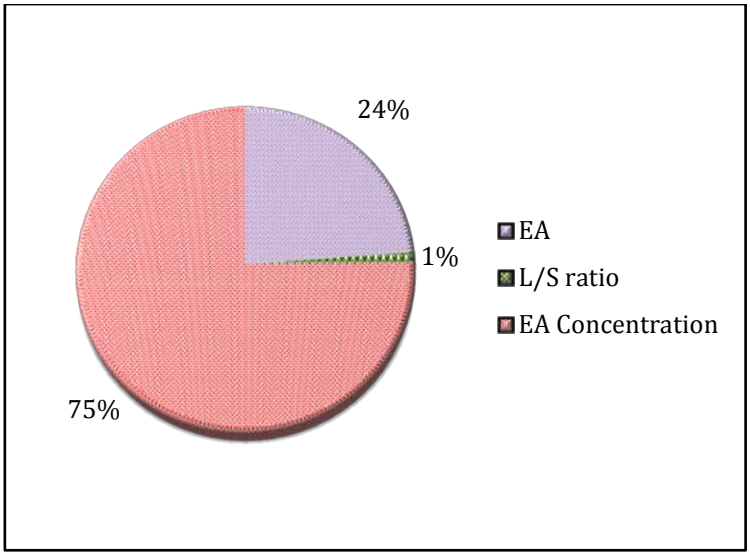

Figure 6.4: Percentage Contribution of factors for zirconium desorption.

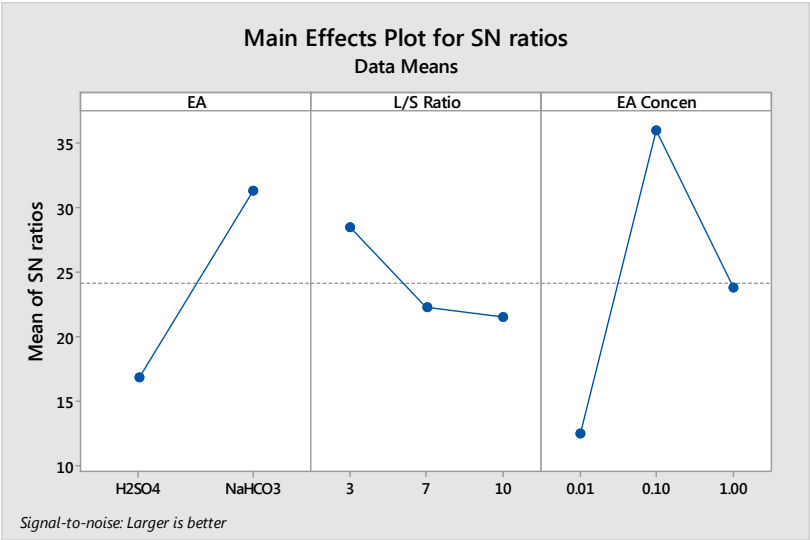

Figure 6.5: Main effect plots of factors by S/N ratios (larger-is-better) in zirconium desorption

The performance of H_2SO_4 and $NaHCO_3$ as eluting agents for zirconium desorption can be explainedby considering the concentration of the eluting agents. Fig. 6.5 displays the main effect plots of factors by S/N ratios (larger-is-better) in zirconium desorption. An increase in eluent concentration leads to an increase in *D*% up to a certain limit and then decreases because a higher number of protons increases the electrostatic repulsion among metal ions thus inhibiting the desorption process. Thus,

the optimised conditions obtained are$A_2B_1C_2$ i.e., 0.1M of the $NaHCO_3$ solution at a L/S ratio of 3 that leads to 69% for D% (Experiment run order 11 in Table 6.3) from the Taguchi OA design for zirconium recovery. In the first cycle of the desorption, 69% of the Zr has been recovered from the loaded biomass. The sorbent can only be recycled after the complete recovery of Zr from the loaded biomass, which means a few more desorption cycles have to be carried out before the biomass is reused.

The results attained in this work agree with the results of many previous studies reported in the literature (Gok and Aytas, 2013, Anirudhan et al., 2010, Akhtar et al., 2008, Bhalara et al., 2014, A. Hanif, 2013). The optimal combinations recommended by the Taguchi mixed level design for the desorption of radionuclides (Th and Zr) were already present in the experimental design; hence no further experimental runs were required for confirmation.

6.3.3. Desorption kinetics evaluation

The experimental kinetic data was validated using linearised pseudo-first order and second order desorption kinetic models (Table 2.3, Chapter 2). The model parameters computed are shown in Table 6.6 along with regression coefficients (R^2).

Table 6.6: Kinetic model parameters obtained for thorium and desorption under optimised experimental conditions.

Radionuclide	q_e, exp	Pseudo first order			Pseudo second order		
		k_{1d}	q_e,model	R^2	k_{2d}	q_e, model	R^2
Thorium	13.19	0.01	98.75	0.85	0.01	13.33	**0.99**
Zirconium	1.52	0.01	8.06	0.98	0.03	1.49	**0.98**

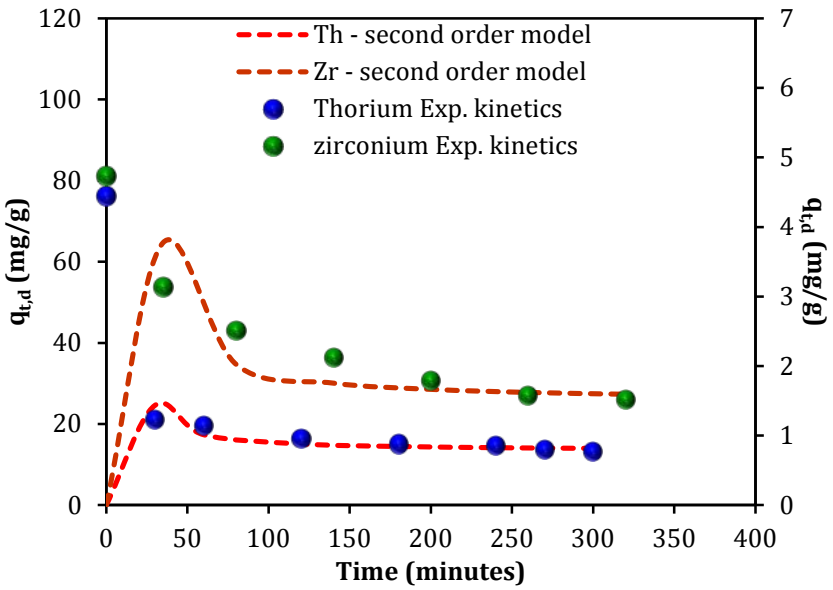

Figure 6.5: Desorption kinetics at optimum process conditions.

Among the two models verified for the desorption kinetics, the pseudo-second order model was shown to provide a better association with the experimental data with *an* $R^2 \geq 0.98$ (higher than the R^2 values obtained for the pseudo-first order model) thus indicating that the desorption kinetics for both thorium and zirconium follow pseudo-second order kinetics. Although pseudo-first order kinetic model also exhibit a good fit to experimental data with $R^2 > 0.97$ for zirconium desorption, the equilibrium value calculated from the model ($q_{e,m}$, model) was significantly higher than the one calculated from the experimental data (q_e, exp). The close agreement between the equilibrium capacity ($q_{e,m}$, model) values predicted using the pseudo-second order model equation and the experimental values (q_e, experimental) show the capability of the model equation in predicting the desorption kinetics for both Th and Zr. This observation was further confirmed by the close agreement between the experimental values of q_e and those predicted by the pseudo-second order model (dashed line) shown in Fig. 6.5 which suggests that the desorption mechanism is due to an ion exchange reaction between the eluant and sorbed metal ions onto the biosorbent across the active sites.

The observations in the present research agree with findings reported in many previous studies in the literature (Njikam and Schiewer, 2012, Jyi-Yeong Tseng and Dar-Ren Ji, 2009, Akin sahbaz, 2015).

6.4. Conclusions

The reversibility of the biosorption process through a desorption method for the recovery of the radionuclides Th and Zr from loaded biosorbentwas investigated to establish a regeneration step for biomass. The process variables that affect the recovery were optimised using the Taguchi mixed level design $L_{18}(2^1 3^2)$ for the maximum desorption efficiency. From the research carried out, it can be concluded that 1M HCl and 0.1M $NaHCO_3$solutions can be used for the efficient recovery of Th and Zr from loaded DKSCwith a maximum $D\%$ of 96% and 69% at a L/S ratio of 7 and 3, respectively. The desorption trend followed pseudo-second order kinetics with calculated R^2> 0.98 for both Th and Zr.

Chapter 7

Characterisation of deoiled Karanja biomass, a novel biosorbent for radionuclides

Summary

The present chapter describes the characterisation of a biosorbent, namely deoiled Karanja biomass. The information about the biomass is not available in the literature. Hence, the characteristics of deoiled Karanja biomass as a sorbent and its behavior in the biosorption and desorption processes wereexplored. The DKSC was characterised using SEM, FTIR and standard NREL methods to determine the possible mechanism involved in the biosorption and desorption studies involving Th(IV) and Zr(IV). SEM analysis demonstrated that a physical pre-treatment method followed increased the porosity and therefore the surface area of the biosorbent. FTIR spectroscopic analysis confirmed the participation of methyl, carboxyl, amine, alkane and nitro functional groups in the biosorption process and the same functional groups were re-established in the desorption process thus validating the regeneration of biomass.

7.1. Introduction

The application of deoiled Karanja biomass as a novel sorbent for the separation of radionuclides from aqueous streams was discussed in previous chapters. This study established the agro-industrial waste as a sorbent for the isolation of Zr and Th radionuclides from aqueous streams. This process can be modified further and adapted as a pollution control technology in nuclear industries dealing with radionuclide waste materials. However, to know the performance of deoiled Karanja biomass as a sorbent in the biosorption of thorium and zirconium, the characteristics of the sorbent need to be identified, and thus the characterisation of deoiled Karanja biomass is necessary. The general characterisation techniques used for the various adsorbents were discussed in Chapter 1 (Introduction).

7.2. Materials and Methods

The materials and methods employed to carry out the present research were described in Chapter 2 (Materials and Methodology).

7.3. Results and Discussions

The DKSC obtained from the local market was pre-treated before using it as a sorbent in the biosorption process as discussed in Section 3.2.1. The metal loaded DKSC and regenerated DKSC was washed with demineralised water on filter paper, dried and subjected to various characterisation techniques. SEM and FTIR analyses, physicochemical properties determination, and elemental analysis was carried out for the native DKSC, the metal loaded DKSC and the regenerated DKSC. The biomass samples are hereafter denoted as DKSC, Th-DKSC, Zr-DKSC, R_DKSCTh andR_DKSC^{Zr} for the pre-treated biomass (sorbent), the thorium-loaded biomass, the zirconium-loaded biomass, and the regenerated biomasses obtained from the thorium and zirconium desorption studies, respectively.

7.3.1. Physico-chemical properties determination through standard NREL methods

Deoiled Karanja biomass was characterised by determining its physicochemical properties using standard National Renewable Energy Laboratory – Laboratory Analytical Procedures (NREL-LAP) and ultimate (CHNS) analyses. The results of the analyses are shown in Table 7.1 for the pre-treated, the metal-loaded and the regenerated DKSC.

Table 7.1: Physico-chemical properties of DKSC at various stages of biosorption and desorption processes.

Properties	DKSC	Th-DKSC	Zr-DKSC	R_DKSCTh	R_DKSC^{Zr}
pH	4.92	3.36	3.55	4.83	4.54
Moisture Content	5.60	8.10	7.32	4.90	4.76
Bulk density (g/cm3)	0.451	0.22	0.31	0.43	0.41
Surface area (m2/g)	119	---	58.2	121	125
pH_{pzc}	6.72	---	---	6.03	6.45
Ultimate (CHNS) Analysis					
C%	50.90	49.08	51.00	49.26	50.23
H%	6.65	7.06	7.96	6.54	6.12
N%	4.44	3.43	3.63	4.27	4.01
S%	0.17	0.14	--	0.13	0.19

R_DKSCTh-Regenerated biomass from thorium desorption

R_DKSC^{Zr}-Regenerated biomass from zirconium desorption

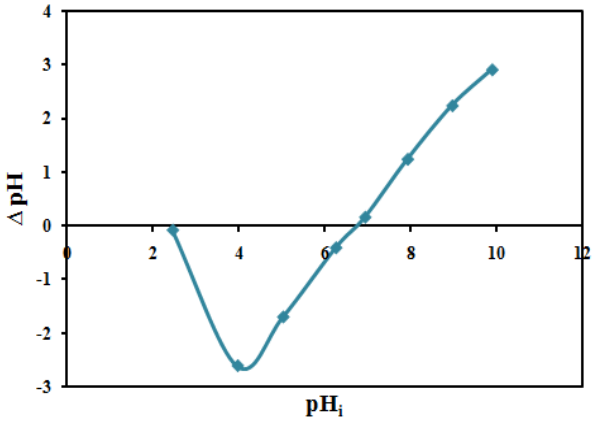

Figure 7.1: ΔpH versus pH_i for the determination of pH_{pzc} of DKSC.

The pH_{pzc} or point zero charge of the sorbent depends on the pH of the metal solution in which the sorbent is suspendedforadsorption. It is an essential characteristic that aids in the determination of the pH at which the sorbent surface has net electrical neutrality. From Table 7.1, it can be concluded that regenerated biomass (R-DKSCTh and

R-DKSC^{Zr}) is analogous to native DKSC in its physicochemicalcharacterisation. In addition to these, the values obtained for the pH_{pzc} of the R-DKSC were consistent with those ofthe native DKSC which indicates that the elution process could regenerate DKSC with properties that are similar to those of pure DKSC.

7.3.2. Fourier Transform Infrared Spectroscopic (FTIR) analysis

FTIR analysis was used to understand and identify the functional groups that participate in the biosorption process.

Native (pure) DKSC; Data shown in Fig.7.2(a) and Fig. 7.3(a) correspond to FTIR spectra of native DKSC before biosorption. The IR spectrum containsfive major peaks at 2925.17, 2854.28, 1709.51, 1628.36, 1106.01, 1027.0cm^{-1}, and also several broad peaks at 3567.69, 3448.96, 1516.02, 1406.18, 1241.81 and 723.93 cm^{-1}. The broad peaks observed at 3567.69cm^{-1} and 3448.96cm^{-1} indicate –OH (alcoholic) and/or N-H(amino) symmetrical stretching groups respectively, while the strong peaks near 2925.17cm^{-1} and 2854.28cm^{-1} correspond to the CH_2symmetrical stretching vibration of the methyl functional group. Other sharp peaks at 1709.51cm^{-1} and 1628.36cm^{-1} may be due to C=O stretching vibrations of the amide group and indicates the presence of either carboxylic (-COO) or quinone (-C=O) groups. A peak at 1516.02cm^{-1} is due to the asymmetric stretching of –NO nitro group, whereas the one at 1460.18cm^{-1} corresponds to the C=O stretching vibration of the amide group. A broad peak observed at 1241.81cm^{-1} is due to a –C-O stretching vibration and/or a –C-O-H asymmetric stretching vibration of the COOH group, and the strong peak observed at 1027.0cm^{-1} indicates a –C-N stretching vibration, while the band at 760.39 cm^{-1} represents the C-H bend of aromatics. These observations confirm the presence of various ionizable functional groups such as hydroxyl, amine, methyl, carbonyl, and carboxyl on DKSC (Deschatre et al., 2015). The

IR spectrum of the metal loaded DKSC (Th-DKSC and Zr-DKSC) is displayed in Fig.7.2(b) and Fig.7.3 (b). It can be seen that they are different from the IR spectrum of pure DKSC. The variations in the IR spectra of the metal loaded DKSC compared to pure DKSC, especially the modifications in the absorption bands in lower or higher wave numbers, indicates the interaction of the functional groups with the radionuclides. An absorption band transfer to lower frequencies designates a weak bond while a shift to higher frequencies indicates a stronger bond (Yuvaraja et al., 2014, G. Yuvaraja, 2014).

Thorium-loaded DKSC (Th-DKSC) (Fig. 7.2(b)): Compared to the spectrum of the original sample (before biosorption), an appearance of a new broad envelope near 3403.89 cm^{-1} in the spectrum of the loaded DKSC is due to the physical adsorption of water molecules and also due to the binding of thorium with hydroxyl and amino groups, i.e., proteins(Yusan et al., 2012, Yuan-You Feng Su Tang Jun Liu Ning, 2015)).Enhancement with a shift in the band at 2924.61 cm^{-1} (originally at 2925.17 cm^{-1}) and an appearance of a prominent band at 2851.54 $cm^{-1}$are both an indication of the increase in aldehydicC-H and alkane C-H stretching vibrations due to the formation of the metal complex after biosorption. A new sharp band at 1517.20 cm^{-1} and the reduction and shift of the band at 1637.65 cm^{-1} (originally at 1628.36 cm^{-1}) represents the possible bonding of amine -NH or amides (–C=O) with Th(IV). The appearance of a sharper peak which has shifted from1460.18 to 1459.07 cm^{-1}can be attributed to increasing interaction of Th(IV) with carboxylic (-COOH) groups during metal complexation reactions. A change of the band at 1025.02 cm^{-1} (originally at 1027.00 cm^{-1}) and a dampening of the band at 1155.10 cm^{-1} are due to a weak electrostatic interaction of Th(IV) with DKSC. Two new weak bands at 760.09 cm^{-1} may be attributable to C-H bending bonds of aromatics after biosorption, and the band at

719.94 cm^{-1}can be assigned to weakly bonding of oxygen atom with thorium as Th-O and O-Th-O bonds (Boveiri Monji et al., 2014, Anirudhan et al., 2010). These shifts may be acknowledged as the biosorption of Th(IV) ions onto DKSC associated with amine/amides, carboxyl, and alkyl functional groups through strong complexation reactions and weak electrostatic forces.

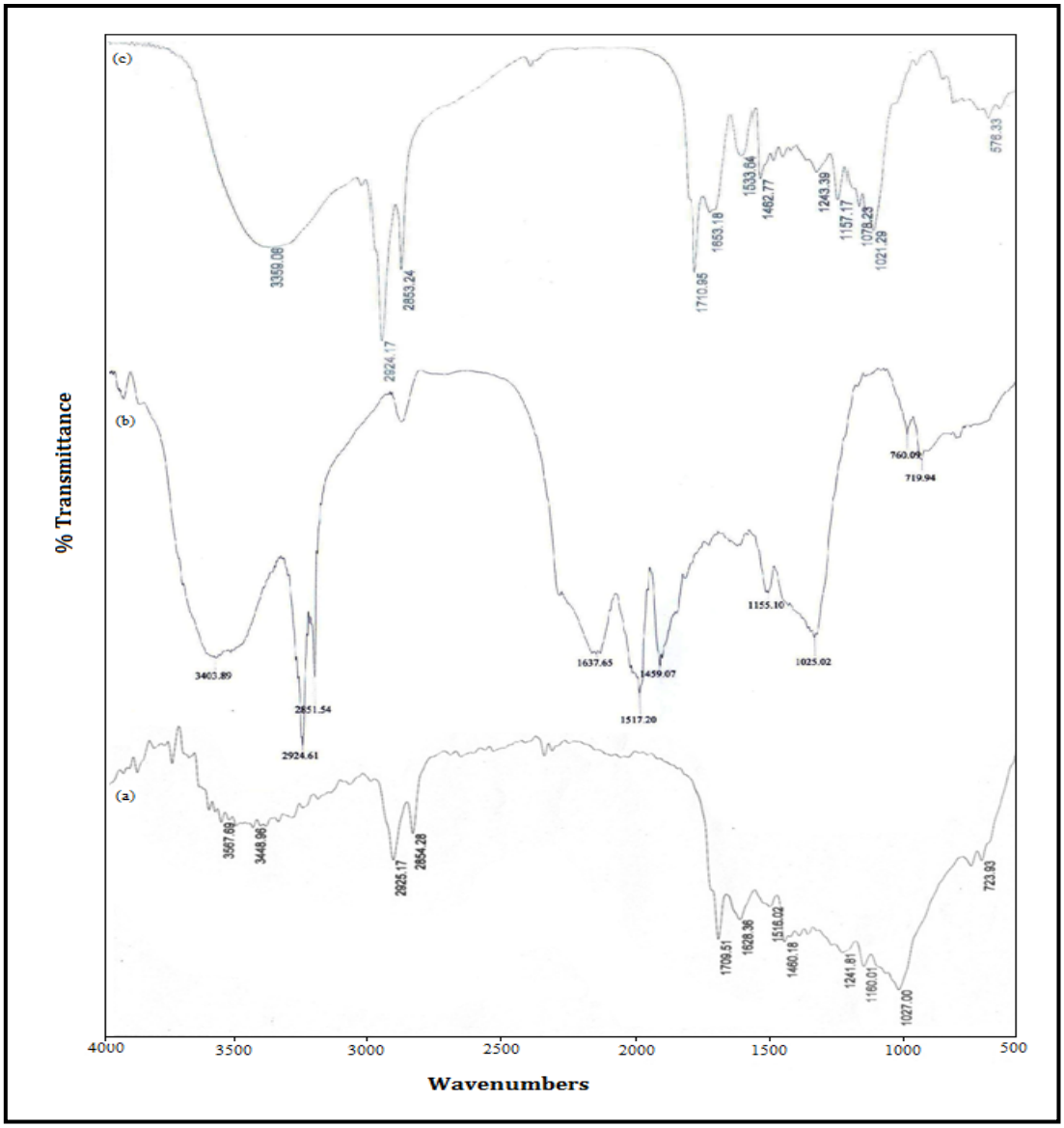

Figure 7.2: FTIR spectrum of (a) Pure DKSC, (b) thorium-loaded DKSC (Th-DKSC) and (c) Regenerated DKSC (R-$DKSC^{Th}$).

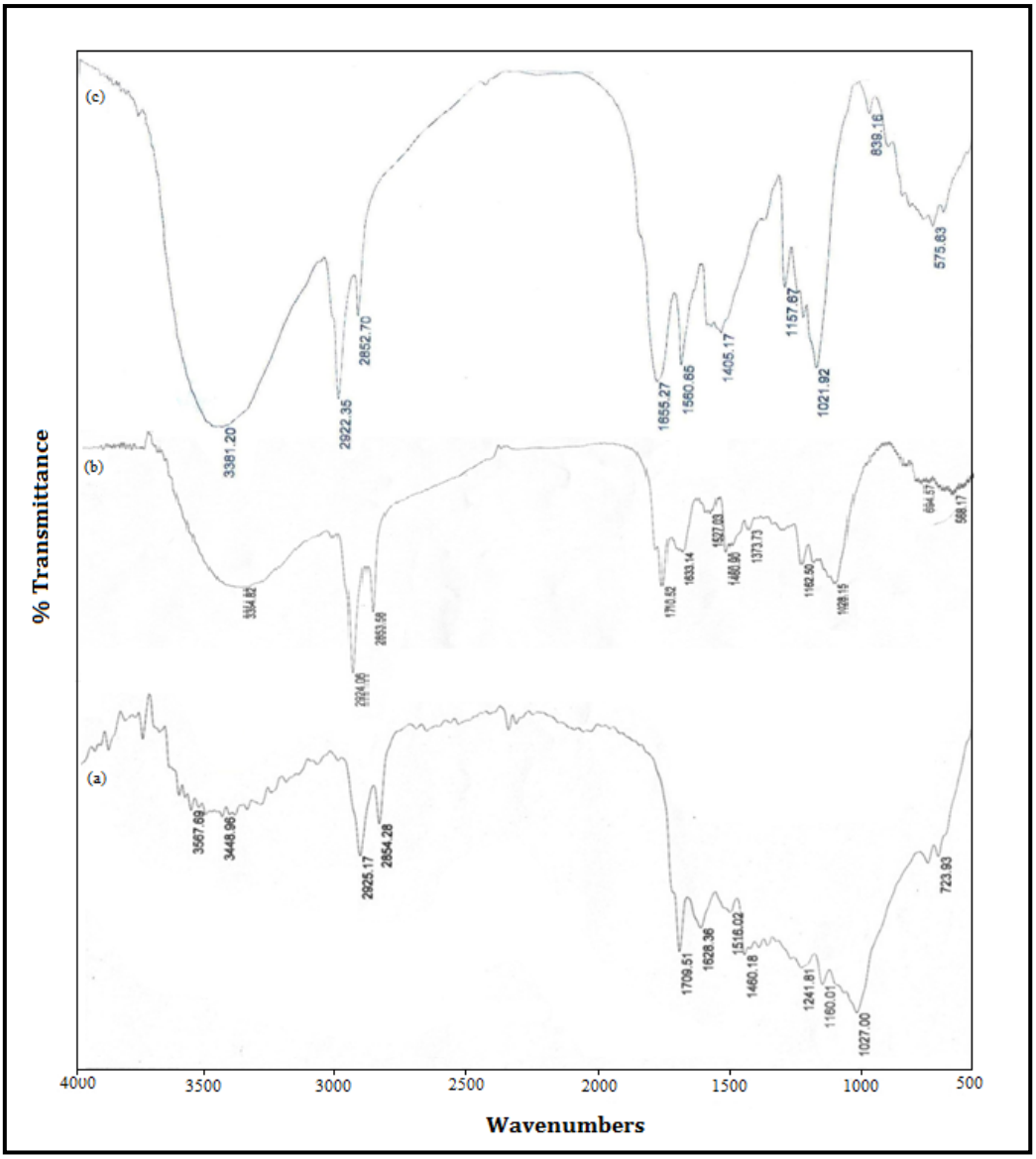

Figure 7.3:FTIR Spectra of (a) Pure DKSC, (b) zirconium-loaded DKSC (Zr-DKSC) and (c) Regenerated DKSC (R-DKSC^{Zr}).

Zirconium loaded DKSC (Zr-DKSC); Fig. 7.3(b) shows the IR spectra of the zirconium-loaded DKSC. After biosorption, five sharp peaks were observed near the frequencies 2924.06, 2853.58, 1710.52, 1460.90, 1162.50cm^{-1}. Similarly broad peaks were seen at 3354.82, 1633.14, 1527.03, 1373.73, 1028.14, 694.57, and 568.17cm^{-1}. Two wide peaks (initially at 3567.69 and 3448.96 cm^{-1}) dissipated and a new peak emerges in the range 3354.82cm^{-1} due to the O-H stretching vibration of aliphatic groups such as alcohols and

carboxylic acids in cellulose and lignin after biosorption (Ai et al., 2013). The two sharp peaks over 2924.06 and 2853.58cm^{-1} (previously at 2925.17 and 2854.28cm^{-1}) were due to C-H symmetrical stretching vibrations of the methyl group. A sharp peak shifted from 1709.51 to 1710.52 cm^{-1} due to the –C=O stretching of COOH group. Also, a wide peak has shifted to 1633.14 (previously at 1628.36cm^{-1}) due to the asymmetric stretching of C=O, C-O and O-H in the fingerprint region (Senthil Kumar et al., 2011). Shifting of the peak from 1516.02 to 1527.03cm^{-1} resembles the asymmetric stretching of a N-O nitro group. The sharp peak at 1460.18cm^{-1}shifted from 1460.90cm^{-1} due to C=O stretching vibration of the amide group. After biosorption, a new peak appeared at 1373.73 cm^{-1} due to a weak symmetrical stretching of the CH_3 group. The sharp peak at 1028.15 cm^{-1}becomes a broad peak after biosorption affecting the C-N stretching vibration. Two new peaks appeared at 594.57 and 568.17cm^{-1} due to the asymmetric stretching vibration of metal ion (Zr-O) and the stretched vibration of weakly bonded oxygen with zirconium. From these observations, the active groups namely methyl, carboxylic, amine and nitro groups played a major role in Zr(IV) metal biosorption onto DKSC. Numerous authors have reported that these are the potential functional groups that are responsible for binding metal ions in the biosorption process (Zolgharnein et al., 2013, Duygu Ozdes 2010, Huseyin Serencam, 2014, Ruhan Altun Anayurt, 2009)).

Regenerated DKSC (R-DKSCTh and R-DKSC^{Zr}); Fig. 7.2 (c) and Fig. 7.3(c)show the FTIR spectra of regenerated biomass obtained from thorium and zirconium desorption process using HCl and $NaHCO_3$ as eluents, respectively.The IR spectrum of R_DKSC (R-DKSCTh and R-DKSC^{Zr}) is similar to that of native DKSC consisting of similar absorption bands in the single and triple bonds region. Furthermore, most of the absorption bands in the fingerprint region of the spectrum coincide with those of pure DKSC. These

observations establish an impression that the desorptionprocess used in this work hasregenerated the biomass with characteristics that are similar to those of pure biomass thereby allowing the regenerated biomass to be reused in multiple biosorption/desorption process cycles.

Table 7.2: Comparision of Shifts in FTIR spectra.

Radionuclide	Band (cm^{-1})	Assignment
Th	3403.89	O-H Stretching
	2924.61	Rocking aldehydic C-H
	2851.54	Oscillation of alkanes C-H
	1637.65	Rocking amides (-C=O) group
	1517.20	Wobbling of amine (-NH)
	1459.07	Rocking carboxylic groups (-COOH)
	760.09	Stretching of C-H bonds of aromatics
	719.94	Weak oxygen bond with thorium ions
Zr	3354.82	O-H stretching vibration of aliphatic groups
	2924.06 and 2853.58	Rocking symmetrical stretching of methyl group
	1710.52	Rocking –C=O of carboxylic group
	1633.14	Asymmetric stretching of C=O, C-O and O-H
	1527.03	Asymmetric stretching of N-O
	1460.90	Rocking C=O
	1373.73	Symmetrical stretching of CH_3 group
	1028.15	C-N stretching vibration
	594.57 and 568.17	Weakly bonded oxygen atoms with Zr ions

7.3.3. Scanning Electron Microscopic (SEM) analysis

Scanning Electron Microscopic (SEM) analysis was carried out for the native and the metal loaded DKSC to determine the surface morphology during biosorption process. Fig. 7.4(a)–(d) show the micrographs of the native, pre-treated, and thorium and zirconium loaded biomass, respectively. As seen from the images, the surface of raw

biomass (Fig. 7.4(a)) exhibits a solid structure with the completely folded non-particulate surface. DKSC (physically treated) (Fig. 7.4(b)) exhibits a homogeneous structure with deep pores, which indicates that the pretreatment method has enhanced the porous nature thereby increasing the surface area of the sorbent. On the other hand, metal-loaded biomass samples (Fig. 7.4 (c) and 7.4 (d)) exhibit a non-folded porous structure formed due to its hydrophilic nature.

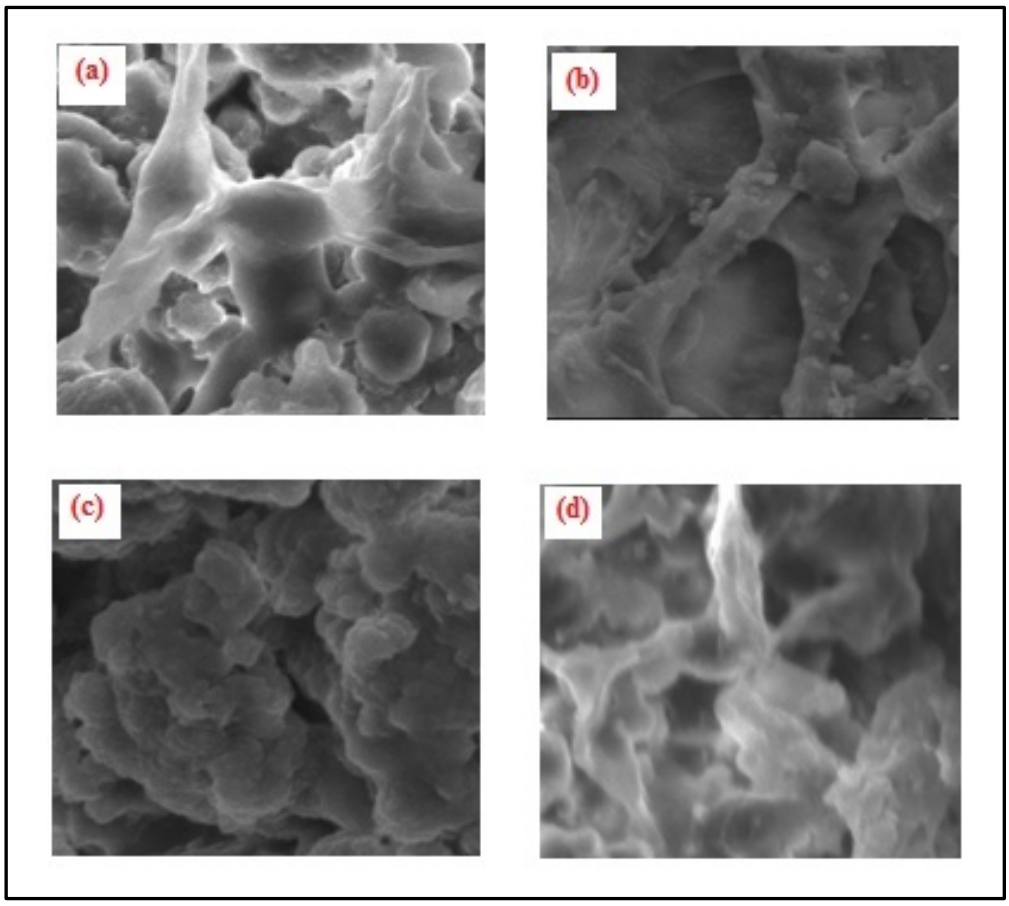

Figure 7.4: SEM micrographs of DKSC. (a) Raw biomass, (b) DKSC (after pretreatment), (c) Th-DKSC and (d) Zr-DKSC..

7.4. Conclusions

The characterisation studies of deoiled Karanja biomass have revealed that the physical pre-treatment followed has enhanced the surface area of the biomass. This was confirmed by SEM analysis. FTIR analysis confirmed that the hydroxyl, carboxyl, and amine are the major functional groups participated in the metal complexation reactions during biosorption. Furthermore, the regenerated biomass has characteristics that are similar to those of native biomass leading to the conclusion that desorption process has regenerated the biomass so that it can be recycled further.

Chapter 8

Conclusions and Recommendations

The research work presented here was about the development of a treatment process that can be used for the removal and recovery of radionuclides (Th and Zr) via a biosorption/desorption method. Literature suggests that extensive investigations are required for recognising relatively suitable biosorbents capable of separating significant quantities of radionuclide ions from aqueous solutions. Recently, agricultural by-products and plant wastes have been identified as important and economic sources to be used as biosorbents. DKSC is one such agricultural waste that can be used as a biosorbent because it is cheap, reusable, environmentally friendly and simple to use, especially for the removal of Th and Zr ions from contaminated sites.

A simple pretreatment method was adopted to enhance the ability of the DKSC biomass to be used as a biosorbent. The property of the new biomass was investigated using characterisation techniques such as SEM, FTIR, EDX, pH_{pzc} and methods for characterising the physicochemical properties. The characterisation techniques (SEM and FTIR) have revealed that the pre-treatment method adopted has enhanced the surface area and porosity of the biomass. FTIR analysis also showed that the functional groups, namely amines, alcoholic, carboxylic, amide and nitro groups present on the DKSC surface participated in the biosorption process by strong complexation reactions and weak electrostatic forces. The research work mainly dealt with the process variables (initial ion concentration, initial pH, sorbent loading) that affect the biosorption/desorption studies. These variables were optimised for achieving the maximum efficiency using DOE concepts such as the Taguchi OA (L_{16} and L_{18}) and Box-Behnken methods in RSM with the desirability approach used in the concentrations considered. Also, equilibrium, kinetic and thermodynamic data have been evaluated to determine the various mechanisms of the sorption process.

Thorium Biosorption; The efficiency of DKSC as a sorbent in removing thorium ions from aqueous solutions was studied by a batch biosorption technique, and process variables were optimised by employing a Taguchi robust OA design approach (L16 (43)). The responses q_e and R% were optimised for their maximum values by adapting the desirability function in the multivariate response optimisation. The optimum conditions were determined to be an initial Th(IV) concentration at level 4 (130 mg/L), an initial pH at level 4 (5) and a DKSC loading at level 1 (0.25 g/L). These conditions gave a maximum value of 260 mg/g for q_e and 99.97% for R%. The Langmuir isotherm model was found to exhibit a good correlation for the equilibrium data. The kinetic study revealed that the data fitted best to a pseudo-second order model signifying that the overall rate of biosorption was affected by chemisorption in the concentration range used in this work. Thermodynamic studies showed that the biosorption process was spontaneous and endothermic.

Zirconium biosorption; The effectiveness of DKSC as a biosorbent for the biosorption of Zr(IV) from aqueous solutions was tested by a batch biosorption technique. The most influential process variables were studied according to a Box-Behnken design in RSM and were optimised by using a desirability approach in a multi-response optimisation. Regression analysis showed that a full-quadratic model provided a good fit to the experimental data with a coefficient of determination (R^2) value of 0.98 and an$F$-Value of 26.96. Optimisation studies showed that the combination of process variables including the initial Zr concentration of 74.99 mg/L, an initial pH of 3.57 and a DKSC loading of 3.00 g/L led to a maximum response of 97.8% for R% and 23.44 mg/g for q_e at a desirability value of 0.99. ANOVA revealed that pH and DKSC loading were the most influential process variables in Zr(IV) biosorption using DKSC. Equilibrium data fitted

best to a Freundlich isotherm model and kinetic data followed pseudo-second-order model in the range of concentration investigated.

Desorption process; Desorption studies is an extension to biosorption method employed for the recovery of bound ions from loaded biomass. It is a useful step for the regeneration of sorbent. The process variables that affect the recovery of these species were found to be L/S ratio, eluent type, and concentration. Therefore, the variables above were optimised using a Taguchi mixed level design L_{18} ($2^1 3^2$) OA for achieving a maximum D%. The results have shown that 1M HCl and 0.1M $NaHCO_3$ can be used for the effective recovery of Th and Zr from loaded biomass with a maximum D% of 96% and 69% at L/S ratios of 7 and 3 for the desorption of thorium and zirconium, respectively. The desorption trend followed pseudo-second order kinetics for both Th and Zr. Also, the regenerated biomass ($DKSC^R$) exhibited similar characteristics as those of native DKSC which was confirmed through the determination of various physicochemical properties and FTIR analysis thereby confirming the possibility of reutilisation of DKSC in multiple cycles.

Overall Outcomes

- Based on the results obtained in this work, it can be concluded that DKSC can be effectively used as a natural and economic biosorbent for the removal and recovery of thorium and zirconium ions from aqueous streams and is therefore suitable as a low-cost biosorbent in the sequestration of radionuclides from effluents produced in nuclear and hydrometallurgical industries.

Limitations

- The present research is limited to the regeneration of the loaded biomass in a single cycle only. The recycling or reuse of the regenerated biomass using more cycles is beyond the scope of the current work.

Recommendations

- Identification of different biomass materials similar to DKSC and their utilisation as biosorbents in the pollution remediation processes.
- Scale-up studies for the commercialisation of biosorption process based on the availability, costs, and uptake capacity of the biomass.
- Investigating the biosorption processes for the treatment of effluent streams containing multi-ions.
- Continuous biosorption studies using packed and fluidised bed.

APPENDIX-A

Table A1: Effect of contact time (preliminary studies)

Time, minutes	C_t, mg/L	q_t, mg/g	R%
0	28.2	0	0
35	5	23.2	82.2695
135	3.9	24.3	86.17021
165	3.6	24.6	87.23404
195	3.6	24.6	87.23404
225	3.5	24.7	87.58865
255	3.3	24.9	88.29787
285	2.3	25.9	91.84397
315	2.3	25.9	91.84397

Table A2: Equilibrium data for thorium biosorption studies

C_i (mg/L)	C_e (mg/L)	q_e (mg/g)	K_d (L/g)	R_L	Θ	R%
25	1.78	23.22	13.04494	0.187529	0.769186	92.88
100	8.9	91.1	10.23596	0.065232	0.930216	91.1
150	46.9	103.1	2.198294	0.045465	0.95237	68.733
200	99.6	100.4	1.008032	0.034892	0.963847	50.2
465	353.1	111.9	0.316907	0.015629	0.984123	24.06
530	424.3	105.7	0.249116	0.013765	0.986043	19.94
625	512.5	112.5	0.219512	0.011722	0.988139	18
700	585.2	114.8	0.196172	0.010492	0.989397	16.4

Table A3: q_e values calculated from isotherm models

Experimental data		Langmuir model	Freundlich model
C_e, mg/L	q_e, mg/g	q_e	q_e
1.78	23.22	23.98	39.05
8.9	91.1	67.83	54.39
46.9	103.1	107.77	76.60
99.6	100.4	116.24	89.46
353.1	111.9	122.40	116.11
424.3	105.7	122.83	120.59
512.5	112.5	123.19	125.37
585.5	114.8	123.42	128.84

Table A4: Thermodynamic studies (effect of temperature)

Temperature, K	C_i, mg/L	C_e, mg/L	q_e, mg/g	K_d, L/g	B%	ΔG
288.15	100	10.721	177.6697	16.57212	89.28	-6726.4
298.15	100	4.944	179.69	36.34506	95.06	-8906.54
308.15	100	1.769	195.6793	110.6158	98.23	-12056.7
318.15	100	8.293	1392.508	167.9137	91.71	-13552

Appendix-B

Table B1: Effect of contact time in Zr biosorption

Time, minutes	C_i, mg/L	R%
0	48.42	0
15	38.1	21.31351
30	35.66	26.35275
60	28.3	41.55308
120	24.72	48.94672
150	24.4	49.6076
200	22.86	52.7881
220	23.3	51.87939
240	23.24	52.0033

Table B2: Equilibrium data for zirconium biosorption studies

C_i, mg/L	C_e, mg/L	q_e, mg/g	K_d, L/g
18.3	1.96	5.41	2.76
22.54	2.67	6.60	2.48
28.42	3.76	8.19	2.18
35.02	4.97	9.99	2.01
44.64	6.74	12.54	1.86
55.05	8.53	15.49	1.82
60.10	9.57	16.81	1.75
67.44	11.05	18.76	1.69
80.08	13.27	22.17	1.67
89.24	15.47	24.47	1.58

Table B3: q_e values calculated from adsorption isotherm models

Experimental data		Langmuir model	Freundlich model	DR	Temkin
C_e, mg/L	q_e, mg/g	q_e, mg/g	q_e, mg/g	q_e, mg/g	q_e, mg/g
1.96	5.41	5.17	5.19	4.24	0.49
2.67	6.60	6.72	6.52	7.59	0.52
3.76	8.19	8.83	8.41	11.18	0.55
4.97	9.99	10.87	10.34	13.47	0.58
6.74	12.54	13.39	12.97	15.22	0.61
8.53	15.49	15.51	15.44	16.13	0.64
9.57	16.81	16.59	16.82	16.47	0.65
11.05	18.76	17.96	18.71	16.80	0.66

13.27	22.17	19.72	21.44	17.12	0.68
15.47	24.47	21.18	24.02	17.32	0.69

Table B4: q_t values calculated from kinetic models

Experimental Data		**Pseudo-first order**	**Pseudo-second order**	**Intraparticle diffusion**	**Elovich**
Time, minutes	***q_t mg/g***	***q_t mg/g***	***q_t mg/g***	***q_t mg/g***	***q_t mg/g***
0	0	2.653314	0	4.194	0
15	4.053333	2.820173	4.846527	5.104151	4.711812
30	6.106667	2.97267	6	5.481148	5.479126
60	6.746667	3.239419	6.810443	6.014302	6.246439
120	6.866667	3.64833	7.303713	6.768296	7.013753
180	7.253333	3.933618	7.484407	7.346856	7.462603
210	7.56	4.04207	7.537688	7.599474	7.633248
240	7.793333	4.132656	7.57815	7.834604	7.781067
270	7.866667	4.208321	--	8.055444	7.911453

Table B5: Thermodynamic studies for Zr biosorption

Temperature, K	**q_e, mg/g**	**LnK_d**	**ΔG, kJ/mole**
288	1.49	-3.89	8.79
298	7.79	-2.16	5.08
308	34.62	0.39	1.37
318	33.47	0.29	-2.35

References

A. Hanif, H. N. B., M. A. Hanif 2013. Removal of zirconium from aqueous solution by Ganoderma lucidum: biosorption and bioremediation studies. *Desalination and Water Treament,* 53**,** 1-11.

Ahmed, S. H., EL Sheikh, E. M. & Morsy, A. M. 2014. Potentiality of uranium biosorption from nitric acid solutions using shrimp shells. *Journal of Environmental Radioacivity,* 134**,** 120-7.

AI, L., Luo, X., Lin, X. & Zhang, S. 2013. Biosorption behaviors of uranium (VI) from aqueous solution by sunflower straw and insights of binding mechanism. *Journal of Radioanalytical and Nuclear Chemistry,* 298**,** 1823-1834.

Akar, S. T., Sayin, F., TurkyilmaZ, S. & Akar, T. 2014. Multivariate optimization of the decolorization process by surface modified biomaterial: Box-Behnken design and mechanism analysis. *Environmental Science and Pollution Research,* 21**,** 13055-68.

Akhtar, K., Akhtar, M. W. & Khalid, A. M. 2008. Removal and recovery of zirconium from its aqueous solution by Candida tropicalis. *Journal of Hazardous Materials,* 156**,** 108-17.

Akin Sahbaz D, Y. A. A. G. U. 2015. Investigation of desorption kinetics and equilibrium of an anionicdye from magnetic polymer adsorbents. *Proceedings of the 14th International Conference on Environmental Science and Technology*.

Akkaya, R. & Akkaya, B. 2013. Adsorption isotherms, kinetics, thermodynamics and desorption studies for uranium and thorium ions from aqueous solution by novel microporous composite P(HEMA-EP). *Journal of Nuclear Materials,* 434**,** 328-333.

Aldor, I., Fourest, E. & Volesky, B. 1995. Desorption of Cadmium, from Algal Biosorbent. *The canadian joijrnal of chemical engineering,* 73**,** 516-522.

Anirudhan, T. S., Rijith, S. & Tharun, A. R. 2010. Adsorptive removal of thorium(IV) from aqueous solutions using poly(methacrylic acid)-grafted chitosan/bentonite composite matrix: Process design and equilibrium studies. *Colloids and Surfaces A: Physicochemical and Engineering Aspects,* 368**,** 13-22.

Aravind kumar, B. P., I.M. MISHRA 2008. Optimization of process parameters for acrylonitrile removal by a low-cost adsorbent using Box-Behnken design. *Journal of Hazardous Materials,* 150**,** 174-182.

Azizian, S. 2004. Kinetic models of sorption: a theoretical analysis. *Journal of Colloid Interface Science,* 276**,** 47-52.

Azouaou, N., Sadaoui, Z., Djaafri, A. & Mokaddem, H. 2010. Adsorption of cadmium from aqueous solution onto untreated coffee grounds: equilibrium, kinetics and thermodynamics. *Journal of Hazardous Materials,* 184**,** 126-34.

Bhalara, P. D., Punetha, D. & Balasubramanian, K. 2014. Kinetic and isotherm analysis for selective thorium(IV) retrieval from aqueous environment using eco-friendly cellulose composite. *International Journal of Environmental Science and Technology,* 12**,** 3095-3106.

Bhatti, H. N. & Amin, M. 2013. Removal of zirconium(IV) from aqueous solution by Coriolus versicolor: Equilibrium and thermodynamic study. *Ecological Engineering,* 51**,** 178-180.

Boveiri monji, A., Ghoulipour, V., Mallah, M. H. & Maraghe-mianji, B. 2014. Selective sorption of thorium (IV) from highly acidic aqueous solutions by rice and wheat bran. *Journal of Radioanalytical and Nuclear Chemistry,* 303**,** 949-958.

Boveiri monji, A., Javad ahmadi, S. & Zolfonoun, E. 2008. Selective Biosorption of Zirconium and Hafnium from Acidic Aqueous Solutions by Rice Bran, Wheat Bran and Platanus Orientalis Tree Leaves. *Separation Science and Technology,* 43**,** 597-608.

Ding, C., Feng, S., Cheng, W., Zhang, J., LI, X., Liao, J., Yang, Y., An, Z., Luo, S., Yang, J., TANG, J. & Liu, N. 2014. Biosorption behavior and mechanism of thorium on Streptomyces sporoverrucosus dwc-3. *Journal of Radioanalytical and Nuclear Chemistry,* 301**,** 237-245.

Diniz, V. & Volesky, B. 2006. Desorption of lanthanum, europium and ytterbium from Sargassum. *Separation and Purification Technology,* 50**,** 71-76.

Douglas, C. & Montgomery Design and Analysis of Experiments. *John Wiley & Sons, Inc.,* fifth ed.

Duygu Ozdes , A. G., Celal Duran& Hasan Basri Senturk 2010. Evaluation of adsorption characteristics of malachite greenonto almond shell (prunus dulcis). *Separation Science and Technology,* 45**,** 2076-2085.

E. Ozdemir, D. D. G., U. Beker, A. O. Avci 2011. Process optimization for Cr(VI) adsorption onto activated carbons by experimental design. *Chemical Enineering Journal,* 172**,** 207-218.

Ercan Özdemir, D. D. G., Ülker beker, Asli özge avci 2011. Process optimization for Cr(VI) adsorption onto activated carbons byexperimental design. *Chemical Engineering Journal,* 172**,** 207-218.

G. Annadurai, R. Y. S. 1998. Use of Box-Behnken design of experiments for the adsorption of verofix red using biopolymer. *Bioprocess Engineering,* 18**,** 463-466.

G. Yuvaraja, N. K., M.V. Subbaiah 2014. Biosorption of Pb(II) from aqueous solution by Solanum melongena leaf powder asa low- cost biosorbent prepared from agricultural waste. *Colloids and Surfaces B: Biointerfaces,* 114**,** 75-81.

Garnham, G. W., Codd, G. A. & Gadd, G. M. 1993. Accumulation of zirconium by microalgae and cyanobacteria. *Applied Microbiology Biotechnology* 39**,** 666-672.

Gok, C. & Aytas, S. 2013. Recovery of Thorium by High-Capacity Biopolymeric Sorbent. *Separation Science and Technology,* 48**,** 2115-2124.

H. Kalantari, S. Y., R. Roostaazad, H. Mohammad-Beigi 2014. Removal of zirconium from aqueous solution by Aspergillus niger. *Transactions C: Chemistry and Chemical Engineering,* 21**,** 772-780.

Huseyin Serencam, D. O., Celal Duran, Hasan Basri Senturk 2014. Assessment of kinetics, thermodynamics, and equilibriumparameters of Cu(II) adsorption onto Rosa canina seeds. *Desalination and Water Treatment,* 52**,** 3226-3236.

Islam, M. A., Sakkas, V. & Albanis, T. A. 2009. Application of statistical design of experiment with desirability function for the removal of organophosphorus pesticide from aqueous solution by low-cost material. *Journal of Hazardous Materials,* 170**,** 230-8.

Jnr, M. H. 2006. Recovery of lead and cadmium ions from metal-loaded biomass of wildcocoyam (Caladium bicolor) using acidic, basic and neutral eluentsolutions. *Electronic Journal of Biotechnology,* 9.

Jyi-Yeong Tseng, C.-Y. C., Chiung-Fen Chang, Yi-Hung Chen, Chia-Chi Chang, & Dar-Ren ji, C.-Y. C., Pen-Chi Chiang 2009. Kinetics and equilibrium of desorption removal of copper from magneticpolymer adsorbent. *Journal of Hazardous Materials,* 171**,** 370-377.

Kamaruddin, S., Khan, Z. A. & Foong, S. H. 2010. Application of Taguchi Method in the Optimization of injection moulding parameters for manufacturing products from plastic blend. *IACSIT International Journal of Engineering and Technology,* 2**,** 574-580.

Kousha, M., Daneshvar, E., Dopeikar, H., Taghavi, D. & Bhatnagar, A. 2012. Box–Behnken design optimization of Acid Black 1 dye biosorption by different brown macroalgae. *Chemical Engineering Journal,* 179**,** 158-168.

Kumar Anupam, S. D., Chiranjib Bhattacharjee, Siddhartha Datta 2011. Adsorptive removal of chromium (VI) from aqueous solution over powderedactivated carbon: Optimisation through response surface methodology. *Chemical Engineering Journal,* 173**,** 135-143.

Kütahyalı, C. & Eral, M. 2010. Sorption studies of uranium and thorium on activated carbon prepared from olive stones: Kinetic and thermodynamic aspects. *Journal of Nuclear Materials,* 396**,** 251-256.

Kuyucak, N. & Volesky, B. 1989. Desorption of Cobalt-Laden AlgalBiosorbent. *Biotechnology and Bioengineering,* 33**,** 815-822.

Mourabet, M., El rhilassi, A., El Boujaady, H., BennanI-Ziatni, M., El Hamri, R. & Taitai, A. 2012. Removal of fluoride from aqueous solution by adsorption on Apatitic tricalcium phosphate using Box–Behnken design and desirability function. *Applied Surface Science,* 258**,** 4402-4410.

Nagpal, U. M. K., Bankar, A. V., Pawar, N. J., Kapadnis, B. P. & Zinjarde, S. S. 2010. Equilibrium and Kinetic Studies on Biosorption of Heavy Metals by Leaf Powder of Paper Mulberry (Broussonetia papyrifera). *Water, Air, & Soil Pollution,* 215**,** 177-188.

Njikam, E. & Schiewer, S. 2012. Optimization and kinetic modeling of cadmium desorption from citrus peels: a process for biosorbent regeneration. *Journal of Hazardous Materials,* 213-214**,** 242-8.

Ofomaja, A. E. 2010. Intraparticle diffusion process for lead(II) biosorption onto mansonia wood sawdust. *Bioresource Technology,* 101**,** 5868-76.

P. Senthil Kumar, S. R., S. Dinesh Kirupha, A. Murugesan, T. Vidhyadevi, S. Sivanesan 2011. Adsorption behavior of nickel(II) onto cashew nut shell: Equilibrium,thermodynamics, kinetics, mechanism and process design. *Chemical Engineering Journal,* 167**,** 122-131.

Plazinski, W., Dziuba, J. & Rudzinski, W. 2013. Modeling of sorption kinetics: the pseudo-second order equation and the sorbate intraparticle diffusivity. *Adsorption,* 19**,** 1055-1064.

Radha kumari, M., Ball, A., Bhargava, S. K., Satyavathi, B. 2014. Optimization of glucose formation in karanja biomass hydrolysis using Taguchi robust method. *Bioresource Technology*, 166, 534-540.

Ruhan Altun Anayurt, A. S., Mustafa Tuzen 2009. Equilibrium, thermodynamic and kinetic studies on biosorption of Pb(II) andCd(II) from aqueous solution by macrofungus (Lactarius scrobiculatus) biomass. *Chemical Engineering Journal,* 151**,** 255-261.

Sayanasree Varala, Alka Kumari, B. Dharanija, Suresh K Bhargava, R. Parthasarathy, & Satyavathi, B. 2016. Removal of thorium (IV) from aqueous solutions by deoiled Karanja seed cake: Optimisation using Taguchi method, equilibrium, kineticand thermodynamic studies. *Journal of Environmental Chemical Engineering,* 4**,** 405-417.

Sharma, P., Singh, L. & Dilbaghi, N. 2009. Optimization of process variables for decolorization of Disperse Yellow 211 by Bacillus subtilis using Box-Behnken design. *Journal of Hazardous Materials,* 164**,** 1024-9.

Singh, R., Chadetrik, R., Kumar, R., Bishnoi, K., Bhatia, D., Kumar, A., Bishnoi, N. R. & Singh, N. 2010. Biosorption optimization of lead(II), cadmium(II) and copper(II) using response surface methodology and applicability in isotherms and thermodynamics modeling. *Journal of Hazardous Materials,* 174**,** 623-34.

Vi´tor J.P. Vilar, C. L. M. S. B., Rui A.R. Boaventura 2007. Copper desorption from Gelidium algal biomass. *Wat er Re s e arch,* 41**,** 1569-1579.

Volesky, M. T. A. B. 1981. Biosorption of Uranium and Thorium. *Biotechnology and Bioengineering,* XXIII**,** 583-604.

Yang, S. K., Tan, N., Wu, W. L., Hou, X. J., Xiang, K. X. & Lin, Y. C. 2015. Biosorption of thorium(IV) from aqueous solution by living biomass of marine-derived fungus Fusarium sp. #ZZF51. *Journal of Radioanalytical and Nuclear Chemistry,* 306**,** 99-105.

Yetilmezsoy, K., Demirel, S. & Vanderbei, R. J. 2009. Response surface modeling of Pb(II) removal from aqueous solution by Pistacia vera L.: Box-Behnken experimental design. *Journal of Hazardous Materials,* 171**,** 551-62.

Yuan-You, Feng su, Tang Jun Liu Ning, L. T. D. C.-C. L. J.-L. L. X.-L. L. X.-L. Z. J. Z. D. Y. J.-J. L. S.-Z. A. Z. W. Q.-Q. Y. 2015. Biosorption behavior and mechanism of thorium on Bacillus sp. dwc-2 isolated from soil. *Nuclear Science and Techniques,* 26.

Yusan, S., Gok, C., Erenturk, S. & Aytas, S. 2012. Adsorptive removal of thorium (IV) using calcined and flux calcined diatomite from Turkey: Evaluation of equilibrium, kinetic and thermodynamic data. *Applied Clay Science,* 67-68**,** 106-116.

Yuvaraja, G., Krishnaiah, N., Subbaiah, M. V. & Krishnaiah, A. 2014. Biosorption of Pb(II) from aqueous solution by Solanum melongena leaf powder as a low-cost biosorbent prepared from agricultural waste. *Colloids and Surfaces B :iointerfaces,* 114**,** 75-81.

Zhang, X. & Wang, X. 2015. Adsorption and desorption of nickel(II) ions from aqueous solution by a lignocellulose/montmorillonite nanocomposite. *PLoS One,* 10**,** e0117077.

Zolfonoun, E., Monji, A. B., Taghizadeh, M. & Ahmadi, S. J. 2010. Selective and direct sorption of zirconium from acidic leach liquor of zircon concentrate by rice bran. *Minerals Engineering,* 23**,** 755-756.

Zolgharnein, J., AsanjaranI, N. & Shariatmanesh, T. 2013. Taguchi L16 orthogonal array optimization for Cd (II) removal using Carpinus betulus tree leaves: Adsorption characterization. *International Biodeterioration & Biodegradation,* 85**,** 66-77.